DESIGN AND IMPLEMENTATION OF A MICROWAVE CAVITY RESONATOR FOR MODULATED BACKSCATTERED WAVE

A THESIS SUBMITTED TO
THE GRADUATE SCHOOL OF NATURAL AND APPLIED SCIENCES
OF
MIDDLE EAST TECHNICAL UNIVERSITY

BY

AHMET AKKOÇ

IN PARTIAL FULFILLMENT OF THE REQUIREMENTS
FOR
THE DEGREE OF MASTER OF SCIENCE
IN
ELECTRICAL AND ELECTRONICS ENGINEERING

AUGUST 2015

Approval of the Thesis:

DESIGN AND IMPLEMENTATION OF A MICROWAVE CAVITY RESONATOR FOR MODULATED BACKSCATTERED WAVE

submitted by **AHMET AKKOÇ** in partial fulfillment of the requirements for the degree of **Master of Science in Electrical and Electronics Engineering Department, Middle East Technical University** by,

Prof. Dr. Gülbin Dural Ünver
Dean, Graduate School of **Natural and Applied Sciences** _____

Prof. Dr. Gönül Turhan Sayan
Head of Department, **Electrical and Electronics Engineering** _____

Prof. Dr. Şimşek Demir
Supervisor, **Electrical and Electronics Eng. Dept., METU** _____

Examining Committee Members

Prof. Dr. Özlem Aydın Çivi
Electrical and Electronics Engineering Dept., METU _____

Prof. Dr. Şimşek Demir
Electrical and Electronics Engineering Dept., METU _____

Assoc. Prof. Dr. Lale Alatan
Electrical and Electronics Engineering Dept., METU _____

Assoc. Prof. Dr. Özgür Ergül
Electrical and Electronics Engineering Dept., METU _____

Assist. Prof. Dr. Mehmet Ünlü
Electrical and Electronics Engineering Dept., YBU _____

Date: 10.08.2015

I hereby declare that all information in this document has been obtained and presented in accordance with academic rules and ethical conduct. I also declare that, as required by these rules and conduct, I have fully cited and referenced all material and results that are not original to this work.

Name, Last name : Ahmet AKKOÇ

Signature :

ABSTRACT

DESIGN AND IMPLEMENTATION OF A MICROWAVE CAVITY RESONATOR FOR MODULATED BACKSCATTERED WAVE

Akkoç, Ahmet
M.S., Department of Electrical and Electronics Engineering
Supervisor: Prof. Dr. Şimşek Demir

August 2015, 160 pages

In this study, the device called "Theremin's Bug" which is a passive microwave cavity resonator is analyzed in detail and a similar device is designed, simulated and implemented. The device being the predecessor of modulated backscatter wave communication devices, RFID devices and microwave wireless sensors is invented by Russian inventor Leon Theremin in 1940s, and used as a covert spy device. The structure is totally passive and contains no electronic component and no battery. It uses the modulation of backscattering electromagnetic waves technique and resembles a passive microphone since it reflects the incoming wave by modulating with the ambient sound.

Since the device was a secret, there is no exact information about the technical details and principle of operation of the device. All the information about the device is consisted of stories and tales. And there are many technical inconsistencies about the device and working principle. In this work, the device is studied analytically and a practical prototype is implemented.

Keywords: Cavity Resonator, Coaxial Cavity, Reentrant Cavity, Evanescent Mode Cavity, Backscatter Wave Modulation, Monopole Antenna, Passive Microphone, Antenna Loading.

ÖZ

KİPLEMELİ DALGA GERİ SAÇILIMI İÇİN
MİKRODALGA KOVUK ÇINLATICI TASARIM VE ÜRETİMİ

Akkoç, Ahmet
Yüksek Lisans, Elektrik ve Elektronik Mühendisliği Bölümü
Tez Yöneticisi: Prof. Dr. Şimşek Demir

Ağustos 2015, 160 sayfa

Bu çalışmada "Theremin'in Böceği" olarak adlandırılan pasif mikrodalga kovuk çınlatıcı sistem detaylı bir şekilde analiz edilerek benzer bir sistemin tasarımı, simulasyonu ve üretimi gerçekleştirilmiştir. Söz konusu aygıt, kiplemeli geri saçılımlı dalga iletişim sistemlerinin, RFID sistemlerinin ve mikrodalga kablosuz sensor sistemlerinin ilk örneği olarak görülmektedir ve Rus mucit Leon Theremin tarafından 1940'lı yıllarda geliştirilerek gizli dinleme amacıyla kullanılmıştır. Sistem tamamıyla pasif yapıdadır ve batarya veya elektronik eleman içermemektedir. Sistem geri saçılan dalganın kiplenmesi tekniğini kulanarak çalışmaktadır ve gelen dalgayı ortam sesi ile kiplediği için pasif bir mikrofon olarak çalışmaktadır.
Söz konusu sistem Sovyet gizli servisine ait olduğundan çalışma mantığı ve teknik detayları ile ilgili kesin bilgi bulunmamaktadır. Var olan bilgiler anı, hikaye ve tevatürlerden ibarettir. Ayrıca sistemin çalışma biçimi ile ilgili olarak teknik manada tutarsız bilgiler bulunmaktadır. Bu tezde, bahsi geçen sistemin yapısı analitik olarak incelenmiş ve çalışan bir örneği gerçeklenmiştir.

Anahtar Kelimeler: Kovuk Çınlatıcı, Eşeksenel Kovuk, Girintili Kovuk, Sönümlenen Kipli Kovuk, Geri Saçılım Dalga Kiplemesi, Monopol Anten, Pasif Mikrofon, Anten Yükleme.

Thanks to the Master of the day of the judgment forever..

To my sweetheart ***Esma***, my cheetah ***Mustafa Deha*** and my honey ***Ece Verda***..

ACKNOWLEDGEMENTS

I would like to express my gratitude to my great supervisor Prof. Dr. Şimşek Demir for his guidance, suggestions and support throughout the study.

I would especially like to thank Dear Mr. Cüneyt for his unique support and contribution, which I will never forget.

I would also like to thank Mr. Fendil, Mrs. Güzide, Mr. Semih, Mr. Okan, Mr. Raşit, Mr. Ufuk, Mr. Tahsin, Mrs. Arzu, Mr. Abdullah, Mr. Orhan, Mr. Ferit, Mr. Ahmet Serbey and Mr. Daniel Ariav for their support and contribution to the thesis.

I would like to thank my friends in METU Antenna and Microwave Laboratory for such friendly research environments they had provided.

Finally, I would like to thank my great family (Esma, Mustafa Deha and Ece Verda) for their love, support, devotion and trust to me.

TABLE OF CONTENTS

LIST OF TABLES

TABLES

LIST OF FIGURES

FIGURES

LIST OF ABBREVIATIONS

CIA	Central Intelligence Agency
NKVD	Narodnıy Komissariyat Vnutrennnih Del
	(People's Commissariat for Internal Affairs)
MI5	Military Intelligence – Fifth
	(National security intelligence agency of United Kingdom)
US	United States
RF	Radio Frequency
RFID	Radio Frequency Identification
RLC	(Involving) Resistance Inductance Capacitance
LC	(Involving) Inductance Capacitance
Q Factor	Quality Factor
TE	Transverse Electric
TM	Transverse Magnetic
RCS	Radar Cross Section
VHF	Very High Frequency
UHF	Ultra High Frequency
IFF	Identification Friend or Foe
AM	Amplitude Modulation
PM	Phase Modulation
FM	Frequency Modulation
HFSS	High Frequency Structural Simulation
SPL	Sound Pressure Level
GSM	Global System Mobile
GSM900	Global System Mobile 900 MHz
NF	Noise Figure
SNR	Signal to Noise Ratio
SMA	Sub Miniature version A (Connector)

PET	Polyethylene Terephthalate
DC	Direct Current
BNC	Bayonet Neill – Concelman (Connector)
Wi-Fi	Wireless Fidelity (Wireless local area network)
TV	Television
MW	Microwave
VSWR	Voltage Standing Wave Ratio
IF	Intermediate Frequency

CHAPTER 1

INTRODUCTION

1.1 History of The Device

In 1952 a covert spy device is found in the American Embassy of the Soviet Union. As it is seen in Figure 1, it had been concealed inside a wooden replica of the Great Seal of America. Since it was a strange device and it could not be explained how it works when discovered, it was named as “The Thing” [1-4].

Figure 1. The Wooden Great Seal of America and the Theremin’s Device [1-4]

The seal had been presented to the American Ambassador Averell HARRIMAN as a peaceful gesture of friendship between the countries by the Soviet school children in 1945. According to some informal sources it was presented to the ambassador by an anonymous Russian as a personal gift.

The bug was not discovered until 1952. The seal had been stayed hung on the wall just behind the ambassador and Russians listened the American ambassadors for nearly 7 years until discovered [5]. The listened ambassadors during the period are

- W. Averell Harriman — October 7, 1943
- Walter Bedell Smith — March 22, 1946
- Alan G. Kirk — May 21, 1949
- George F. Kennan — March 14, 1952

Actually Americans had discovered a mysterious signal and realized that Soviets were bombarding the embassy with a microwave signal for a long time before the discovery of the device but they could not be able to explain the reason of the signal bombardment. The CIA counterespionage team had performed technical search operations at the building (Spaso House, Residence of American Ambassadors in Moscow) several times but they had found nothing always. Nevertheless, they had several theories that it might be a mind control attack (at that time, the mind control was a popular scientific research area) by NKVD (Soviet internal intelligence service) or NKVD might had been trying to get the people in the embassy depressed spiritually by microwave signals.

Afterwards they discovered the speech signal by accidentally and then searching in detail, they found the device and thus solved the signal mystery in 1952. But they faced with a new mystery, the device itself.

The device was a small tiny metal cylindrical box with a tail and it contained neither electrical component nor battery. It was a passive device. Soviets were sending a signal towards the device and device reflects back the signal with a modulation of the sound.

CIA worked on the device for a long time but could not explain the working principle of the device. They asked English Service MI5 for help. MI5 dealt with the device but no solution is found. Eventually English scientist Peter Wright worked on the device for several months and solved the mystery. The device was a passive cavity resonator. Later on English service made new devices for themselves and for Americans [6].

The inventor of the device is Leon Theremin who was a Russian scientist and inventor. He had many practical inventions and innovations. Theremin is the inventor of first electronic musical instrument called Theremin and the interlace techniques on video. He had become very famous and had gone to US in 1927. In 1938 he had been kidnapped by Soviet agents and had been brought to Soviet Union and was imprisoned in the Butyrka Prison and later sent to work in the Kolyma Gold Mines. Theremin was supposed to be executed but in fact put to work in Sharashka (a secret laboratory in the Soviet Gulag Camp System, where the prisoners work for army research activities) together with some other well-known scientists and engineers. Where he worked for Soviet Army and Soviet intelligence, and invented "The Thing" [7].

1.2 Motivation to Work And Objective

The English scientist Peter Wright discovered the working principles of the devices and he created a similar system called "Satyr" for British intelligence by working for 18 months [7]. The mystery of the device had been solved, but since the issue was related with the intelligence services and secret spy operations, the details of the device has been never explained formally. The operation and the device are disclosed in general aspect but the details of working principle and the properties of the device were not disclosed so far.

Theremin's bug had been a great and new technology and it opened a new era at that time. It was the first practical device using passive communication technique which had been a theoretical issue up to then. Thus Theremin's bug became a pioneer for modulated backscatter wave, passive wireless communication, passive microwave sensors and RFID applications.

There are many informal references which give information about the device but almost all of them are consist of memories, rumors and recollection stories. So, nearly all data about the device are inconsistent. The only consistent information is the general mechanical structure of the device.

In this thesis the device will be analyzed and tried to be clarified technically. After the analysis of the structure, a similar system will be designed, produced and implemented.

In addition, in this work the structure is used for perception of the sound but the structure is a promising design for a variety of different applications to sense or detect many physical parameters wirelessly, remotely and passively.

1.3 The Device Properties

All the descriptions about the device from all kind of references define physically the same structure. The device is consisted of a metal cylinder and an aerial protruding from the cylinder. One circular face of the cylinder is closed by a thin metallic diaphragm. Inside the cylinder, there is a mushroom shaped post in the middle which has a disc shaped plate parallel to the diaphragm. The inner part of the antenna having disc shaped head near to the central post [8]. The available picture and drawings of the device are given in Figure 2. In Appendix A, all the data and information collected from all sources about the issue are given in detail.

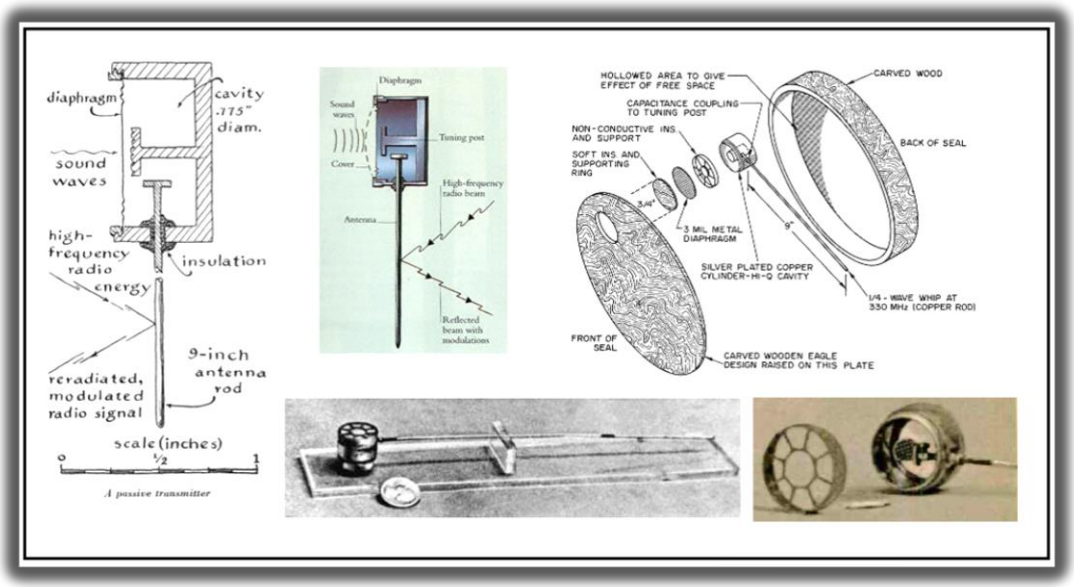

Figure 2. The pictures and drawings of the Theremin's Device [2, 9-12]

There are many stories about the device. Only few of them are first-hand information and few of those first-hand stories mention the details. The device is generally described as a passive cavity resonator. And some references say that the device used modulated backscattering technique. In any case an electromagnetic signal is sent to the device; the device modulates the signal with the surrounding sound and reflects or sends back. The information carrying reflected signal is then detected and demodulated.

The more explanatory definition can be done in the following way. A high powered microwave signal is sent from a van parked near to the building by using a highly directive antenna to the region of the building where the device is placed. The device resonates at a certain frequency and this frequency changes in accordance with the sound hitting the thin diaphragm of the device. Because the sound hitting the diaphragm changes the resonance characteristic of the device, the reflected wave from the antenna of the device is modulated by the sound.

In the Table 1 below it is given the most general dimensional parameters of the device [2,10,13,14].

Table 1 The most general dimensional parameters of the device

Dimension	Measure
The Diameter	0.775 inch
The Cylindrical Height	0.6875 inch
The Plate Diameter	0.25 inch
The Antenna Length	9 inch
The Diaphragm Thickness	3 mil
The Weight	1.1 oz
The Cavity Inductance	10 nH

1.4 Organization of the Thesis

This thesis aims to research on the Theremin's Device and describe the structure and working principle of the device by analyzing technically in detail, making

simulations, designing and producing a prototype having similar structure and making experimental work on this prototype. In accordance with this goal;

Chapter 1 (Introduction) gives the history of the device and explains the motivation and objectives of the thesis and introduces a broad overview of the thesis.

Chapter 2 (Theoretical Background) provides the relevant technical knowledge about the involving issues such as resonance and resonators, microwave cavities, antennas and backscatter modulation technique.

Chapter 3 (Theoretical Work) includes the theoretical analysis of the device structure, calculations, derivations and simulations related with the structure; design, analysis and simulations of the prototypes.

Chapter 4 (Measurements & Results) describes the experimental set-up, prototype measurements and experiments. Moreover, Chapter 4 gives experimental results of the listening experiments.

Chapter 5 (Conclusions) includes a summary of the thesis, conclusions drawn from the work and several suggestions for future works about the issue.

There are two appendices at the end of the thesis. Appendix A provides more detailed information relevant to the main text. It contains the pictures, drawings and existing information about the device in all kind of sources. Appendix B is a CD-ROM which is attached in an envelope on the back cover of the document. It contains the audio files related with the sound receive experiments.

The thesis ends with the list of used reference materials following the appendices.

CHAPTER 2

THEORETICAL BACKGROUND

This chapter gives the relevant information and provides a theoretical background about the subjects relating the topics studied in this work. All the information is presented from the thesis' point of view and necessary to understand the further parts.

2.1 Resonance And Resonators

2.1.1 Resonance

Resonance is a very general phenomenon that happens so often and in so many kinds of systems. Resonance can be in any media, in any form and in a vast range of spatial scales. But across this wide range of spatial scales and diverse media, there are certain general properties of resonance that are common to all of them. They all tend to oscillate at some characteristic frequency and at its higher harmonic frequencies that are integer multiples of the fundamental frequency. They all exhibit spatial standing waves, whose wavelength is inversely proportional to their frequencies. In the most general sense, resonance represents that the energy in a system exchanges from one form into another form at a particular rate. However, while exchanging there happen some losses from cycle to cycle. A resonance system has low quality if its energy is lost quickly during the energy exchange process. Losses may be caused by “friction” in mechanical systems and “resistance” in electronic systems. In this thesis, our main interests are the electrical resonance and the electromagnetic wave (or microwave) resonance [15].

In electrical circuits, resonance occurs as electrical energy stored in capacitors and magnetic energy stored in inductors exchange back and forth.

Electromagnetic or microwave resonance occurs in a medium as standing waves by reflections from the boundaries in a frequency related with the medium size. In some special type microwave resonators, the energy also exchange between the electric and the magnetic fields.

2.1.2 Resonators

A resonator is a physical system providing the resonance. There is at least one fundamental frequency at which the resonance takes place for every resonator. This is called the resonant or resonance frequency. In resonance, the oscillating energy is converted from one form to another and vice versa. If it is supplied more energy to the system at the frequency of resonance then the energy is absorbed by the system and stored in the continuing oscillation. So a resonator is a system which can store the energy that is oscillating from one kind to another.

There are many structures functioning as a resonator. In acoustic resonators, the air molecules oscillate back and forth such that the energy changes from pressure to kinetic energy and vice versa. In mechanical resonators, energy change occurs between stress force and movement or kinetic energy. The parameters like dimension, size, shape and stiffness affect the speed of energy oscillation, i.e., the resonant frequency [15].

In electrical resonators, the alternation of energy occurs between electrical energy and magnetic energy. In a circuit, the electrical energy is stored in capacitance as charge separation and the magnetic energy is stored in inductance as charge movement or current. The energy in the circuit is therefore transformed between these two forms or between capacitance and the inductance of the circuit. Hence, the frequency of the oscillation is determined by the inductance and capacitance of the circuit.

In electromagnetic or microwave resonators, the resonance is created by the reflection of the wave between the boundaries of the structure and forming a standing wave oscillation. In some special case of microwave resonators, the energy exchange takes place between electric and magnetic fields inside the resonator as very like in electrical resonator.

In electromagnetic waves, the electric and magnetic field is already transformed each other periodically while propagating. The resonant frequency of microwave structure depends on the dimensional parameters like size and shape and also the electrical and magnetic properties of the involving structures.

2.1.3 Electrical Resonators

Near the resonant frequencies, a microwave resonator can be modeled by lumped-element equivalent circuit which may be series RLC or parallel RLC resonator circuit. So in the following sections it is reviewed some basic properties of the electrical resonator circuits [15,16].

2.1.3.1 Ideal LC Resonators

Electrical resonator circuits are ideally and simply consist of a capacitance and an inductance forming a loop as in Figure 3 below.

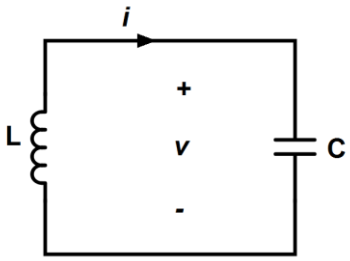

Figure 3. Ideal LC Resonator

This LC circuit is an idealized model since it assumes there is no dissipation of energy due to resistance. Any practical implementation of an LC circuit will always include loss resulting from small but non-zero resistance within the components and connecting wires.

The LC resonator circuit has two configurations according to the connection type; series and parallel LC circuit which are shown in Figure 4 below.

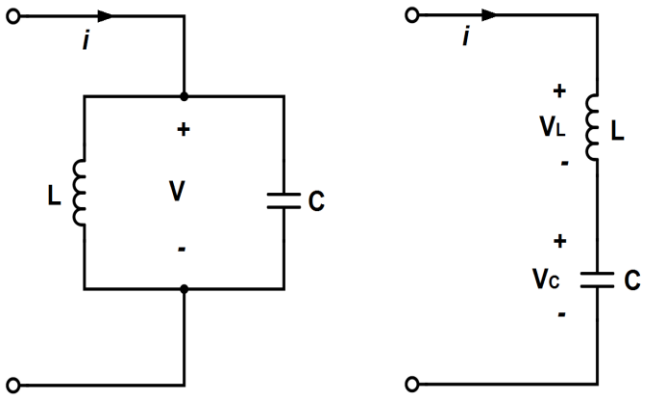

Figure 4. Parallel and Series LC Resonant Circuit

These circuits are called simple LC resonant circuits, and act as an electrical resonator, storing energy oscillating at the circuit's resonant frequency.

LC circuits are used either for generating signals at a particular frequency, or picking out a signal at a particular frequency from a more complex signal. They are key components in many electronic devices, particularly radio equipment and used in circuits such as oscillators, filters, tuners and frequency mixers.

Resonance occurs when an LC circuit is driven from an external source at a frequency at which the inductive and capacitive reactances are equal in magnitude. The frequency at which this equality holds for the circuit is called the resonant frequency. The resonant frequency of the LC circuit is given as

$$\omega_0 = \frac{1}{\sqrt{LC}} \qquad (2.1)$$

where L is the inductance in Henries, and C is the capacitance in Farads.

The angular frequency ω_0 has units of radians per second. The equivalent frequency in hertz is

$$f_0 = \frac{1}{2\pi\sqrt{LC}} \tag{2.2}$$

The *L/C* ratio of the LC circuit is one of the factors that determine its Q Factor (Quality Factor). The Q Factor is a dimensionless quantity that describes how under-damped (or lossy) a resonator as well as characterizes a resonator's bandwidth relative to its center frequency. The two common definitions of Q Factor are as follows

$$Q \triangleq \frac{f_0}{\Delta f} = \frac{\omega_0}{\Delta\omega} \tag{2.3}$$

$$Q \triangleq 2\pi \frac{Energy\ Stored}{Energy\ Dissipated\ per\ cycle} = 2\pi f_0 \frac{Energy\ Stored}{Power\ Loss} \tag{2.4}$$

where f_0 is the resonant frequency, Δf is the half power bandwidth.

These two definitions are not necessarily equivalent. They become approximately equivalent as Q becomes larger, meaning the resonator becomes less damped. Higher Q indicates a lower rate of energy loss relative to the stored energy of the resonator, i.e., the oscillations die out more slowly.

The two-element LC circuit described above is the simplest type of inductor-capacitor network (or LC network). It is also referred to as a second order LC circuit to distinguish it from more complicated (higher order) LC networks with more inductors and capacitors. Such LC networks with more than two reactive structures may have more than one resonant frequency.

2.1.3.2 RLC Resonators

Any practical implementation of an LC circuit will always include loss resulting from small but non-zero resistance within the components and connecting wires.

In LC circuit the charge flows back and forth between the plates of the capacitor, through the inductor. The energy oscillates back and forth between the capacitor and the inductor until (if not replenished from a source) internal resistance makes the oscillations die out. There must be a source to drive continuous oscillations. If the excitation frequency of the source is at the resonant frequency of the circuit then resonance will occur.

There are two types of RLC resonators depending on the connection, series and parallel RLC resonator as given in the Figure 5 below. It will be noted that the only difference between the series and parallel circuit is in the manner of connection.

At resonance, parallel circuit offers high impedance and the series circuit offer low impedance to the source.

2.1.3.2.1 *Series RLC Resonators*

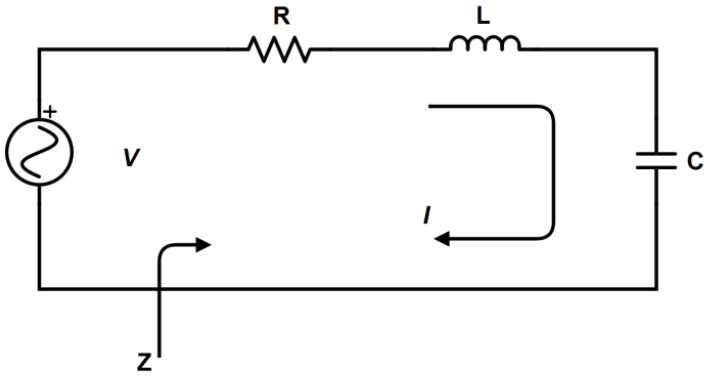

Figure 5. Series RLC Resonant Circuit

A circuit consisting of resistance, inductance and capacitance connected in series with a voltage applied as shown in Figure 5 is termed as a series resonant circuit. In many cases, practically R represents the loss resistance of the inductor, which in the case of air core coils simply means the resistance of the winding. The resistances associated with the capacitor are often negligible.

When the resistance is low, as is normally the case, the current depends upon the frequency of the applied voltage. The current is a maximum and in phase with the applied voltage at the resonant frequency. At the resonant frequency the inductive reactance and capacitive reactance are equal in magnitude. At lower frequencies the current falls off and leads, while at higher frequencies it drops and lags.

The resonant frequency of the series RLC circuit is as given in Eq. (2.2). Another important parameter of a resonant circuit is its Q Factor, or quality factor, which is

$$Q = \omega \frac{Average\ Energy\ Stored}{Energy\ Loss/Second} \tag{2.5}$$

Thus Q is a measure of the loss of a resonant circuit. Lower loss implies a higher Q. Resonator losses may be due to conductor loss, dielectric loss, or radiation loss and are represented by the resistance R of the equivalent circuit. An external connecting network may introduce additional loss. Each of these loss mechanisms will have the effect of lowering the Q. The Q of the resonator itself, disregarding external loading effects, is called the unloaded Q, denoted as Q_0.

For the series resonant circuit of Figure 5, the unloaded Q can be evaluated from Eq. (2.5) above, as follows

$$Q_0 = \frac{\omega_0 L}{R} = \frac{1}{\omega_0 RC} = \frac{1}{R}\sqrt{\frac{L}{C}} \tag{2.6}$$

The circuit impedance Z illustrated in the Figure 5 is

$$Z = R + j\omega L + \frac{1}{j\omega C} \tag{2.7}$$

$$Z = R + j\left(\omega L - \frac{1}{\omega C}\right) \tag{2.8}$$

The resistance and reactance components of the impedance of the series circuit vary with frequency.

In the small frequency region around the resonance, the circuit resistance is substantially constant. The reactance, on the other hand, varies substantially linearly from a relatively high capacitive value below resonance to a relatively high inductive value above resonance, and becomes zero at the resonant frequency. The absolute value of the impedance is at the minimum in the resonance.

2.1.3.2.2 *Parallel RLC Resonators*

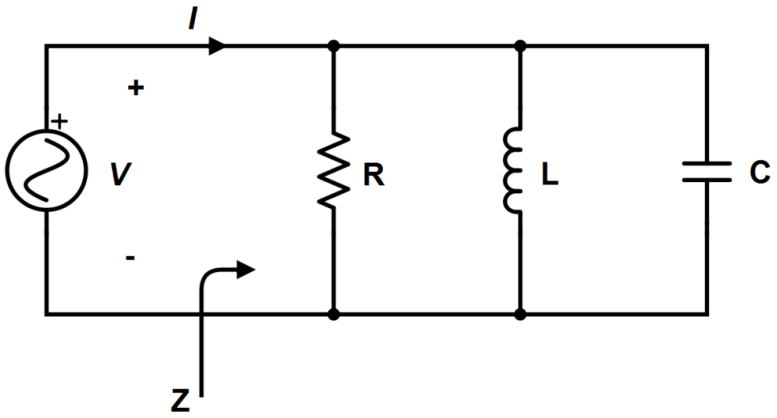

Figure 6. Parallel RLC Resonant Circuit

A parallel resonant circuit is the dual of the series RLC circuit. It is obtained when the voltage is applied to an inductance and capacitance connected in parallel, as in the Figure 6. The resonant frequency of a parallel circuit can be defined in several ways as follows:

- The frequency at which "$\omega L = 1/\omega C$", i.e., the resonant frequency of the same circuit when operating in series resonance.
- The frequency at which the parallel impedance of the circuit is maximum.
- The frequency at which the parallel impedance of the circuit has unity power factor.

These three definitions lead to frequencies that differ by an amount depending upon the circuit Q and the division of the resistance between the branches.

When the circuit Q is at least moderately high ($Q \geq 10$), for all practical purposes the resonant frequency of a parallel resonant circuit can be taken as the resonant frequency of the same circuit when connected in series. The only difference between series and parallel resonance under these conditions is that the phase angles are reversed, i.e., the phase angle of parallel impedance has the opposite sign from the phase angle of the current in the series circuit.

The resonant frequency and the Q factor of the parallel RLC circuit are given in Eq. (2.2) and Eq. (2.6).

The circuit impedance Z is

$$Z = (\frac{1}{R} + \frac{1}{j\omega L} + j\omega C)^{-1} \tag{2.9}$$

The unloaded Q factor of the Parallel RLC circuit is

$$Q_0 = \frac{R}{\omega_0 L} = \omega_0 RC = R\sqrt{\frac{C}{L}} \tag{2.10}$$

As it is seen in Eq. (2.10) above that the Q of the parallel resonant circuit increases as R increases.

2.1.3.3 Loaded and Unloaded Q Factors

The unloaded quality factor Q_0 is a characteristic of the resonator itself in the absence of any loading effects caused by external circuitry. In practice, however, a resonator is invariably coupled to other circuitry which will have the effect of lowering the overall or loaded quality factor Q_L, of the circuit [16].

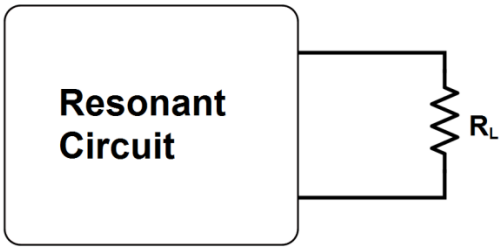

Figure 7. Resonant Circuit connected to an external Load R_L

A resonator coupled to an external load resistor R_L is seen in Figure 7. If the resonator is a series circuit, the load resistor R_L adds in series with R, so the effective resistance increases. If the resonator is a parallel RLC circuit, the load resistor R_L combines in parallel with R, so the effective resistance decreases. If we define an external quality factor Q_e, as

$$Q_e = \frac{\omega_0 L}{R_L} \qquad for\ series\ resonator \tag{2.11}$$

$$Q_e = \frac{R_L}{\omega_0 L} \qquad for\ parallel\ resonator \tag{2.12}$$

Then the loaded quality factor Q_L can be written as

$$\frac{1}{Q_L} = \frac{1}{Q_e} + \frac{1}{Q_0} \tag{2.13}$$

2.2 Microwave Cavities

Any closed surface with conducting walls can support resonance of electromagnetic waves within it, and it possesses certain resonant frequencies when excited by electromagnetic fields. In the volume enclosed by the conducting walls, electric and magnetic energy is stored and by exchanging from one form to other establishes a resonance condition.

These resonators are commonly termed microwave cavity resonators and are extensively used as resonant circuits at extremely high frequencies. For such use of high frequency, cavity resonators have several advantages like simplicity, manageable physical size, high Q and very high shunt impedances. At wavelengths well below one meter, microwave cavity resonators become vastly superior to the corresponding resonators with lumped components.

Cavity resonators have less power dissipation according to the lumped resonators. In cavities, power is dissipated in the metallic walls of the cavity as well as in the dielectric material that may fill the cavity.

Cavities are used in many kinds of microwave circuits and systems like microwave generators (e.g. Klystrons, Magnetrons), frequency meters, material measurements, heating applications and microwave filters.

The information in this section is compiled from [16-19] in general.

2.2.1 Types of Cavity Resonators

Cavity resonators can be in any shape and physical form. The physical structure of the cavity depends on the application required. As general, practical cavity resonators can be divided into two groups of physical structure. The first group is the cavities having regular geometric shapes and structures like rectangle, cylinder, sphere, prism, ellipsoid etc. as shown in

Figure 8.

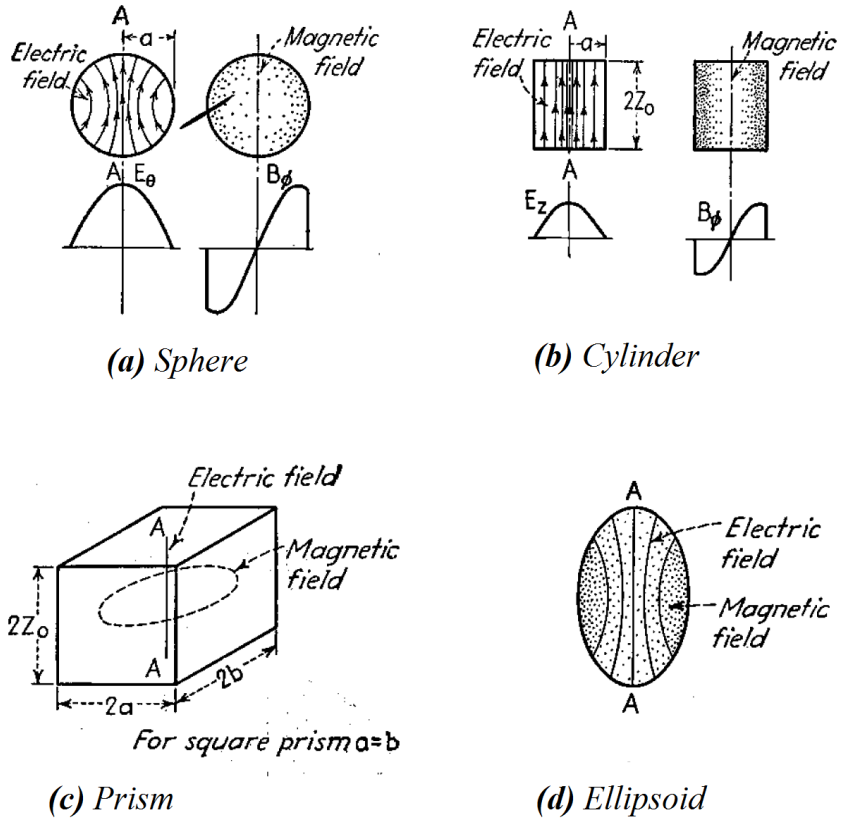

Figure 8. Cavities having regular shapes [16]

The second group cavities, as illustrated in Figure 9, are in various physical forms and shapes. They are combination of some idealized and some practical forms. Since there are some types of protrusions and bulges inwards of the cavities, these cavities are called as reentrant type.

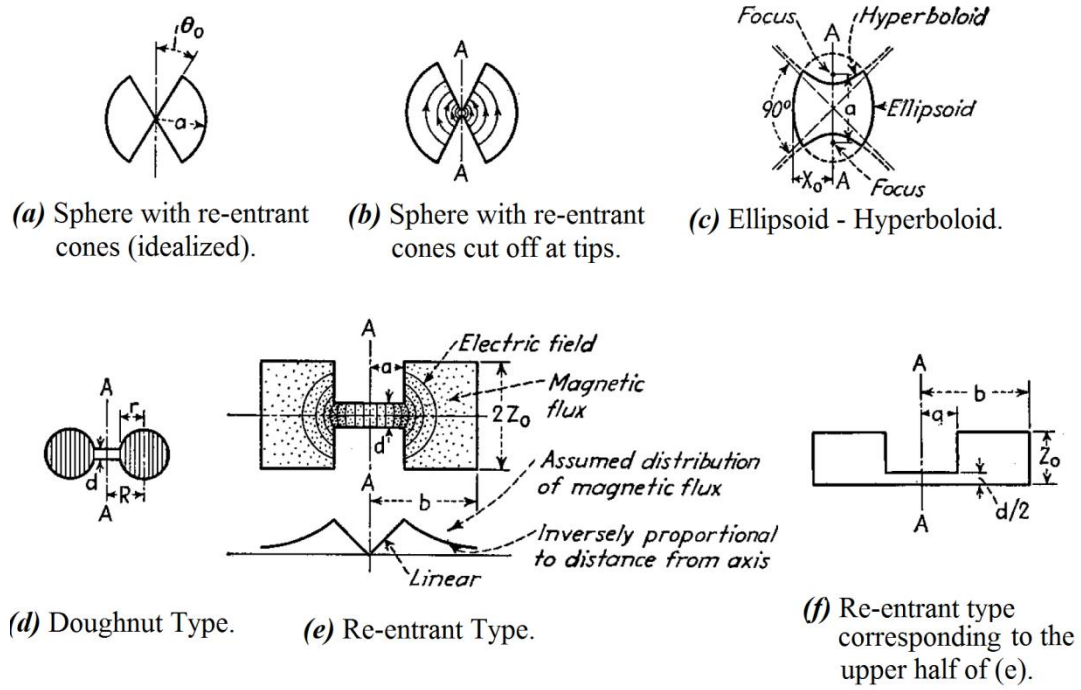

Figure 9. Reentrant Type Cavities [16]

2.2.2 Modes of Cavity Resonators

In a cavity, the resonating electromagnetic fields can be in various forms. These forms are called as modes. Resonance modes depend on the excitation frequency, excitation style and the dimensions of the cavity. The mode having the minimum resonance frequency is called as the fundamental mode of the cavity. Higher order modes correspond to a higher resonance frequency than the fundamental mode. Q factor and the shunt impedance of the cavity also depend upon the mode, and may be either greater or less than for the fundamental mode. In particular, certain types of higher order modes have very low losses and give unusually high Q and shunt impedance. The fields corresponding to the second order mode in a spherical and a cylindrical cavity resonators are shown in Figure 10.

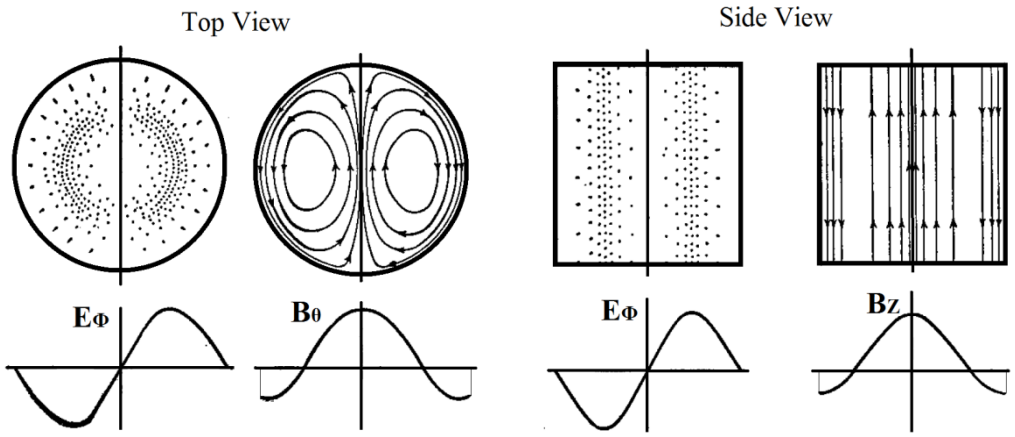

Figure 10. Second order mode in a spherical and a cylindrical cavity [16]

In a cylindrical resonator, the oscillations can be explained crudely as the electric charges or currents flow up and down in the sidewalls of the cylindrical cavity and provide the charging of the capacitance formed by the top and bottom walls of the cavity. The sphere is analogous.

For the reentrant type cavities the electric field is concentrated largely in the region of the reentrant portions, and the most of the magnetic fields existing in the other regions encircle the reentrant portions. Since the electric and magnetic fields concentrate in different parts, this kind of resonator is much more closely related to a circuit with lumped parameters than the other forms of cavities.

2.2.3 Resonant Frequency of Cavity Resonators

Possible solutions of Maxwell's equations satisfying the boundary conditions for the electric and magnetic fields within the cavity resonator give the resonant frequency of the cavity. For the cavities having regular physical forms such as cylinders, spheres, cubes, prisms and some idealized forms involving reentrant portions, the calculation of resonant frequency can be exactly carried out. But for some others having complex physical forms and shapes, approximate solutions are derived.

The resonant wavelength is proportional to the resonator size, i.e., if all dimensions are doubled, then the resonant wavelength will likewise be doubled. Using this fact, the resonators having complex shapes that cannot be calculated can be constructed easily. In order to obtain a desired resonant frequency, first it is constructed a resonator of proper size and shape. Then the resonant frequency is measured. The ratio of this frequency to the desired resonant frequency gives a scale factor that is applied to all dimension of the resonator to obtain the resonator operating at the desired wavelength.

The resonant frequency of resonators such as illustrated in

Figure 9 (d to f) above, which have a large capacitance, can be calculated approximately by using the capacitance and inductance.

The resonant frequency of a cavity resonator can be changed by changing the mechanical dimensions or by coupling reactance into the resonator or by means of a conductive paddle. Small changes in dimensions can be realized by flexible walls, while large changes require some movable parts. The resonant frequency of the reentrant type resonators is particularly sensitive to the gap that constituting a capacitance between the reentrant portions, especially when this gap is small. Reactance can be coupled into the resonator by coupling loops or probes in the manner discussed below and affects the resonant frequency. A copper paddle placed inside the resonator in such a way that intercepts some of the flux lines will increase the resonant frequency. Changing the position of the paddle will change the effect. This can be used to adjust the resonant frequency.

2.2.4 Q Factor of Cavity Resonators

The Q Factor of a cavity resonator is the ratio of the energy stored in the fields of the resonator to the energy lost per cycle, according to the relation below.

$$Q = 2\pi \frac{Energy\ Stored}{Energy\ Lost\ per\ cycle} \tag{2.14}$$

It has the same significance as for a lumped resonant circuit. So it can be defined as

$$\Delta f = f_2 - f_1 \tag{2.15}$$

$$Q = \frac{f_c}{\Delta f} \tag{2.16}$$

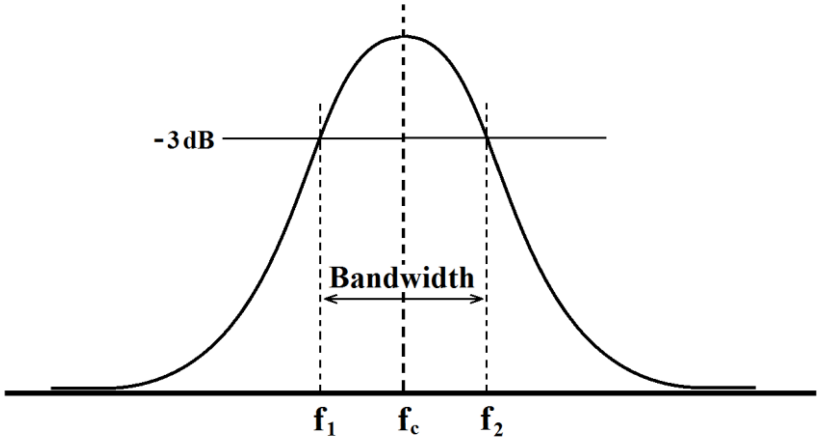

Figure 11. Q Factor of the resonator

An important implication of Eq. (2.14) is that to achieve a high Q value, the resonator should have a large ratio of volume to surface area. The physical explanation for this is that all the energy is stored in the volume of the resonator, whereas all dissipation occurs at the walls. As a result, resonators such as spheres, cylinders, and prisms can in general be expected to have higher Q than the resonators having the same shape with reentrant sections. The drop in Q resulting from reentrant portion is excessive if the reentrant portions have very sharp spines. With resonators of the same proportions but different size, Eq. (2.14) shows that the Q will be proportional to the square root of the wavelength and thus the size.

For practical cavity resonators, typical values of Q are extremely high, compared with those encountered with common resonator circuits.

2.2.5 Shunt Impedance of Cavity Resonators

The shunt impedance of a cavity resonator can be defined as the square of the line integral of voltage across the resonator, divided by the power loss in the resonator. This impedance corresponds to the parallel resonant impedance of a tuned circuit, and at resonance becomes purely resistive and called the shunt resistance of the resonator.

The shunt impedance of cavity resonators having regular shapes can be calculated by analytically. The values obtainable are very large. The shunt resistance of the reentrant type cavity resonators is less than without reentrants. But if the distance across which the impedance is developed is very short then the reentrant type of cavity resonator gives much greater shunt impedance in inverse proportion with the distance [20]

2.2.6 Conducting Material of Cavity Resonators

In terms of cavity performance or quality factor, the conductor material which the microwave cavity is made of is important. The conductor must be chosen accordingly with the expected performance. Using materials having better conductivity provide the lower loss. The materials that can be used for cavity production and their conductivity values are Copper (5.813 x 107 S/m), Aluminum (3.816 x 107 S/m) and Brass (2.564 x 107 S/m) [15].

Since copper is very expensive it is not proper for massive structures generally. It is more common use for applications involving strip conductors, grounds in micro strips lines, which they have a very small thickness (around 17um ~35um) or even for wires. Aluminum has the soldering problem with the conventional method using tin, and the softness of it causes some mechanical difficulties. So finally, brass is suitable in many aspects for microwave cavity applications. It eliminates the drawbacks of copper and aluminum for bulky structures. In this work, brass is also used as cavity material.

2.2.7 Coupling to Cavity Resonators

Transferring the electromagnetic energy into a cavity is called as coupling. The energy is transferred from the external structure to the cavity via the coupling device. For the TE and TM mode, the coupling devices will be different. Coupling to a cavity resonator can be realized by electron beaming, coupling loops, coupling probes or coupling slots. Coupling by means of an electron beam can be accomplished by passing the beam through the resonator, as indicated in Figure 12.

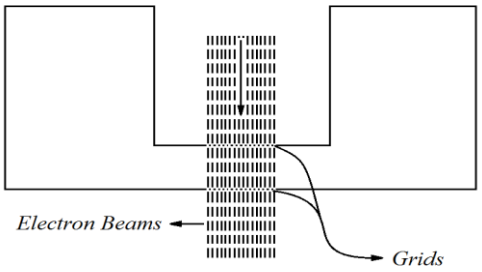

Figure 12. Coupling by means of electron beaming [16]

Since it is necessary for electron beam coupling that the transit time for the electrons to reach across the resonator must be small compared with the resonance period. This requires particularly the use of the reentrant type resonators, in order to keep short the distance the electrons must travel within the resonator.

A coupling loop is used for coupling to a cavity resonator magnetically. The loop is oriented in such a way to enclose magnetic flux lines corresponding to the desired mode of operation. Thus a current passing through the loop will then raise the oscillations of desired mode. Conversely any existing oscillation in the resonator will induce a voltage in such a coupling loop. Hence the coupling mechanism works in both ways.

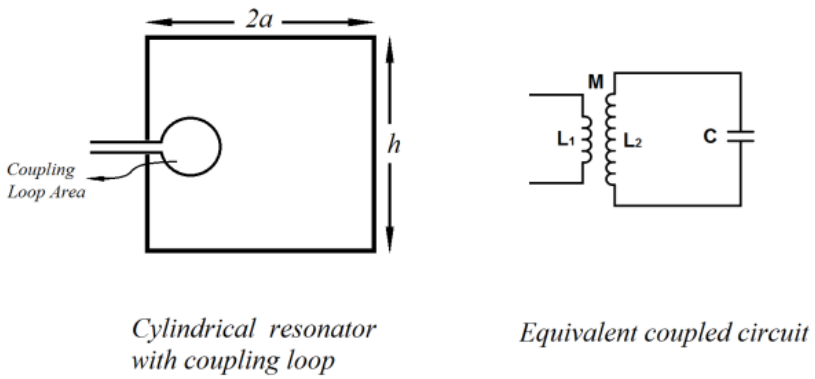

Figure 13. Coupling loop [16]

In order to maximize coupling, the coupling loop must be placed on a location inside the cavity where the magnetic flux density is maximum or it must be provided that the loop area is in the most favorable position for enclosing much more magnetic flux. The magnitude of coupling can be readily changed by simply rotating the loop; the coupling reduces to zero when the plane of the loop is parallel to the magnetic flux.

The coupling probe functions as like an antenna inside the cavity. Excitation of a cavity resonator by means of a coupling probe is shown in Figure 14. It is the equivalent of a short antenna which provides electric or capacitive coupling to the field inside the cavity. Probe coupling is useful only in providing coupling to modes in which the electric field terminates on the surface of the cavity in the vicinity of the coupling device. The coupling probe must be located on a place inside the cavity where the electric field of the desired excitation mode is maximal. The coupling probe produces an electric field component in the same direction as the electric field of the desired mode of oscillation in the resonator. In this circumstance the voltage applied to the probe will excite oscillations in the cavity resonator and conversely the oscillations in the cavity resonator will create a voltage on the probe.

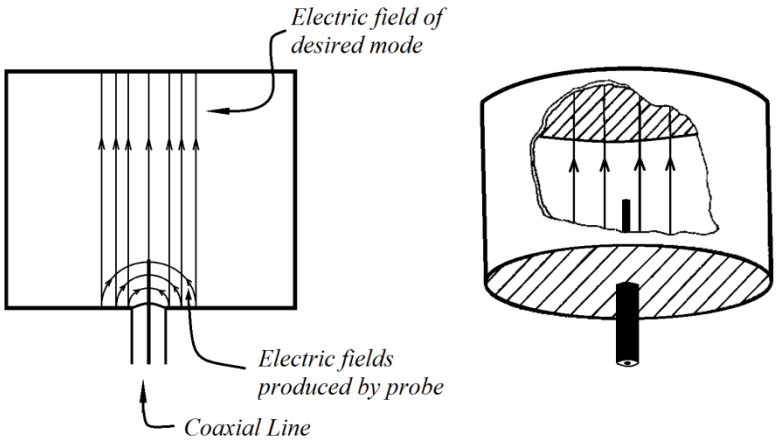

Figure 14. Coupling probe [16, 21]

Waveguide coupling or slot coupling is accomplished by arranging so that the waves entering the cavity from the waveguide or slot produce a field within the cavity that corresponds to the desired mode of oscillation in the cavity resonator (Figure 15). Coupling slots or coupling holes are designed is the natural coupling mechanism. The electromagnetic fields, either the magnetic field or the electric field penetrate the aperture and couple to cavity resonator. The location, position and the shape of the slot determines the resonance mode and the magnitude of coupling [15].

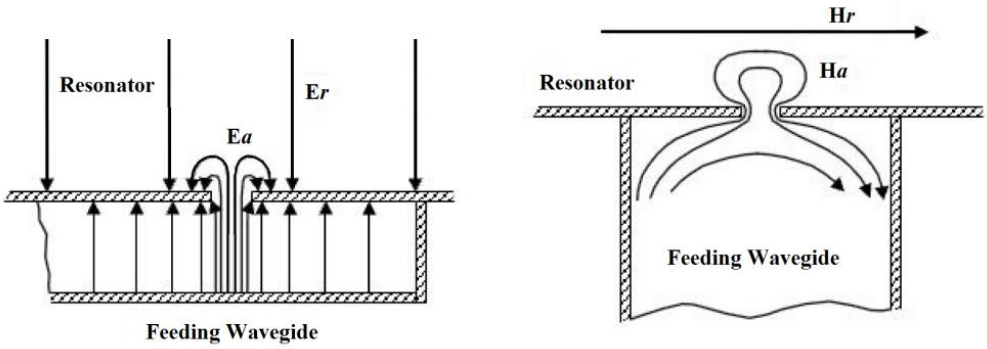

Figure 15. Slot Coupling of the cavity resonator [22]

2.2.8 Cylindrical Cavity

Cylindrical cavity can be constructed from circular waveguide shorted at both ends. The basic theory of the cylindrical cavity resonator is similar to circular waveguide. The geometry of a cylindrical cavity resonator is given in Figure 16 below [22].

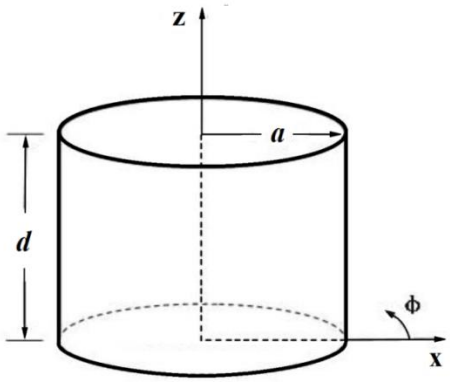

Figure 16. Cylindrical cavity resonator

2.2.8.1 Resonant frequency of Cylindrical Cavity

The resonant frequency of the cylindrical cavity resonator has the same properties with cylindrical waveguide. The dominate modes of the cylindrical cavities are TE_{111} and TM_{010}. The resonant frequency depends on the dimension of the cavity and the filling materials. Equations below give the resonant frequency of the cylindrical cavity [23].

$$(f_c)_{mnp}^{TM^z} = \frac{1}{2\pi\sqrt{\mu\epsilon}} \sqrt{\left(\frac{x_{mn}}{a}\right)^2 + \left(\frac{p\pi}{d}\right)^2} \qquad (2.17)$$

m= 0,1,2..
n= 1,2,3..
p= 0,2,3..

$$(\boldsymbol{f_c})_{mnp}^{TE^z} = \frac{1}{2\pi\sqrt{\mu\epsilon}}\sqrt{\left(\frac{x'_{mn}}{a}\right)^2 + \left(\frac{p\pi}{d}\right)^2} \quad (2.18)$$

m= 0,1,2..
n= 1,2,3..
p= 1,2,3..

where $(f_c)_{mnp}^{TM^z}$ is the resonant frequency for the TM_{mnp} mode and $(f_c)_{mnp}^{TE^z}$ is the resonant frequency for the TE_{mnp} mode. x_{mn} is the nth zero of the mth order Bessel function of the first kind and x'_{mn} is the nth zero of the derivative of the mth order Bessel function of the first kind. a is the radius and d is the height of the cylindrical cavity.

Table 2 Same $\boldsymbol{x_{mn}}$ and $\boldsymbol{x'_{mn}}$ values

$\boldsymbol{x_{mn}}$	**Value**	$\boldsymbol{x'_{mn}}$	**Value**
x_{01}	2.4049	x'_{01}	3.8318
x_{11}	3.8318	x'_{11}	1.8412
x_{21}	5.1357	x'_{21}	3.0542
x_{12}	7.0156	x'_{12}	5.3315
x_{22}	8.4173	x'_{22}	6.7062

2.2.8.2 TM_{010} Mode of Cylindrical Cavity

The TM_{010} mode is the dominant mode for the cylindrical cavity, with $\boldsymbol{x_{mn}}$= 2.4049. Figure 17 shows that the electric and magnetic field form of the TM_{010} mode inside the cylindrical cavity resonator. Within the cavity the magnetic field is parallel to the cavity bottom and perpendicular to the cylindrical axis and the electric field. The electric field is parallel to the cylindrical axis.

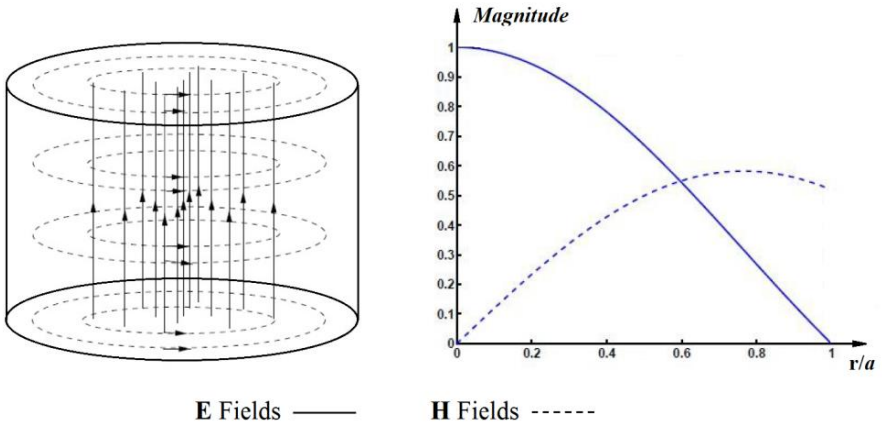

Figure 17. The electric and magnetic fields inside a cylindrical cavity [22]

The graph in Figure 17 shows the relationship between the fields, the dashed line is the magnetic fields and the solid line is the electric fields. The magnetic field strength is increasing from the center to the outer boundary, and the electric field is inversely.

2.2.8.3 Quality Factor of Cylindrical Cavity

Q factor is an important parameter for estimating the quality of cavity resonators. The Large Q-value indicates the high accuracy and the narrow bandwidth for the cavity. The unloaded Q factor (Q_0) is the value for the cavity resonator with no connection of any circuit. Q_0 is related to the conductivity of the cavity material as well as the filling materials within the cavity as follows.

$$Q_0 = \left(\frac{1}{Q_c} + \frac{1}{Q_d}\right)^{-1} \tag{2.19}$$

where Q_c is the Q value due to the conducting walls, Q_d is the Q value due to the filled material.

For an air filled cylindrical cavity the unloaded Q factor for the TM_{010} mode is

$$Q_0 = Q_c \frac{2V}{S\sqrt{\frac{2}{\omega\mu\sigma}}} \tag{2.20}$$

where V is the cavity volume, S is the internal surface area of the cavity, σ is the conductivity of the walls.

When the cavity resonator is connected to an external circuit which has a Q factor Q_e, the external circuit will have the effect of decreasing the overall Q value of the system. The unloaded Q factor (Q_0), the external Q factor (Q_e) and the loaded Q factor (Q_L) are given below as

$$\frac{1}{Q_L} = \frac{1}{Q_0} + \frac{1}{Q_e} \tag{2.21}$$

$$Q_0 = \frac{R}{\omega_0 L} \tag{2.22}$$

$$Q_e = \frac{R_L}{\omega_0 L_L} \tag{2.23}$$

2.2.8.4 The Equivalent Circuit of Cylindrical Cavity

The cylindrical cavity resonator can be equivalently regarded as a parallel RLC resonant circuit illustrated in Figure 18 [20].

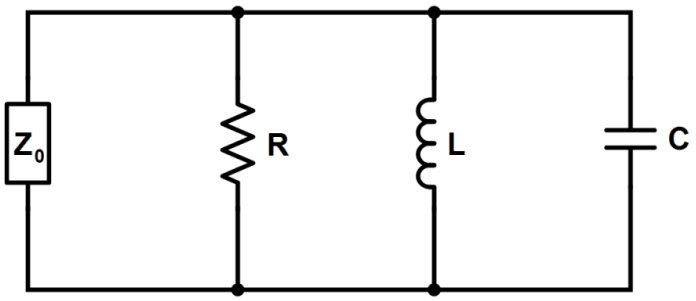

Figure 18. The equivalent circuit of a cylindrical cavity

The input impedance of the resonator is represented as,

$$Z_{in} = (\frac{1}{R} + \frac{1}{j\omega L} + j\omega C)^{-1} \tag{2.24}$$

Making some algebra and manipulation the input impedance can be written as

$$Z_{in} = \frac{R}{1 + jQ_0 2\Delta} \tag{2.25}$$

Where

$$\Delta = \frac{\omega - \omega_0}{\omega_0} \tag{2.26}$$

$$Q_0 = \frac{R}{\omega_0 L} \tag{2.27}$$

The coupling factor for a Parallel Resonant circuit is given as

$$g = \frac{R}{Z_0} \tag{2.28}$$

$g < 1$: Under coupled resonator

$g = 1$: Critically coupled resonator

$g > 1$: Over coupled resonator

The input impedance of the parallel resonant circuit can be written in terms of g is as follows

$$Z_{in} = \frac{gZ_0}{1 + jQ_0 2\Delta} \tag{2.29}$$

The reflection coefficient of the circuit can be written as follows

$$\Gamma = \frac{Z_{in} - Z_0}{Z_{in} + Z_0} \tag{2.30}$$

$$\Gamma = \frac{g - 1 - jQ_0 2\Delta}{g + 1 + jQ_0 2\Delta} \tag{2.31}$$

At resonance, $\Delta = 0$, so the imaginery part of the reflection coefficient is zero and the it is purely real as follows

$$\Gamma_{real} = \frac{g - 1}{g + 1} \tag{2.32}$$

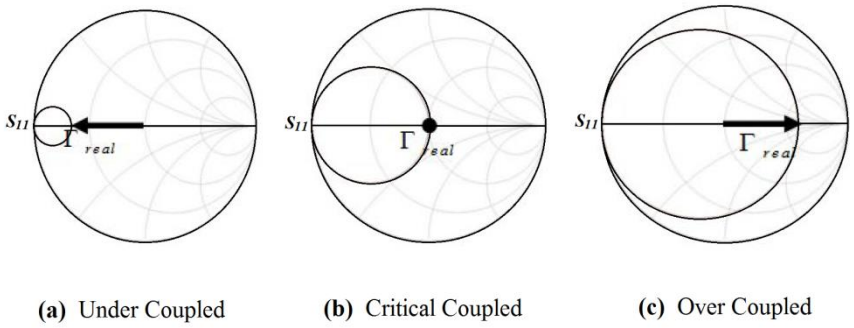

(a) Under Coupled **(b)** Critical Coupled **(c)** Over Coupled

Figure 19. Smith Chart representation of coupling to a parallel RLC circuit [22]

The unloaded and the loaded Q factors can be written in terms of g as follows

$$Q_0 = gQ_e \tag{2.33}$$

$$Q_L = \frac{Q_0}{1 + g} \tag{2.34}$$

The loaded Q factor can be obtained from the graph of reflection coefficient with the following expression

$$Q_L = \frac{f_0}{\Delta f} \tag{2.35}$$

where f_0 is the resonant frequency of the resonator circuit and Δf is the half power bandwidth.

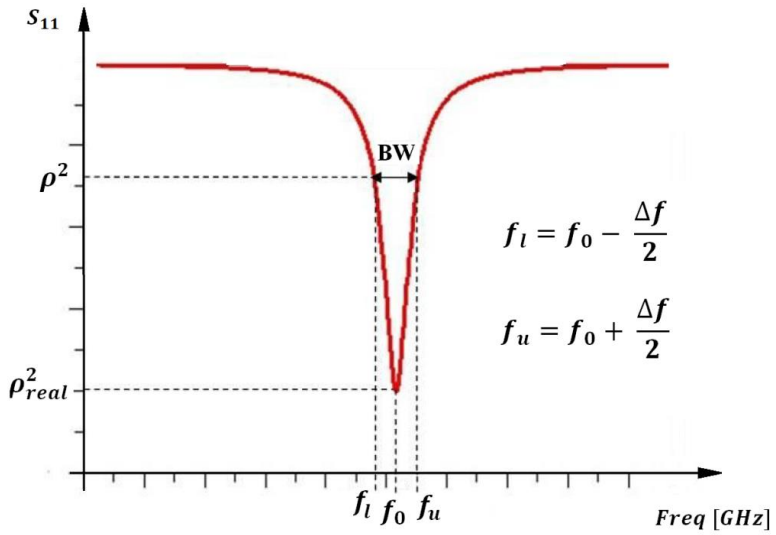

Figure 20. Q calculation from the reflection coefficient curve [22]

2.2.9 Reentrant, Evanescent Mode and Coaxial Cavities

2.2.9.1 Reentrant Cavities

Reentrant cavity is one in which metallic boundaries extend into the interior of the cavity. Introducing some protrusions and bulges to a cylindrical cavity it can be obtained cylindrical reentrant cavity. Some reentrant cavity types are illustrated in Figure 21.

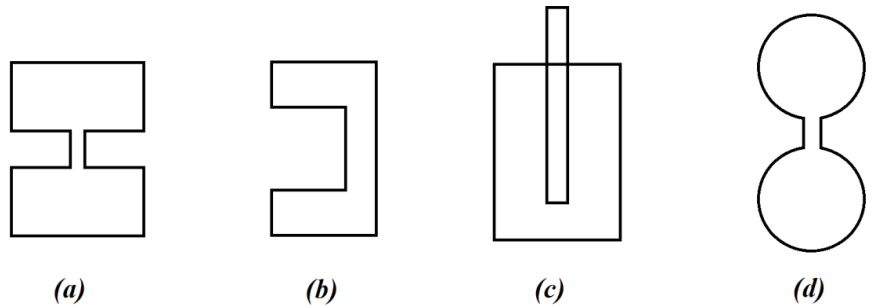

Figure 21. Some reentrant type cavities [24]

2.2.9.2 Evanescent Mode Cavities

Cavities are often bulky and heavy and it is highly desirable to reduce the size and weight. Since the resonant frequency of a cavity is inverse proportional to its dimensions, there will be a limit to the size for a given frequency of interest. By introducing some structures or reactance inside the cavity, creating a discontinuity or changing the shape of the cavity the resonant frequency can be reduced. Such structural transformations can change the resonant frequency to a lower value than the original one. Cavities that operate using this technique are referred to as evanescent-mode cavity. In other words an evanescent-mode cavity is one that whose resonance frequency is somehow lower than its original fundamental mode frequency. By evanescently loading a cavity, the frequency can be brought down by an order of magnitude, while still maintaining a high-Q [25].

2.2.9.3 Coaxial Cavity Resonator

A coaxial cavity resonator is a cylindrical cavity structure resembling a finite length coaxial transmission line which is closed at both end and it is shorted at one end as illustrated in the Figure 22.

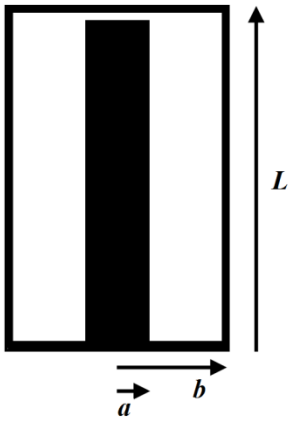

Figure 22. Coaxial Cavity Structure

One end of the coaxial transmission line is shorted but there is a small gap at the other end. This gap creates a capacitance between inner and outer conductor as like a parallel plate capacitor.

At sufficiently high frequencies, a short section of a transmission line with completely reflecting terminations acts as an inductor if it is less than quarter wavelength long. For a short circuited transmission line of fixed length, the impedance is given as

$$Z_s = jZ_0 \tan \beta l \tag{2.36}$$

This formula shows how the reflecting impedance changes with the frequency.

For a short-circuited line, impedance is zero for the zero frequency, but as the frequency increase it behaves as an increasing inductive reactance. However, as the frequency is raised higher, the tangent function becomes negative, this means that Z_s is capacitive and its reactance decreases.

At the point where Z_s passes from plus infinity to minus infinity the structure behaves like a parallel resonant circuit, i.e., anti-resonance. When the frequency reaches the value at which the length of the line is equal to the half wavelength, Z_s becomes zero. At this point the line behaves like a series resonant circuit. Just beyond this frequency Z_s becomes a positive reactance and so on, this is illustrated in Figure 23.

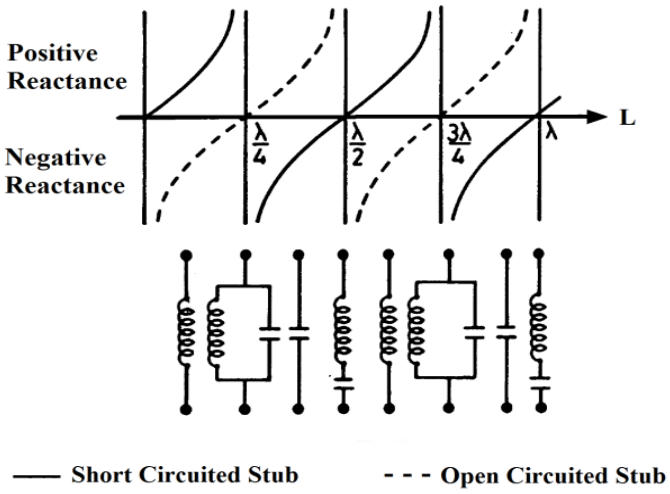

Figure 23. Variation of input impedance with frequency for a short circuited coaxial line [26].

The above theory can be applied to a coaxial cavity in which case the inductance created by a line length of less than $\lambda/4$ can resonate with either a lumped capacitance or a capacitance due to the gap between the inner and the outer conductor.

In order to have such a coaxial resonant cavity of high performance, many points must be taken into account. To decrease the losses of the electromagnetic wave inside the cavity the inner surface must be made as smooth as possible. Also the inner and outer conductor dimensions have to be chosen to give high quality factor and low losses. A good short circuit between the inner and outer conductors is very important.

The loaded quality factor must be high and transmission loss low to provide a sharp resonance at the frequency of the signal transmitted through the cavity. This may be achieved by careful tuning of the inner post and further improved by loose coupling if the unloaded quality factor is high [26].

In coaxial cavity, the central post constitute a capacitive structure together with the upside wall of the cavity. The E-field inside the cavity is concentrated inside the capacitive gap between the top of the post and the cavity wall. On changing the gap width, the frequency changes according to the equation below

$$f_0 = \frac{1}{2\pi\sqrt{L(C_c + C_p + C_f)}} \tag{2.37}$$

where L and C_c are the inductance and the capacitance of the cavity, C_p is the capacitance between the post and the roof of the cavity, C_f is the capacitance due to the fringing fields near the post edges.

These parameters can be calculated by using the following expressions.

$$C_p = \frac{\in_0 \pi a^2}{d} \tag{2.38}$$

$$C_c \cong \frac{2h\pi \in_0}{\ln\frac{b}{a}} \tag{2.39}$$

$$C_f \cong \kappa_1 a \in_0 \ln\frac{h}{d} \tag{2.40}$$

$$L \cong \frac{\mu h}{2\pi}\ln\frac{b}{a} \tag{2.41}$$

where κ_1 is an empirically fitted constant which is sensitive to *a/b* ratio.

For $a/b \leq 0.3$, this constant has been found to be 2.78 [27,28].

2.2.9.3.1 Quality Factor of Coaxial Cavity Resonator

In general, the electromagnetic energy in a cavity at resonance is stored in the electric and magnetic fields. The stored energy in each field will vary during the cycle, but their summation is always equal to the total energy stored in the cavity. If the loaded quality factor of the cavity is high, the rate of the stored energy to dissipated energy is high, and the average magnetic field density is equal to the average electric field density over a cycle.

At some instants in the cycle the energy will be entirely in the magnetic field, and at other instants the energy will be entirely in the electric field. With this fact, by finding the peak magnetic or electric field energy, the total stored energy can be calculated.

The unloaded quality factor of a cylindrical coaxial cavity can be analytically approximated using the following equation [27,29]

$$\frac{1}{Q_0} \cong \frac{R_s}{2\pi\mu f_0}\left(\frac{\left(\frac{1}{a}+\frac{1}{b}\right)}{\ln\frac{b}{a}}+\frac{2}{h}\right) \tag{2.42}$$

where a is post radius, b is cavity radius, h is the height of the post and R_s is the sheet resistance of the cavity sidewalls.

As it is seen on the expression above the unloaded Q of a coaxial cavity mainly depends on the cavity dimensions and the sheet resistance. Increasing the radius and the height of the cavity increases the quality factor because this provides more volume for energy storage inside the cavity as long as *b* and *h* are much smaller than the resonant wavelength. It can be mathematically validated from the above formula that when the ratio of the post radius and the cavity radius a/b is 0.28 then the quality factor is maximized.

Sheet resistance R_s is the resistance offered by the cavity walls to the RF currents and it can be approximated as follows

$$R_s = \frac{\rho}{t} \cong \frac{1}{\sigma\delta} \tag{2.43}$$

$$\delta = \frac{1}{\sqrt{\pi\mu f_0 \sigma}} \tag{2.44}$$

where ρ is the resistivity and σ is the conductivity of the cavity material [27]. The cavity thickness t can be replaced by the skin depth δ, provided $t \gg \delta$. So, materials having higher conductivity provide higher Q for cavity resonators.

2.2.9.3.2 *Shunt Resistance of Coaxial Cavity Resonator*

In a cavity, the losses due to the finite conductance of the wall is represented with an equivalent shunt resistance or an equivalent series resistance. These resistances are directly related with the cavity material, physical structure, dimensions and the operation frequency. The shunt resistance of the coaxial cavity can be analytically approximated by using the following expression [20].

$$R_{sh} \cong \frac{2\pi\delta\sigma\ \omega^2 L^2}{\left(\frac{p_1}{a} + \frac{h - p_1}{a_1} + \frac{h_2}{b} + 2\ln\frac{b}{a}\right)} \tag{2.45}$$

where δ is the skin depth, σ is the conductivity of the cavity material, ω is the angular frequency and L is the inductance of the cavity.

The series resistance of the coaxial cavity can be approximated as the following expression.

$$R_{se} \cong \frac{\omega^2 L^2}{R_{sh}} \tag{2.46}$$

2.2.9.3.3 *Cylindrical Cavity to Coaxial cavity*

The coaxial cavity is defined here as a length of short circuited transmission line terminated with a capacitive reactance formed by the gap between the inner conductor and the end plate. As seen in Figure 24 below the coaxial cavity is a special form of the cylindrical cavity.

Figure 24 shows the transition of a perfect cylindrical cavity to a perfect coaxial cavity with the illustration of possible electric fields of the lowest mode during transition. The perfect cylindrical cavity mode TM_{010} becomes the usual capacitively loaded coaxial mode TM_{00p} for a small gap between reentrant portions. When the reentrant portion (i.e., the center conductor) is started to be inserted into the cylindrical cavity, the resonant frequency decreases slowly at first and then rapidly until zero frequency is approached asymptotically for full insertion (i.e., center

conductor shorted to the end plate). Thus, low frequencies may be obtained by making the gap sufficiently small.

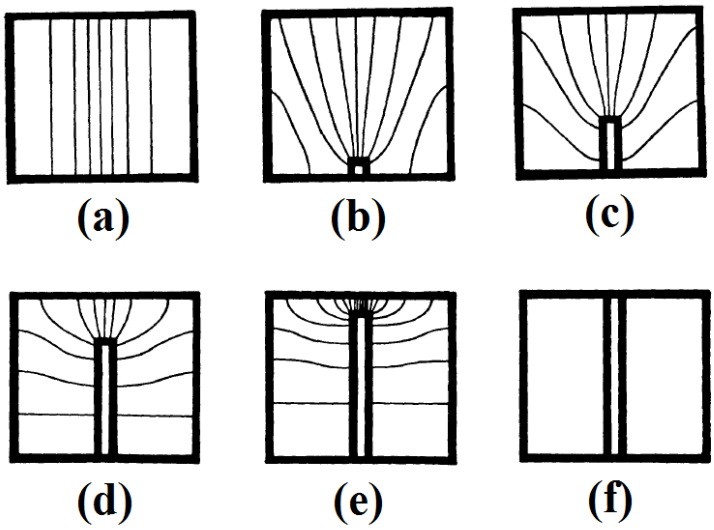

Figure 24. Transition from cylindrical cavity to coaxial cavity [30]

In a coaxial cavity with a small gap, the electric field is concentrated between the end of the inner conductor and the end plate and the magnetic field is concentrated near the opposite end of the resonator, a typical quasi-stationary electromagnetic system [30].

2.2.9.3.4 *Fringing Field Effect*

In a coaxial cavity, not only the gap capacitance (C_p) is considered, but the capacitance due to fringing field (C_f) should also be taken into account. Since the fields extending slightly beyond the end of the post (i.e., the fringing fields) create capacitive reactance which consequently affects the behavior of the cavity.

The effect of additional inductance and capacitance between the tip of the inner conductor and the adjacent cavity wall should also be considered if a more accurate electrical circuit equivalent of the cavity is to be established.

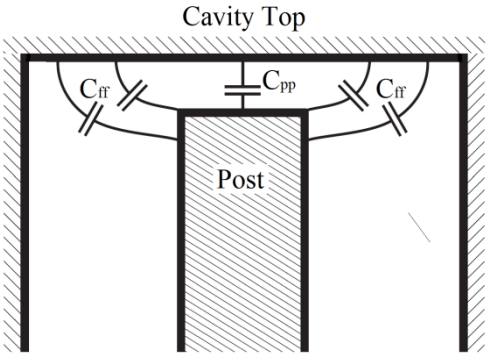

Figure 25. Fringing fields inside the coaxial cavity

2.2.10 Cavity Perturbation Technique

When a resonant cavity is perturbed, i.e., when an object is introduced into the cavity or when a general shape of the cavity is changed, the electromagnetic fields inside the cavity change accordingly. The underlying assumption of cavity perturbation theory is that the electromagnetic fields inside the cavity after the change differ by a very small amount from the fields before the change. Then Maxwell's equations for the original and perturbed cavities can be used to derive expressions for resulting resonant frequency shifts.

When a general shape of a resonant cavity is changed, a corresponding change in resonant frequency can be approximated as

$$\frac{\omega - \omega_0}{\omega_0} \cong \frac{\iiint_{\Delta V}(\mu|H_0|^2 - \epsilon|E_0|^2)dv}{\iiint_V(\mu|H_0|^2 + \epsilon|E_0|^2)dv} \tag{2.47}$$

The expression above for change in resonant frequency can additionally be written in terms of time-average stored energies as follows

$$\frac{\omega - \omega_0}{\omega_0} \cong \frac{\Delta W_m - \Delta W_e}{W_m - W_e} \tag{2.48}$$

where ΔW_m and ΔW_e represent time-average magnetic and electric energies contained in ΔV.

This expression can also be written in terms of energy densities as follows

$$\frac{\omega - \omega_0}{\omega_0} \cong \frac{(\bar{w}_m - \bar{w}_e)\Delta V}{W} \tag{2.49}$$

It is clear from the above equation that, an inward perturbation will raise the resonant frequency if it is made at a point of large H (high $\bar{w}_m$), and will lower the resonant frequency if it is made at a point of large E (high $\bar{w}_e$). The opposite behavior results for an outward perturbation. It is also evident that the greatest changes in resonant frequency will occur when the perturbation is at a position of maximum E and zero H, or vice versa [18].

2.3 Antennas

2.3.1 Monopole Antenna

The primary interest for this work is monopole antenna. A monopole antenna is half of a dipole antenna placed on top of a ground plane, as illustrated in Figure 26.

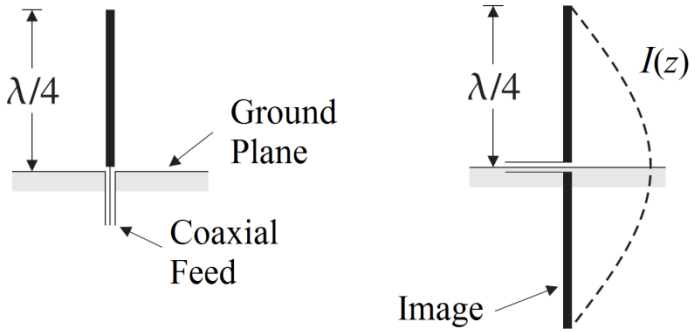

Figure 26. Monopole antenna and an equivalent dipole antenna [31]

Assuming the plane is infinite and perfectly conducting, the monopole antenna will be equivalent to a dipole whose lower half is the image of the upper half.

Thus, the radiation pattern (in the upper hemisphere) will be identical to that of a dipole [31]. Because the fields are radiated only in the upper hemisphere, the total radiated power will be half that of a dipole, and hence the corresponding radiation resistance will also be halved:

$$P_{monopole} = \frac{1}{2} P_{dipole} \tag{2.50}$$

$$R_{monopole} = \frac{1}{2} R_{dipole} \tag{2.51}$$

In the same manner, the directivity doubles because the isotropic radiation intensity is a half of its dipole value:

$$D_{monopole} = 2D_{dipole} \tag{2.52}$$

2.3.2 Reflection from antennas

In general, a reflected wave from an antenna is composed of two parts. One is due to the reflection from the conducting structure of the antenna, i.e., structural mode and the other is due to the reflection from the mismatch between the antenna and the circuit behind the antenna, i.e., antenna mode [32].

So the reflected power from a receiving antenna system can be written as the sum of two terms, one is the scattered power due to the structural mode and the other is due to the antenna mode. This phenomenon is illustrated in Figure 27. Consequently, it is not correct to assume that a matched receiving antenna scatters as much as it absorbs. In general, the reflected power from a receiving antenna may be greater, equal to, or lower than the absorbed power.

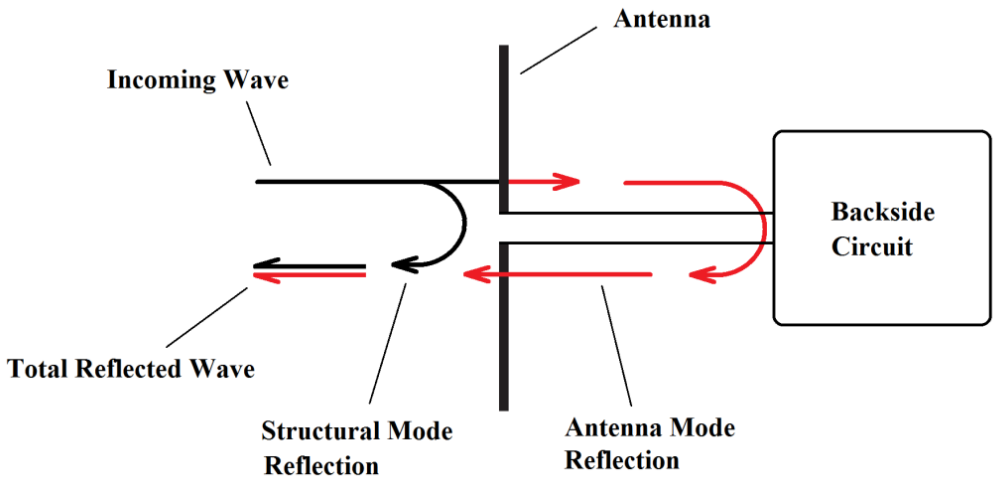

Figure 27. Reflection from antenna

The reflected power due to the antenna mode depends on the load impedance of the antenna, but the power reflected due to structural mode is not affected by load impedance. Thus the antenna mode reflection can be used for communication or a modulation by changing properly [33].

2.3.3 Antennas as Scatterers

Antennas have several important properties such as pattern, gain, and impedance which are both transmitting and receiving antennas. But a receiving antenna has an additional important property, scattering. In general, the scattering is considered in absorption efficiency issues. Absorption efficiency is the ratio between the absorbed power and the received power that is the sum of the absorbed and the scattered powers. It is generally believed that absorption efficiency is less than or equal to 50%, but it has been shown that this is not true. The scattering from an antenna have two mode : one that is due to mismatch behind the antenna, called the antenna scattering or re-radiation since it has the same pattern as the transmitting antenna; and one that is what is left when the antenna is matched, called the residual or structural scattering [34].

Figure 28 represents a transmitting antenna (a) and a scattering antenna (b) which is loaded with Z_L. The voltage across terminals of (a) due to the currents on the scattering antenna is called scattered voltage and given as

$$V_s = I_0 \left(\Delta Z_0 - \frac{Z_{ab} Z_{ba}}{Z_b - Z_L} \right) \tag{2.53}$$

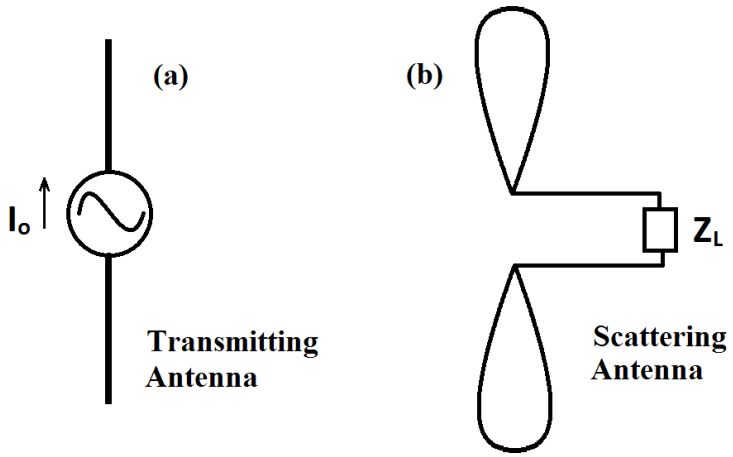

Figure 28. Scattering from a loaded antenna [34]

where I_0 is the input current at antenna (a), ΔZ_0 is the change in the input impedance at (a) because of the existence of the unloaded scattering antenna, Z_{ab} and Z_{ba} are the mutual impedances between the antennas, Z_b is the input impedance of the scattering antenna and Z_L is the load impedance of the scattering antenna.

In the case of far zone scattering, relating to the above equation, the Radar Cross Section σ is given as

$$\sigma = \frac{\lambda^2}{\pi} \left| \Delta Z_0{}' - \frac{Z_{ab}{}' Z_{ba}{}'}{Z_b - Z_L} \right|^2 \tag{2.54}$$

where λ is wavelength, and the primed Z's are obtained from the unprimed Z's by a limiting procedure.

The gain and the effective area of the scattering antenna are given as

$$G = \frac{\left|Z_{ba}{}'\right|^2}{R_b} \tag{2.55}$$

$$A = \frac{\lambda^2}{4\pi}\frac{\left|Z_{ab}{}'\right|^2}{R_b} \tag{2.56}$$

where G is the transmitting gain of the scattering antenna, A is the effective area of the scattering antenna with matched load, and R_b is the radiation resistance ($\mathcal{R}e\{Z_b\}$) of scattering antenna. So it is seen that, all of the factors except for λ in the σ expression above are related to common antenna parameters. If the first term of the RCS expression above is small compared to the second term, i.e., if the scattered field of the unloaded antenna is small compared to that of the loaded antenna, then the RCS expression can be written as

$$\sigma \cong \frac{4AG{R_b}^2}{|Z_b + Z_L|^2} \tag{2.57}$$

As it is seen in the expression above, the incoming wave is received with an effective area A and then reradiating some part of the energy with a gain G. Practically, this approximation usually applies for small antennas, like dipoles and monopoles, which are less reflecting body.

If all the media involving are reciprocal then the effective area A and the gain G have a relation as follows

$$A = \frac{\lambda^2}{4\pi}G \tag{2.58}$$

So the RCS expression can be written as

$$\sigma \cong \frac{\lambda^2}{\pi}\left|\frac{GR_b}{Z_b + Z_L}\right|^2 \tag{2.59}$$

In the case of bi-static scattering, i.e., the transmitter and the receiver are at different places, formulas similar to Eqns. (2.56) to (2.59) can also be written. The RCS expression is as follows

$$\sigma = \frac{\lambda^2}{\pi} \left| \Delta Z_0{}' - \frac{Z_{tb}{}' Z_{br}{}'}{Z_b - Z_L} \right|^2 \tag{2.60}$$

where $Z_{tb}{}'$ and $Z_{br}{}'$ are the mutual impedances between scattering antenna and transmitting and receiving antennas respectively.

In Eqns. (2.57) to (2.59), G becomes the gain of the scattering antenna in the direction of the receiver, and A the effective area of the scattering antenna in the direction of the transmitter. In bi-static case even for the reciprocal media Eqns. (2.59) and (2.60) are not valid. In the nonreciprocal case, there is in general a G and an A associated with each direction, for which a special type of reciprocity relationship applies [34].

2.4 Backscatter Wave Technique

When an electromagnetic wave is reflected or scattered from a target, some parameters of the scattered or reflected wave is effected from the properties of the target. The properties of the target affect the way in which the signal is reflected back. Antenna properties such as cross sectional area, gain, impedance etc. all have an effect on how the target reflects the incident wave. Thus the scattered wave properties can be accordingly changed by changing those properties.

Backscattering is a communication technology used at UHF or microwave frequencies. It is the process of collecting an RF signal (energy), processing the signal with the data it will carry, and reflecting it back to where it came from. It works like a reader that sends the electromagnetic wave to a target at a specific frequency; the target receives the wave, encodes the information into the wave, and scatters it back to the reader [35].

2.4.1 History of Passive Backscatter Communication

Backscatter communication can be realized in several ways. The key point is that a modulation of reflected or scattered wave must be provided by means of some parameters. For example, modulation can be provided by a Doppler shift, so that the receiver detects the motion or vibration of the target or by a deliberately designed target that modulates the reflections. This is achieved by electronics attached to an antenna called load modulation. During the Second World War, there was early interest in modulation sidebands scattered from both radar targets and loaded antennas. An important issue to be handled was the identification of friend or foe (IFF), i.e., distinguishing between friendly and enemy aircraft on radar.

Wattson-Watt in Britain tried load modulation with a dipole antenna stretched across the wings of a fighter aircraft in the late 1930s. By mechanically or electronically shorting and opening the antenna, pilots would send their codes by reflecting signals to identify themselves. The received signals were so weak, but it was an active transponder system developed to transmit IFF codes. Later on, more sensitive and successful systems including mechanical vibrations and rotating propellers are developed.

The first public paper about the backscatter communication was published by Harry Stockman in 1948 [35]. Presumably he did not know about Theremin's earlier work. Stockman discussed different approaches to load modulation and mechanical modulation by translating or rotating reflectors. Load modulation also used for field measurements, starting with J.H. Richmond's paper published in 1955 [37].

The first commercial applications of backscatter communication that are similar to RFID were patented in the mid-1970s. These were targeted at inventory management, making them true precursors to modern RFID [36].

2.4.2 Modulated Backscatter Technique

A backscatter communication system is a wireless communication that takes place between a transmitter/receiver and a target.

The transmitter/receiver transmits RF signals to the target which resends the signals by modulating the electromagnetic waves scattered from it. The amplitude and phase of the backscattered waves can be varied by creating an impedance mismatch between the antenna and the back structure of the target.

A backscattering target can be constructed by integrating a transducer that changes its impedance as a function of an input physical parameter. The impedance of the transducer changes accordingly with the physical parameter and this causes a variation of amplitude and phase in the backscattered signal. Thus changing physical parameter modulates the backscattered signal. This modulation can be detected and demodulated at the receiver [37,38].

2.5 Amplitude Modulation

In Amplitude Modulation, the information signal varies the amplitude of the carrier wave. The instantaneous value of the carrier amplitude changes in accordance with the modulating signal. Figure 29 below shows a single frequency sine wave data signal modulating a higher frequency carrier. The carrier frequency remains constant during the modulation process, but its amplitude varies in accordance with the modulating signal. An increase in the amplitude of the modulating signal causes the amplitude of the carrier to increase. Both the positive and the negative peaks of the carrier wave vary with the modulating signal. An increase or a decrease in the amplitude of the modulating signal causes a corresponding increase or decrease in both the positive and the negative peaks of the carrier amplitude.

The sine wave carrier can be expressed with the simple expression

$$v_c = V_c \sin 2\pi f_c t \tag{2.61}$$

In this expression, v_c represents the instantaneous value of the carrier wave voltage at a specific time in the cycle.

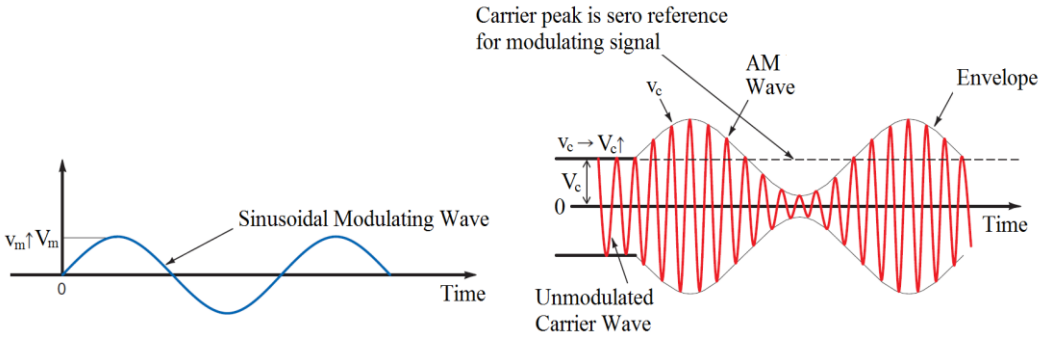

(a) The modulating or information signal **(b)** The modulating carrier

Figure 29. Amplitude Modulation [39]

A sine wave modulating signal can be expressed with a similar expression

$$v_m = V_m \cos 2\pi f_m t \tag{2.62}$$

In amplitude modulation, it is particularly important that the peak value of the modulating signal be less than the peak value of the carrier, i.e., $V_m < V_c$.

The instantaneous value of either the top or the bottom voltage envelope can be computed by using the equation

$$v_1 = V_c + v_m = V_c + V_m \cos 2\pi f_m t \tag{2.63}$$

This expresses the fact that the instantaneous value of the modulating signal algebraically adds to the peak value of the carrier. Thus we can write the instantaneous value of the complete modulated wave v_2 by substituting v_1 for the peak value of carrier voltage V_c as follows:

$$v_2 = v_1 \sin 2\pi f_c t \tag{2.64}$$

Now substituting the previously derived expression for and expanding, we get the following:

$$v_2 = (V_c + V_m \cos 2\pi f_m t) \sin 2\pi f_c t$$

$$= V_c \sin 2\pi f_c t + (V_m \cos 2\pi f_m t\ ) \sin 2\pi f_c t$$

$$= V_c \sin 2\pi f_c t + \frac{V_m}{2} \sin 2\pi (f_c + f_m) t + \frac{V_m}{2} \sin 2\pi (f_c - f_m) t \qquad (2.65)$$

Thus, as it is seen in the expression above, the modulated signal has three components: the carrier wave and two pure sine waves (known as sidebands) with frequencies slightly above and below the carrier frequency f_c [39].

CHAPTER 3

THEORETICAL ANALYSIS OF THE STRUCTURE AND DESIGN OF THE PROTOTYPES

In this chapter the theoretical analysis and design works are presented. The physical and functional details of the device are studied. By creating an HFSS model of the cavity structure the eigenmode analysis and parametric analysis are realized.

3.1 Analysis of The Theremin's Device

3.1.1 Physical Structure

All the descriptions about the device from all kind of sources define physically the same structure for the device. That is shown in the Figure 30.

According to the existing descriptions, drawings and pictures of the device; it composed of a cylindrical box and an aerial protruding from the sidewall. The cylindrical body of the device is copper and interior is silver-plated. Inside the body a mushroom shaped central post is attached to the backside. Front side of the cylinder is covered with a thin metallic diaphragm. The post plate and the diaphragm together constitute a capacitive gap. The back plate of the cylinder is threaded so that the post can be positioned relative to the diaphragm to adjust the gap length. The antenna extending through the side of the cylinder has a disc shaped head terminates near the central post but does not touch it [10-12,40].

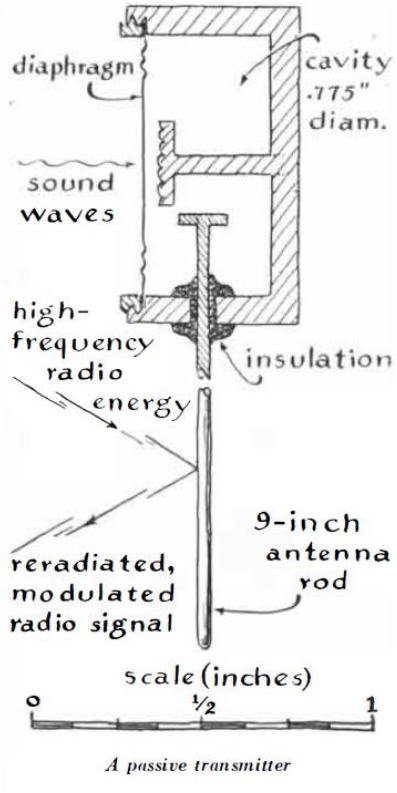

Figure 30. A Drawing of Theremin's Device [10]

3.1.2 Functional Structure

The general definition according to the references is that the device is a passive cavity transmitter. Nearly all sources say that device is a passive device, i.e., a microwave signal is directed to the device and the device receives those signals and reflects back but the reflected wave conveys the information of change in the resonance frequency. Because, one surface of the cavity is a diaphragm and the movement of the diaphragm changes the resonant frequency of the cavity. Thus the sound in the environment is transported via the reflected wave from the device.

The mushroom shaped central post and the diaphragm on top of the cavity constitutes a parallel plate capacitance and since the gap is very small this capacitance is very sensitive to the gap distance between post and diaphragm.

As it will be detailed in further sections, when the sound wave hits the diaphragm it moves and this movement changes the gap capacitances and thus the resonant frequency of the cavity. Hence the coupling and re-radiating property of the structure change accordingly for a specific frequency and this accordance creates modulation on the returning wave.
After this general explanation, in the following sections the device and its components and functions are analyzed in details.

3.2 Analysis of The Structure

3.2.1 The Antenna Analysis

The antenna of the device consists of a metal rod entering to the body of the device. The section inside the body has a disc shaped head. Considering the overall structure since it has only one arm, the antenna of the device must be a monopole antenna. And the structure of the device implies that the body of the cylindrical cavity is a finite ground plane for the monopole antenna.

There are two possibilities for the connection of the antenna to the cavity.

- First, the antenna section inside the cavity can be a mushroom shaped exciting probe for the cavity.
- Second, the disc shaped head of the antenna probe section constitutes a parallel plate capacitance together with the central post of the cavity. Thus the probe can capacitively couple the antenna to the post or cavity.

The position of the probe section of the antenna with respect to the central post affects the cavity characteristics. With tight coupling (i.e., the disc head of the antenna is close to the central post), the loss at the resonance frequency is less and the Q factor is higher. With loose coupling (i.e., the disc head of the antenna is away from the central post) the loss at the resonance frequency is more and the Q factor is lower [41].

On the assumption of quarter wave monopole antenna, we can try to estimate the functioning or resonance frequency of the antenna. In the Table 3 below, the antenna length information extracted from all existing sources are listed. In the table, the corresponding frequencies are also given.

Table 3 The antenna length of the device from the references

Assumed Antenna Length	**Corresponding Operation Frequency (λ/4)**
9” (22.86cm) [2,10,13,14]	328 MHz
8.5” (21.59cm) [8]	347.4 MHz
8” (20.32cm) [51]	369.1 MHz
18cm (from picture) [2]	416.7 MHz
20.2cm (from picture) [40]	371.3 MHz
23cm (from picture) [1]	326.1 MHz
12.6cm (from old CIA replica, 7-diameter length) [13]	595.2 MHz
14.56cm (from CIA replica, 8-diameter length) [13]	515.1 MHz

As it is seen on the above table the possible frequency values are inside the VHF-UHF range. As given in Appendix A, there are many values such as 330 MHz, 800 MHz, 1600 MHz, and 1800 MHz for the operation frequency of the device. According to the table, the only frequency value that seems reasonable among the mentioned frequency values is 330 MHz for the device. There is no evidence for other frequency values yet. For now the existing antenna length values point to the 330 MHz frequency. But the multiples of this frequency value are also possible.

3.2.2 The Cavity Analysis

It is apparent from the physical structure that Theremin’s device is an electromagnetic cavity resonator. Its outer shape is a cylinder but due to its internal structure it is not a regular cylindrical cavity. It is a reentrant type evanescent mode cavity resonator.

It is reentrant because it has a part extended into the interior of the cavity as central post and nearly reaching to the other side but does not touch it. Because of this internal structure the resonant frequency is to be lower than a true cylindrical cavity. So it is an evanescent mode cavity.

In reentrant type evanescent mode cavity class, the structures resembling the device's form are called as radial cavity, coaxial cavity or tunable cavity. As the whole structure depicts, the device looks like a coaxial cavity most.

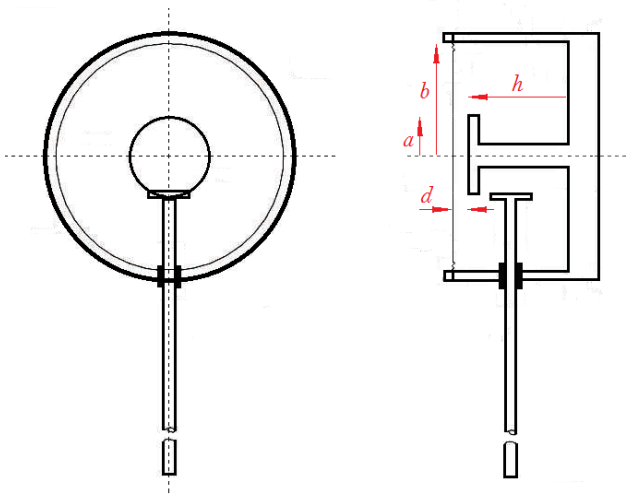

Figure 31. Device's structural drawing

The central post of the device has a mushroom shape which increases the quality of the cavity resonator. The quality factor of the cavity is directly proportional with volume since the energy stored inside the volume and inversely proportional with the internal surface since the energy is dissipated in the surface. So by thinning the central post increases the volume and decreases the surface area and thus increases the quality factor.

But the end part of the post is enlarged as a thin plate like a disc in order to increase the parallel plate capacitance. The thin form of the plate reduces the fringing fields emanating from the post edges and ending in the diaphragm and the side walls of the cavity. These fringing fields increase the undesired capacitances which diminish the effect of the gap capacitance over the resonance characteristic.

The thin plate increases the sensitivity of the resonance frequency to the gap length by reducing the unwanted capacitances.

In coaxial cavity, the fundamental resonating mode fields are the same with the TM_{010} mode in cylindrical cavities, as illustrated in Figure 17. In this mode, the electric fields are in the direction of the cylindrical axis from one circular face to other and the magnetic fields are encircling these electric fields as parallel to the side walls.

In a cylindrical cavity, from Eq. (2.17) given in the cylindrical cavity section, the resonant frequency for TM_{010} is given as

$$(\boldsymbol{f_c})_{010}^{TM^z} = \frac{1}{2\pi\sqrt{\mu\epsilon}}\left(\frac{2.4049}{a}\right) \tag{3.1}$$

From this expression the resonance frequency for the TM_{010} modes is only affected from the materials involving the structure and the diameter of the cylindrical cavity. The height of the cavity does not have an effect on the resonance frequency.

In the case of coaxial cavity the account differs such that the electric and magnetic fields inside the coaxial cavity are placed in different part of the cavity as illustrated in Figure 32.

The electric fields are strictly confined to the capacitive gap region between the post plate and the top wall or the diaphragm of the cavity, whereas the magnetic fields are in the remaining part of the cavity and encircling the central post. Because of this field distribution, the resonance frequency of the coaxial cavity depends on mostly the lumped parameters created by the structure. That is the capacitance and the inductance of the cavity.

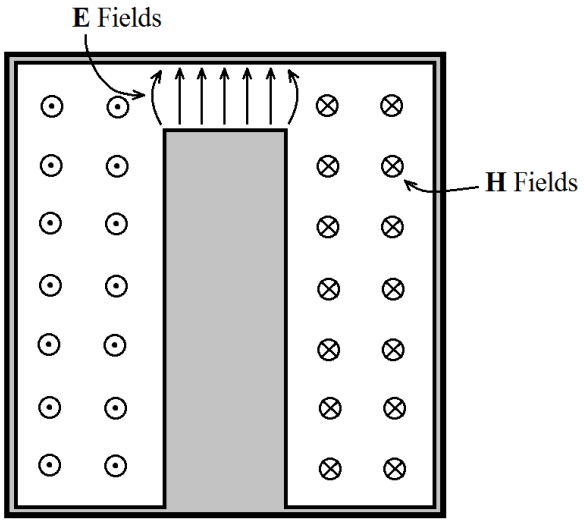

Figure 32. The field distribution of coaxial cavity

If the gap is sufficiently small, then the capacitance constituted by the post and the diaphragm dominate the overall capacitance of the cavity so being the determinant for the resonant frequency. This dominance stems from the fact that any small change in the gap has a great effect on the gap capacitance but very little effect on the other lumped characteristics.

3.2.2.1 The Analytical Calculation of the Resonance Frequency

The dimension information of the device existing in some source is listed in Table 18 in Appendix A. Some references contain many parameters of the device and some others only few. And some parameters are very different from each other. So it is reasonable to make calculations by using all alternatives in order to reach a result that can be commented and evaluated. In Table 19 in Appendix A there exist also the proportions of the dimensions from some references. So those can be used as a crosscheck to support calculations.

The parameters which will be used for calculations are given in the Table 4 below. The resonance frequency will be calculated for three alternatives.

The cavity capacitances C_c are calculated as separately for three parts as the post body portion, the post plate portion and the gap portion as illustrated in Figure 33. Since the gap length is very small according to the cavity height, the capacitance resulting from that part will be very small so it is neglected.

The analytical expression involving the lumped parameters of the cavity is given in coaxial cavity section 2.2.9.3.

Table 4 The device dimensions that will be used for calculations.

Parameter	**Reference-1 [14]**	**Reference-2 [10]**	**Reference-3 [2,13]**
Internal Radius (b)	0.98425 cm	0.98425 cm	0.98425 cm
Internal Height (h_2)	1.00 cm	0.9463 cm	0.95 cm
Post Plate Radius (a)	0.3400 cm	0,325 cm	0.3175 cm
Post Plate Thickness (p_1)	0.0585 cm	0.1162 cm	0.08735* cm
Post Height (h)	0.9815 cm	0.8467 cm	0.891 cm
Post Body Radius (a_1)	0.114 cm	0.0747 cm	0.09435* cm
Gap Length (d)	0.185 mm	0.9961mm	0.59* mm
Diaphragm Thickness (T_d)	76.2** μm	76.2** μm	76.2 μm
Antenna Plate Radius (r_{ap})	0.1750 cm	0.1826 cm	0.247 cm
Antenna Plate Thickness (H_{ap})	0.040 cm	0.0880 cm	0.064* cm
Antenna Body Radius (r_a)	0.0488 cm	0.0440 cm	0.0464* cm
Antenna Length (H_{ao})	22.86 cm	22.86 cm	22.86 cm
Antenna Probe Height (H_{apr})	0.65 cm	0.7886 cm	0.7193* cm
Cylinder Body Thickness (T_w)	0.089 cm	0.2158 cm	0.0905 * cm
Quality Factor (Q)	1000**	1000**	1000
Inductance (L)	10** nH	10** nH	10 nH
* Since there is no any value in the reference this is taken as the average of the other two ** Since there is no any value in the reference this data is taken from the other reference			

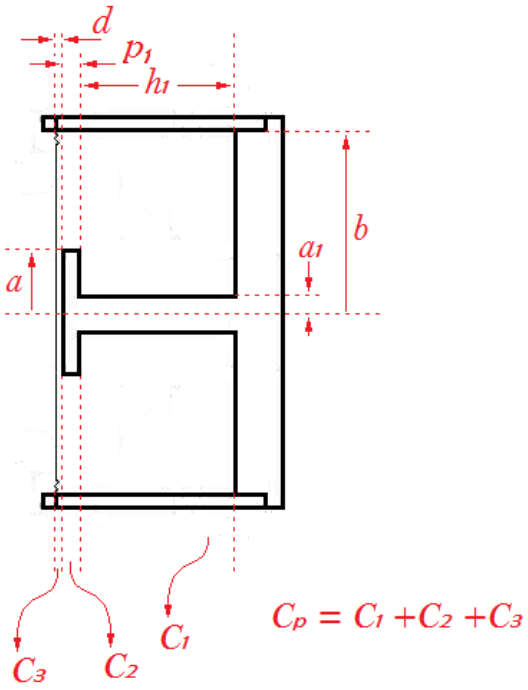

Figure 33. Capacitance calculation, the cavity is divided into three part

The cavity capacitances (i.e., capacitance due to the coaxial structure) are calculated by using the following expression.

$$C_c \cong \frac{2h\pi \in_0}{\ln \frac{b}{a}} \tag{3.2}$$

where $\in_0 = 8.854187817 \times 10^{-12}\ F/m$

Since the cavity is divided into three parts, all cavity capacitances are calculated separately and added together.

$$C_c \cong C_1 + C_2 + C_3 \tag{3.3}$$

$$C_c \cong \frac{2(h-p_1)\pi \in_0}{\ln\frac{b}{a_1}} + \frac{2p_1\pi \in_0}{\ln\frac{b}{a}} + C_{c_{gap}} \rightarrow (neglected) \quad (3.4)$$

Since the central post discontinues at the gap region and the gap is very small the capacitance corresponding to that part is neglected for simplicity.

The parallel plate capacitances created by the post plate and the diaphragm are calculated by using the following expression.

$$C_p = \frac{\in_0 \pi a^2}{d} \quad (3.5)$$

The fringing field capacitances (C_f) are calculated by using the following expression.

$$C_f \cong \kappa_1 a \in_0 \ln\frac{h}{d} \quad (3.6)$$

where κ_1 is the empirical constant related with the *a/b* ratio[27,28]. For *a/b* ≤ 0.3, $\kappa_1 = 2.78$.

Thus the total capacitance for the cavity is

$$C = C_c + C_p + C_f \quad (3.7)$$

The inductance values of the device are calculated for three parts and added together to obtain the total inductance. The inductance corresponding to the gap region is also neglected.

$$L \cong \frac{\mu h}{2\pi}\ln\frac{b}{a} \quad (3.8)$$

$$L \cong L_1 + L_2 + L_3 \quad (3.9)$$

$$L \cong \frac{\mu(h-p_1)}{2\pi}\ln\frac{b}{a_1} + \frac{\mu p_1}{2\pi}\ln\frac{b}{a} + \left(L_{gap}\right) \rightarrow (neglected) \tag{3.10}$$

where $\mu = 4\pi \times 10^{-7}$ H/m

By using the obtained capacitance and inductance values the resonant frequencies are calculated by using the following expressions.

$$f_0 = \frac{1}{2\pi\sqrt{LC}} \tag{3.11}$$

The calculated parameters and the resonance frequencies calculated from those parameters are given in the Table 5 below.

Table 5 The calculation results (lumped parameters & resonance frequencies)

Parameters	**Alternative 1**	**Alternative 2**	**Alternative 3**
$\boldsymbol{C_c}$	0.2688 pF	0.2159 pF	0.2337 pF
$\boldsymbol{C_p}$	1.7382 pF	0.2950 pF	0.4753 pF
$\boldsymbol{C_f}$	0.3324 pF	0.1712 pF	0.2122 pF
$\boldsymbol{C}$	2.3394 pF	0.6821 pF	0.9212 pF
$\boldsymbol{L}$	4.1038 nH	4.0245 nH	3.9666 nH
$\boldsymbol{f_0}$	**1.6244 GHz**	**3.0377 GHz**	**2.6329 GHz**

The calculated resonance frequency values are 1.6244 GHz, 3.0377 GHz and 2.6329 GHz for all three alternatives respectively. The first result seems reasonable since the reported value for alternative 1 is 1800 MHz in the reference and the frequency value of 1600 MHz is referenced in some of the other sources. But two of them are much higher than the possible values given in Appendix A. The gap length values which are used in those are in the order of millimeters, i.e., 0.9961 mm and 0.59 mm, while the gap length of the first alternative is 185 um.

When the gap length is sufficiently small, i.e., in the order of tens of micrometers then the frequency values will be much lower.

The low gap length also provides much more frequency change by an amount of diaphragm deflection. The next section presents the relationships between the gap length, sound level and frequency shift by calculations.

3.2.2.2 Gap Length Estimation

The movement of the diaphragm changes the resonance frequency and thus the reflection characteristics of the antenna loaded by the cavity also change.
In the Table 6 there are SPL (Sound Pressure Level) values for various sound levels.
A normal conversation sound level at 1 m away is ranging from 50 to 70 dB. It is 60 dB averages.
The whispering level is 40 dB. So the system must work for approximately 30 dB range between 40 dB and 70 dB.In order to calculate the amount of the frequency change, it must be calculated the displacement of the diaphragm by sound.

Table 6 The SPL levels for some sounds [42]

Sound Sources	**Sound Pressure Level (dB)**	**Sound Pressure Level (Pa)**
Threshold of Pain	120 - 130	20 - 63.25
Rock Concert	110 - 120	6.33 - 20
Loud Crowd Noise	100	2
Diesel Truck (10m away)	90	0.63
Busy Road or Cafeteria	80	0.2
Conversation (1m away)	50 - 70	0.0063 - 0.063
Quiet Office or Average Home	50	0.0063
Whisper	40	0.002
Bedroom	30 - 40	0.00063
Background in TV Studio	20	0.0002
Threshold of Hearing	10	0.000063

When the sound waves hit the diaphragm, it moves with the sound back and forth. This displacement of the diaphragm is dependent on the sound pressure level, speed of the sound, the density of the air in the medium and the frequency of the sound.

This relation is expressed as follows

$$\Delta d = \frac{\Delta P_m}{\upsilon \rho 2\pi f} \tag{3.12}$$

where Δd is the displacement of the air molecule in meter, ΔP_m is the pressure amplitude of the acoustic wave in Pa (the maximum increase or decrease in pressure), υ is the velocity of the sound (which is 346.13 m/s at 25^{o}C), ρ is the density of the air in the medium (which is 1.184 kg/m^3 at 25^{o}C) and f is the frequency of the sound (during normal conversations humans produce sounds from 80 Hz to about 8,000 Hz but the most normal speech occurs between 300 Hz and 3,000 Hz).

The maximum, minimum and average displacements of an air molecule by a speech sound are calculated by using Eq. (3.12) and the parameters given in Table 6 above.

$\Delta d_{max} = 81.5546$ nm
$\Delta d_{min} = 0.8156$ nm
$\Delta d_{av} = 7.7671$ nm

The maximum deflection is obtained from a 70 dB (0.063 Pa) and 300 Hz sound, the minimum deflection is from a 50 dB (0.0063 Pa) and 3 kHz sound and average deflection is from a 60 dB (0.02 Pa) and 1 kHz sound.

As it is seen on the results above, the displacements of the molecules are in the order of nanometers. So the displacement of the diaphragm will be less than this amount because of the stiffness of the membrane which is used as diaphragm.

There are two types of membranes, thick membranes and thin membranes [43]. A membrane is called as thick when its maximum deflection X_m (seen in the Figure 34) is much smaller than its thickness t and thin when the deflection is larger than the thickness. In our case the thickness of the diaphragm is 76.2 μm and so the deflections are much smaller than the thickness.

Thus the diaphragm of the device is a thick type membrane. In some source [8,50] it is said about the diaphragm of the device that it is a metallic diaphragm and silver plated thin copper sheet. So we can assume the diaphragm of the device is a circular membrane of thin copper sheet.

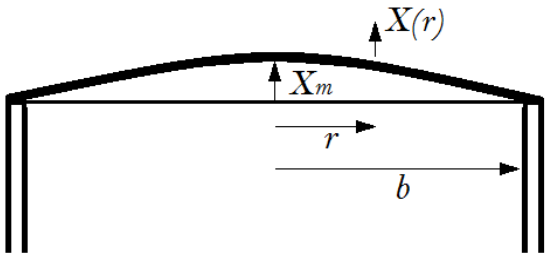

Figure 34. Deflection of diaphragm

The deflection $X(r)$ of a circular thick membrane with radius b is described by the following equation

$$X(r) = X_m \left(1 - \frac{r^2}{b^2}\right)^2 \tag{3.13}$$

For a thick circular membrane the maximum deflection is given as

$$X_m = \frac{3}{16} \frac{b^4}{t^3} \frac{1-\upsilon}{E} \Delta P \tag{3.14}$$

where t is the thickness of the membrane, υ is the Poisson's Ratio of the membrane material (it is 0.33 for copper), E is Young's Modulus for membrane material (it is 117 Gpa for copper) and ΔP is the pressure difference.
The maximum deflection amounts for maximum, minimum and average sound levels (70 dB, 60 dB and 50 dB) are calculated by using Eq. (3.14) as follows.

$X_{m_{max}} = 1.4348$ nm

$X_{m_{min}} = 0.1435$ nm

$X_{m_{av}} = 0.4555$ nm

The maximum deflection takes place in the middle point of the diaphragm and this also coincides to the midpoint of the post plate. At the edge of the post plate, the deflections for three alternatives are calculated by using Eq. (3.13) as follows

$$X(r)_1 = X_m\, 0.7756 \tag{3.15}$$

$$X(r)_2 = X_m\, 0.7938 \tag{3.16}$$

$$X(r)_3 = X_m\, 0.8027 \tag{3.17}$$

Thus the maximum edge deflections are

$X_1 = 1.1128\ nm$

$X_2 = 1.1389\ nm$

$X_3 = 1.1517\ nm$

In order to calculate the capacitance difference due to the diaphragm deflection, we will take the deflection as the average of the maximum deflection at the center of the diaphragm and the deflection at the edge of the posts. Thus the deflection amounts which will be used to calculate the capacitance differences are

$\Delta d_1 = 1.2738$ nm

$\Delta d_2 = 1.2869$ nm

$\Delta d_3 = 1.2933$ nm

The parallel plate capacitances for three alternatives when the deflection is maximum are calculated by using Eq. (3.5) and the resonant frequency differences with these capacitance values are calculated by using Eq. (2.37) and given in Table 7 below.

Table 7 The calculation results (parallel plate capacitances & resonance frequency changes)

Parameters	Alternative 1	Alternative 2	Alternative 3
C_p (Deflected max.)	1.738151785050 pF	0.294959878516 pF	0.475264091393 pF
C_p (Not deflected)	1.738139817170 pF	0.294959497446 pF	0.475263049598 pF
ΔC_p	**11.967880 aF**	**0.381070 aF**	**1.041795 aF**
f_0 (Deflected max.)	1.62434872070 GHz	3.03775618727 GHz	2.63294888422 GHz
f_0 (Not Deflected)	1.62435287572 GHz	3.03775703587 GHz	2.63295037309 GHz
Δf_0	**4.155 kHz**	**848 Hz**	**1.489 kHz**

As it is seen on the frequency shift results, the deflections are extremely small according to the gap length which is in the order of millimeters.

Since the first alternative has a very small (185 um) gap length, the frequency shift in that case are so high than the other alternatives those have larger gap. So this result shows that the gap length which is in the order of millimeter seems unreasonable for the device.

In order to obtain higher frequency shift the gap length must be very small. When the gap length is so small the parallel plate capacitance dominates over the other capacitances, i.e., fringing field and cavity capacitances. Thus the change in gap length affects the capacitance much more and thus the resonance frequency as well.

3.2.2.3 Quality factor of the Device

The quality factor of the device can be calculated by using the expression 2.42 for a rough estimation.

$$\frac{1}{Q_0} \cong \frac{R_s}{2\pi\mu f_0}\left(\frac{\left(\frac{1}{a}+\frac{1}{b}\right)}{\ln\frac{b}{a}}+\frac{2}{h}\right) \tag{3.18}$$

where R_s is the sheet resistance.

$$R_s = \frac{\rho}{t} \cong \frac{1}{\sigma\delta} \tag{3.19}$$

where δ is the skin depth.

$$\delta = \frac{1}{\sqrt{\pi\mu f_0 \sigma}} \tag{3.20}$$

The device is said to be copper or brass and silver plated according to the references. The copper and the brass are reasonable for such an application. In both case it is silver plated so it will be used to silver parameters for conducting surface related parameters. The conductivity of silver is 6.3×10^7 S/m, resistivity is 1.59×10^{-8} Ω.m and the relative permeability is 0.99998.

The calculated resonant frequencies were 1.6244 GHz, 3.0377 GHz and 2.6329 GHz so by using these frequency values the skin depth is calculated by using Eq. (3.20).

The skin depths for three alternatives are

$\delta_1 = 1.5733 \times 10^{-6}$ m

$\delta_2 = 1.1505 \times 10^{-6}$ m

$\delta_3 = 1.2358 \times 10^{-6}$ m

The sheet resistances, by Eq. (3.19), are

$R_{s_1} \cong 10.0089$ mΩ

$R_{s_2} \cong 13.7966$ mΩ

$R_{s_3} \cong 12.8443$ mΩ

Hence the unloaded quality factors, by Eq. (3.18), are

$Q_{0_1} \cong 1948$

$Q_{0_2} \cong 2187$

$Q_{0_3} \cong 2249$

These Q factor values are higher than the value (1000) given in references [2,13]. The reason for obtaining the high Q value is that the formulation used here is valid for a true coaxial cavity, i.e., the post has a uniform cylindrical shape. But in our case the post has a mushroom shape and only the body diameter is used in calculation. And the post plate and antenna probe sections are not taken into account. Since these unaccounted portions have a negative effect on the quality factor by increasing the surface area and decreasing the cavity volume, the actual values must be lower than the calculated values for all alternatives.

The bandwidth of the device can be obtained from the Q value and the resonance frequency value.

$$Q = \frac{f}{\beta} \quad \Rightarrow \quad \beta = \frac{f}{Q} \tag{3.21}$$

$\beta_1 \cong 0.8339\ MHz$

$\beta_2 \cong 1.3890\ MHz$

$\beta_3 \cong 1.1707\ MHz$

3.2.2.4 The Equivalent Circuit of the Structure

The equivalent circuit of the cavity resonator is given in Figure 35 below as a parallel resonant circuit.

The cavity capacitance and the inductance values are calculated previously for three alternatives of the cavity (Table 5). So the equivalent circuit of the device for three alternatives can be calculated.

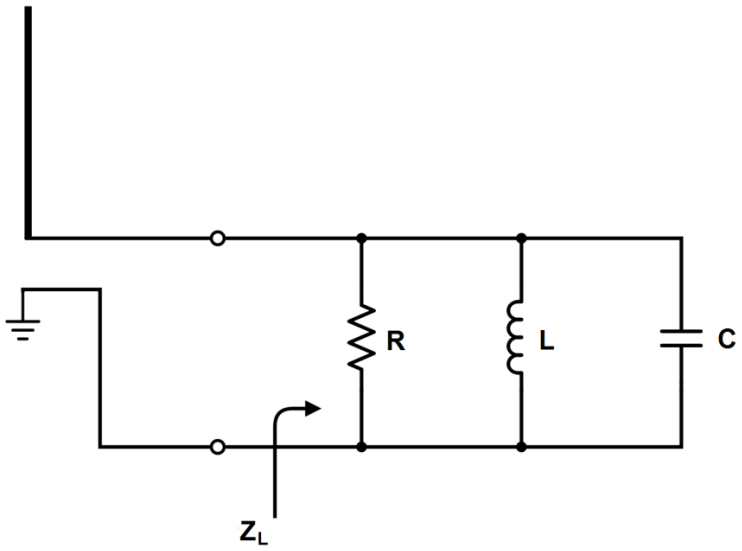

Figure 35. The equivalent circuit of the cavity resonator

The shunt resistances of the cavities are calculated by using the expression 2.45 as follows.

$$R_{sh} \cong \frac{2\pi\delta\sigma\ \omega^2 L^2}{\left(\frac{p_1}{a} + \frac{h - p_1}{a_1} + \frac{h_2}{b} + 2\ ln\frac{b}{a}\right)} \tag{3.22}$$

$R_{sh_1} \cong 95.752\ k\Omega$
$R_{sh_2} \cong 201.820\ k\Omega$
$R_{sh_1} \cong 175.226\ k\Omega$

Since the antenna is a quarter wave monopole, the antenna impedance Z_a can be assumed as (36.5 + j21.25) Ω. The antenna load impedance or the cavity input impedances are

$$Z_L = (\frac{1}{R} + \frac{1}{j\omega L} + j\omega C)^{-1} \tag{3.23}$$

$Z_{L_1} = 95.7500 - j0.3827\ k\Omega$
$Z_{L_2} \cong 201.1583 - j11.5375\ k\Omega$
$Z_{L_3} \cong 175.2216 - j0.8646\ k\Omega$

Thus the approximate equivalent circuit parameters are determined.

Table 8 The equivalent circuit parameters

Parameters	Alternative 1	Alternative 2	Alternative 3
R (kΩ)	95.752	201.820	175.226
L (nH)	2.3394 pF	0.6821 pF	0.9212 pF
C (pF)	4.1038 nH	4.0245 nH	3.9666 nH
$\mathbf{Z_L}$ (kΩ)	95.7500 - j0.3827	201.1583 - j11.5375	175.2216 - j0.8646

3.2.2.5 Modulation By The Structure

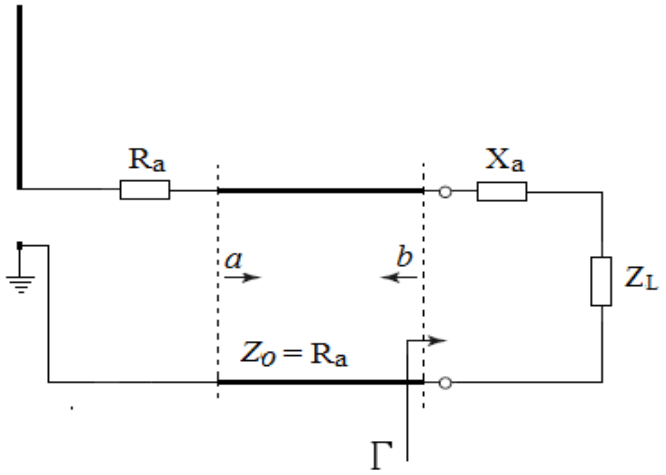

Figure 36. Equivalent circuit of the device expanded by a fictitious transmission line

In order to express analytically the modulation process the equivalent circuit of the device is redrawn in Figure 36. In the figure, the equivalent circuit is expanded by a lossless transmission line to understand what happens within the circuit.

This transmission line is fictitious, i.e., it has zero length. The line is not inserted between the antenna and the load or cavity, but between the real and imaginary part of the antenna impedance. As the line length is set to zero, it has no influence on the circuit behavior, but it helps for understanding. The characteristic impedance Z_0 of the line is equal to the real part of the antenna impedance [44].

The real part of the antenna impedance consists of the radiation resistance R_r and R_l representing the antenna losses.

$$R_a = R_r + R_l \tag{3.24}$$

The available power received by a matched antenna can be written as

$$P_{max} = \frac{1}{8}\frac{|U_0^2|}{R_a} \tag{3.25}$$

Since the characteristic impedance of the line is the same with the antenna, the wave *a* shown in Figure 36 has a relationship as

$$P_{max} = \frac{1}{2}|a^2| \tag{3.26}$$

The reflected wave *b* at the right end of the line is then

$$|b| = |\Gamma . a| \tag{3.27}$$

where Γ is the reflection coefficient at right end of the line.

$$\Gamma = \frac{Z_L + jZ_a - R_a}{Z_L + jZ_a + R_a} = \frac{Z_L - Z_a^*}{Z_L + Z_a} \tag{3.28}$$

The power reflecting from the load and entering into the antenna can be written as

$$P_{in} = \frac{1}{2}|b^2| \tag{3.29}$$

The radiated power P_r from the antenna

$$P_r = \eta_a P_{in} = \frac{\eta_a}{2}|b^2| \tag{3.30}$$

where η_a is the antenna efficiency.

$$\eta_a = \frac{R_r}{R_a} \tag{3.31}$$

The radiated power P_r is the power that reflecting from the antenna load and reradiating through the antenna. This power does not contain the part which is reflected by antenna structure.

The formulation so far is in the frequency domain. The signals are represented by their complex amplitudes, i.e., no time dependence by definition. In order to obtain the modulation expression, a transition into the time domain must be done.

Let the gap length of the device is a function of time as *d(t)*. Then the capacitance of the cavity and thus the impedance of the cavity is a function of time as $Z_L(t)$. Eventually the reflection coefficient of the antenna load is a function of time as $\Gamma(t)$.

$$\Gamma = |\Gamma| e^{j\varphi_\Gamma} \tag{3.32}$$

where φ_Γ is the phase of the reflection coefficient.

The complex wave amplitudes *a* and *b* can be written in time domain as

$$S_a(t) = \mathcal{R}e\{a.e^{j\omega t}\} = |a|\cos(\omega t + \varphi_a) \tag{3.33}$$

$$S_b(t) = \mathcal{R}e\{b.e^{j\omega t}\} = |b|\cos(\omega t + \varphi_b) \tag{3.34}$$

By inserting Eq. (3.27) into Eq. (3.34) it is obtained that

$$S_b(t) = |\Gamma . a| \cos(\omega t + \varphi_a + \varphi_\Gamma) \quad (3.35)$$

where the wave *a* and its phase φ_a are constants.

The magnitude and phase of the reflected wave *b* change, because the reflection coefficient changes. So the reflected wave *b* can be written as

$$S_b(t) = M(d) \cos(wt + \varphi_a + m(d)) \quad (3.36)$$

This is a form of time varying signal whose amplitude and phase are function of some other parameter, i.e., the gap length of the cavity. *M(d)* and *m(d)* show the gap length dependency of the amplitude and the phase respectively.
Eq. (3.36) shows apparently that the reflected wave from the device is amplitude modulation (AM) of the sound that changes the gap between the diaphragm and the post and thus the loading of the antenna. Beside that the reflected signal is also phase modulation (PM) of the sound.

3.2.2.6 Estimated Link Budget of the Device Operation

The operation of Theremin's device is different from the conventional radio because it involves two distinct links: power-up or forward link and the reverse or backscatter link [45,46].

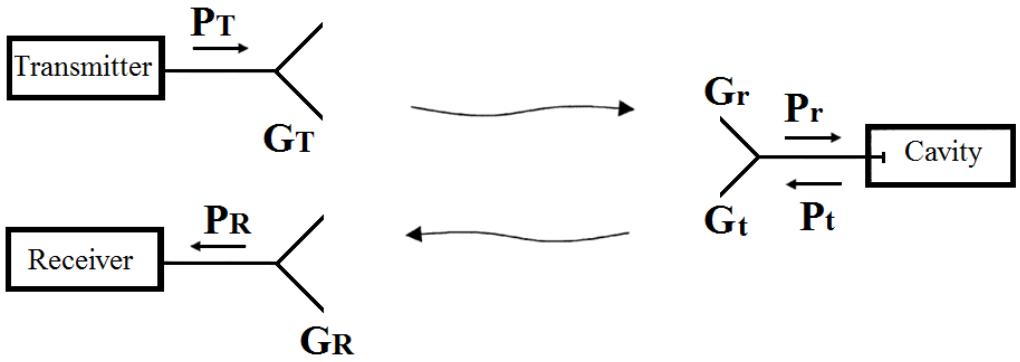

Figure 37. Bi-static collocated communication link of the device

As seen on Figure 37 the operation architecture of the device is bi-static and collocated. The transmitter and the receiver are separate units and located in the same place. So the linear scale link budget for the received modulated backscatter power P_R for bi-static collocated configuration can be written as follows [47].

$$P_R = \frac{P_T G_T G_R {G_r}^2 \lambda^4 X^2 M}{(4\pi R)^4 \Theta^2 B^2 F_\alpha} \tag{3.37}$$

where the parameters are as follows:

P_T : Transmitter power
G_T : Transmitter antenna gain
G_R : Receiver antenna gain
G_t : Device antenna gain (G_r)
λ : Wavelength of the EM signal
X : Polarization mismatch
M : Modulation factor
R : The distance between Transmitter-Receiver and backscatterer
Θ : On-object gain penalty
B : Path blockage loss factor
F_α : Fading factor

Eq. (3.37) can be written in dB format as

$$P_R = 10\,log\,P_T + 10\,log\,G_T + 10\,log\,G_R + 20\,log\,G_r - 40\,log\frac{4\pi R}{\lambda} - 10\,log\,L_T$$

$$P_R = P_T + G_T + G_R + 2G_r - L_{FWD} - L_{BACK} \qquad \text{(in dB)}$$

Where L_T represents the total losses, L_{FWD} represents the forward link losses and L_{BACK} represents the backscatter (reverse) link losses.

Since Yagi-Uda antenna was invented in 1926 and it was used in World War II by Soviets Radar Systems it can be assumed that a Yagi-Uda antenna with a moderate gain of 13 dBi is used for both transmitter and the receiver for the device operation.

The quarter wave monopole antenna of the device is not an ideal one since it has not a perfect ground. A perfect quarter wave monopole antenna has a 5 dBi gain ideally. So the antenna gain of the device can be assumed to have a gain of 2 dBi approximately as a degraded value.

A reasonable operational distance for the device is assumed to be 50 m and the assumed frequency of operation is 330 MHz (as most commonly cited value). Corresponding wavelength of EM signal is about 90.91cm. So these parameters correspond to a one-way free space loss of 56.8 dB.

The polarization mismatch *X* between the antennas may vary from 0 to 1 in a linear scale. It accounts for the power lost due to polarization mismatch. It is not possible to determine the exact value, since the antennas have unpredictable orientations with respect to each other. So an average value of 0.5 can be assumed for the one-way link. This means a 3 dB one-way loss of polarization mismatch.

The modulation factor *M* indicates the effects of changing load states to the reflection. The changing load states change the reflection coefficient and so the reflected power.

The reflection coefficient has a range from -1(Short) to +1 (Open) but in the case of this study it can be assumed as a reasonable assumption that the reflection coefficient range is ±0.5 to balance the backscattered and absorbed power by the cavity resonator. The modulation factor is calculated for two different states of reflection coefficient A and B as

$$M = \frac{1}{4}(\Gamma_A - \Gamma_A)^2 \tag{3.38}$$

So the assumption of ± 0.5 range corresponds to a modulation factor of 0.25 and hence 6 dB loss.

The On-object gain penalty is a factor that accounts for the effects of the objects near the antennas. These objects change the radiation characteristics of the antenna and so the gain. It is defined as the ratio of actual gain to the gain changed by surrounding objects. Practically this factor causes a loss of range 1 dB to 10 dB. So for our case it can be assumed a moderate on-object gain penalty loss of 5dB.

Path blockages in a microwave link result in serious but surmountable losses in the link budget. In these cases, the standard modeling techniques for path blockages in conventional wireless systems is the log-normal distribution. In this model, the distribution of possible aggregate blockage losses *B* can be modeled with the following probability density function [48]:

$$f_B(b) = \frac{1}{\sigma_B\sqrt{2\pi}} exp\left[\frac{(b - \mu_B)^2}{2{\sigma_B}^2}\right] \tag{3.39}$$

where b is the index of the probability density function, μ_B is the average value of the aggregate blockage loss, and σ_B is its standard deviation, all with units of dB.

In the case of our study path blockage is caused mainly by the building and environmental structures. The exact calculation of the path blockage loss is nearly impossible. So it is suitable to use an approximate value. In the literature the path blockage loss can be at a range of 0 to 30 dB depending on the specific conditions.

For a GSM900 signal, the indoor path loss is approximately 5.7 dB average. Actual values are 5dB for light conditions, 6 dB moderate conditions and 9dB for heavy indoor conditions [49]. So for our case it can be assumed that 10 dB is a reasonable path blockage loss for a worst case approach.

In a microwave link, the power received may vary drastically as a function of antenna positions, even for a line of sight communication. This is caused by the constructive and destructive interference of waves scattered from objects in the vicinity of the communication system and known as small scale fading. The effect of small scale fading is also determined in a probabilistic way and involves many parameters. It generally ranges from 5 dB to 20 dB for a variety of practical applications and upper limit may be higher. In our case, for this effect it can be used a reasonable practical value of 20 dB as a fading loss.

Table 9 The estimated link budget of the device operation

Parameter	**Value**
Transmitter Power (P_T)	-
Transmitter Antenna Gain (G_T)	13 dBi
Backscatter Device Antenna Gain (G_t)	2 dBi
Receiver Antenna Gain (G_R)	13 dBi
Free Space Loss (L_{FSL})	- 56.8 dB
Polarization Miss-match Loss (L_X)	- 3 dB
Modulation Loss (L_M)	- 6 dB
On-Object Gain Penalty (L_Θ)	- 5 dB
Path Blockage Loss (L_B)	- 10 dB
Fading Loss (L_F)	- 20 dB

The forward and backscatter link losses are

$$L_{FWD} = L_{FSL} + L_X + L_\Theta + L_B + L_F$$
$$= (-56.8) + (-3) + (-5) + (-10) + (-20)$$
$$= -94.8 \text{ dB}$$

$$L_{BACK} = L_{FSL} + L_X + L_M + L_\Theta + L_B + L_F$$
$$= (-56.8) + (-3) + (-6) + (-5) + (-10) + (-20)$$
$$= -100.8 \text{ dB}$$

The total received power

$$P_R = P_T + G_T + G_R + 2G_r - L_{FWD} - L_{BACK}$$
$$= P_T + (13) + (13) + 2(2) - (94.8) - (100.8)$$
$$= P_T - 165.6 \text{ dB}$$

In order to calculate the signal to noise ratio (SNR), first the noise floor is determined. So the thermal noise is

$$N_{THR} = kT\beta \quad (3.40)$$

where $k = 1.38 \times 10^{-23} J/K$ is Boltzman's constant, T is the temperature of the receiver system in Kelvin, that is assumed to be 300K and β is the bandwidth.
For a sound receiving system must be at least twice the audio bandwidth of 3 kHz.

$$N_{THR} = (1.38 \times 10^{-23})\ (300)\ 2(3)$$
$$= -196\ dB$$

A typical noise figure (NF_{Rec}) of an AM radio receiver that was possible to be used for the device can be assumed as a moderate value of about -20 dB.
So the SNR level of the receiver

$$SNR = P_R - N_{THR} - NF_{Rec}$$
$$= P_R - (-196) - (-20)$$
$$= (P_T - 165.6) - (-176)$$
$$= (P_T + 10.4) \text{ dB}$$

According to this result the SNR values for several transmitter powers are given in Table 10 below.

Table 10 Estimated SNR values for several transmitter power values

Transmitter Power	**SNR**
1 W	10.4 dB
2 W	13.4 dB
5 W	17.4 dB
10 W	20.4 dB
25 W	24.4 dB
50 W	27.4 dB
100 W	30.4 dB

These SNR values seem to be within the detectable range so it can be say that the operation scenario which we define is reasonable and feasible for such an application.

3.3 Simulation of the Theremin's Device

In order to see the field distribution and to find the resonance frequency of the structure, a simulation will be made by modeling the device with HFSS (High Frequency Structure Simulator) software. The model created is shown in the Figure 38. According to the references the device is either copper or brass and silver plated. However, in order to simplify the simulation process the material of the device will be specified as copper in the model. The resonant characteristics of the model are then determined by using eigenmode analysis.

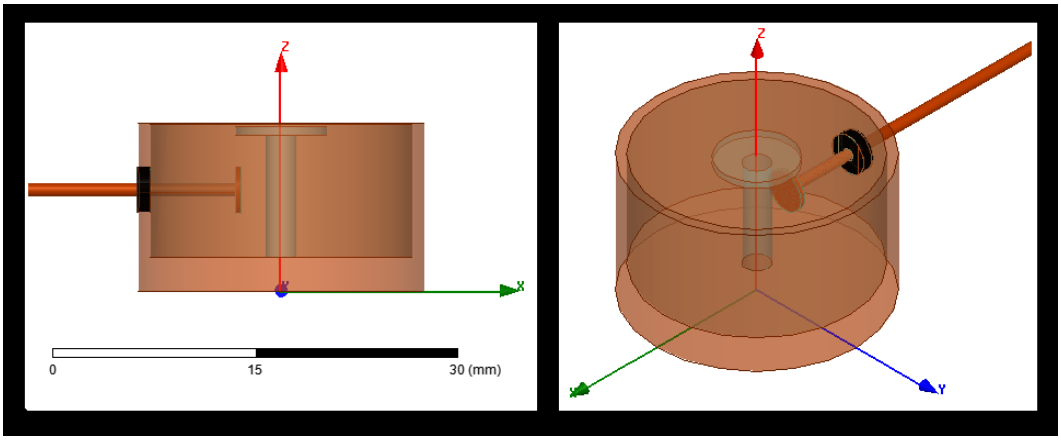

Figure 38. HFSS model of the cylindrical body of the device

The drawing in Figure 39 below illustrates the mechanical dimensions of the cavity to create the HFSS model and the parameters. The parameter values are given in Table 12.

The results of the eigenmode analysis for the first four modes are given in the Table 11 below.

Table 11 First four mode resonant frequencies of the cavity.

Eigenmode	Frequency (GHz)	Q Factor
Mode 1	1.58704	1642.22
Mode 2	5.87324	1636.14
Mode 3	15.6887	4150.06
Mode 4	16.5061	4404.65

Table 12 Cavity resonator dimensional parameters values used in simulation

Parameter	Value (mm)
R_i	19.685
T_w	0.89
H_i	10
T_b	2.5
T_d	0.0762
R_p	2.28
d	0.185
H_{pl}	0.585
H_p	9.23
R_{pl}	6.8
R_o	21.4650
H_o	12.5762
H_{ao}	228.6
R_a	0.976
d_a	2.2
H_{ap}	0.4
H_a	6.4425
R_{ap}	3.5
H_r	1
T_r	1.2
c	5

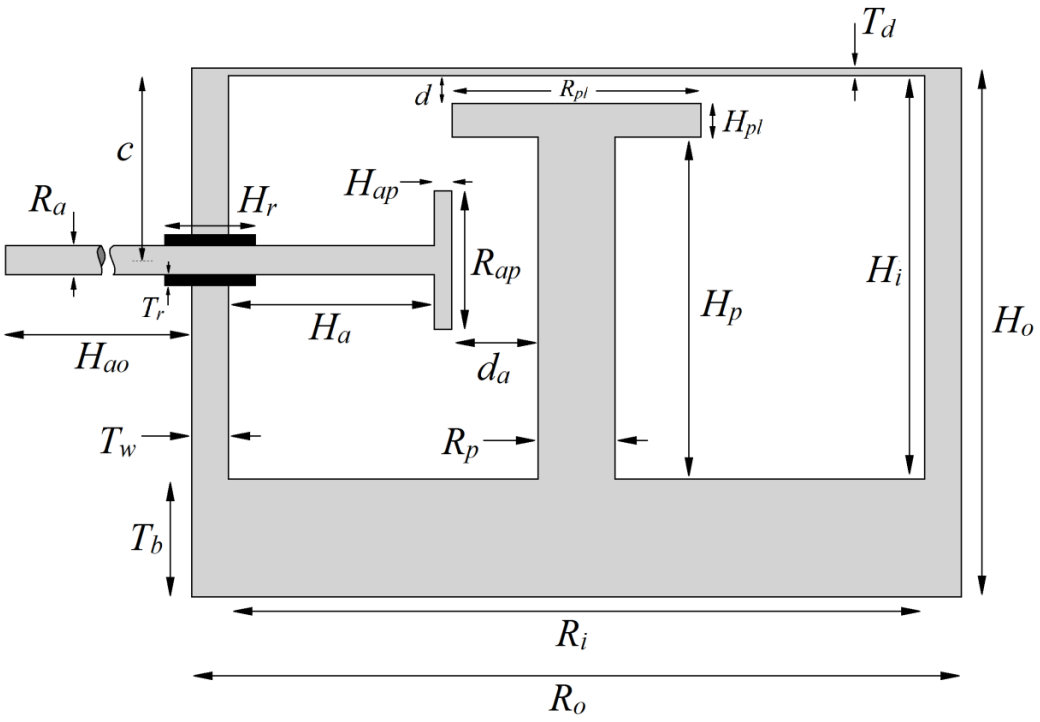

Figure 39. Cavity resonator mechanical structure and dimensional parameters

These results indicate that the higher mode resonant frequencies are too high. However, the resonant frequency value of the first mode seems reasonable for the device. In addition, it can be seen on the Figure 40 that since nearly all electric fields are confined in the gap, the first mode couples strongly to the diaphragm and so should be very sensitive to the gap width between the post and the diaphragm. A diaphragm movement or vibration induced acoustically causes the resonance frequency to change significantly.

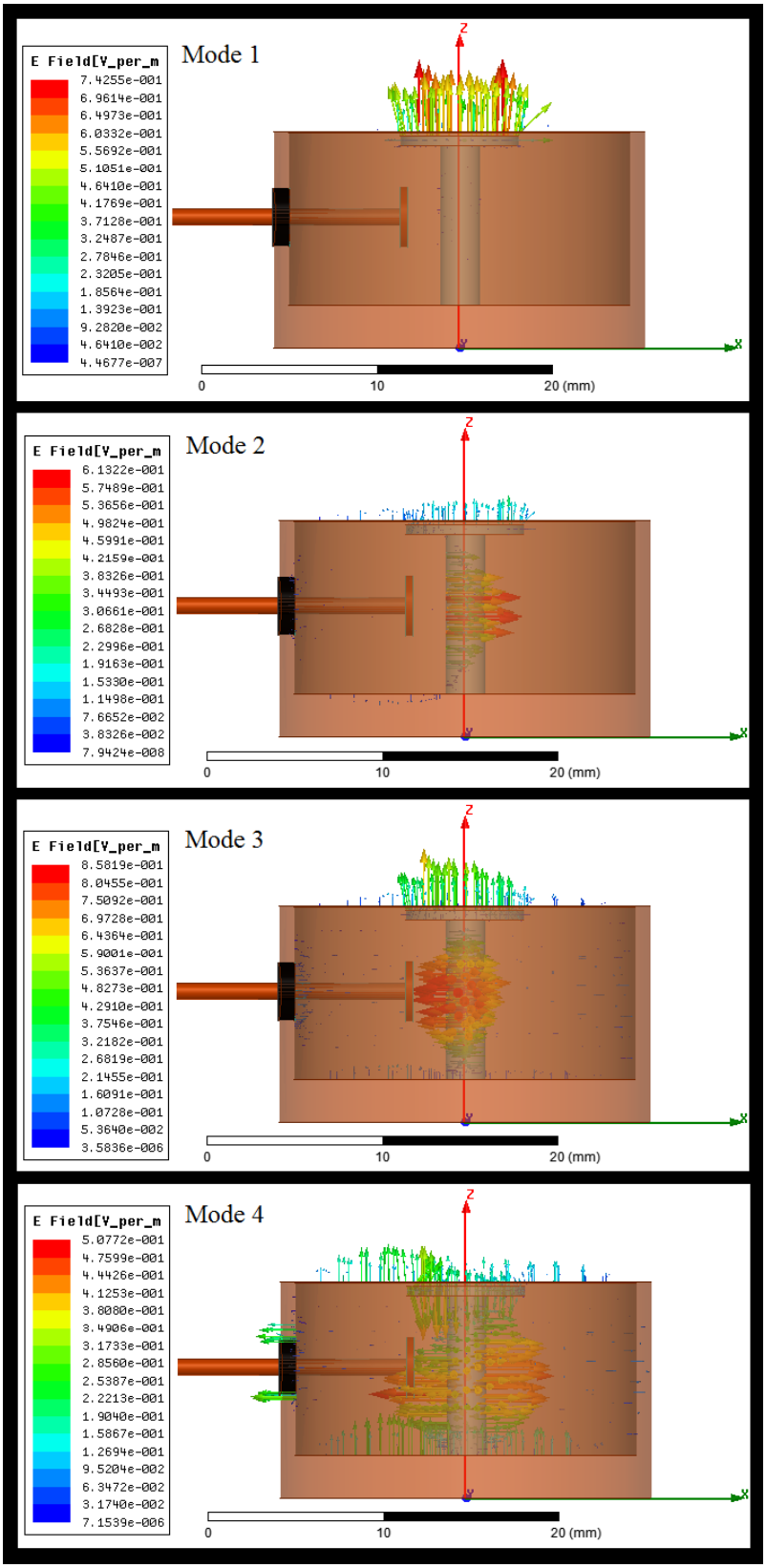

Figure 40. Electric fields within the cavity related to the first four modes

The resonance frequency of the device is also affected by the physical parameters of the device. Some parameters affect much and some less. The graphical representations of these dependencies are illustrated in the Figure 41.

As seen in the graphs in Figure 41 below, the parameter most affecting the resonance frequency of the cavity is the gap width. The "f vs d" graph shows this relationship. The parameter having the second major effect on the frequency is the diameter of the post plate. The "f vs R_{pl}" graph shows this effect. The post plate width is directly related with the parallel plate capacitance so as with the resonance frequency. The internal diameter of the cavity is the parameter having minimal effect on the frequency among the others in Figure 41. It has nearly no effect on the frequency. The internal height of the cavity, as seen on the "f vs H_i" graph, slightly affects the frequency. This effect is due to that any increase of the height provides more space for magnetic fields and this causes an increase of the inductance and thus a decrease in resonance frequency.

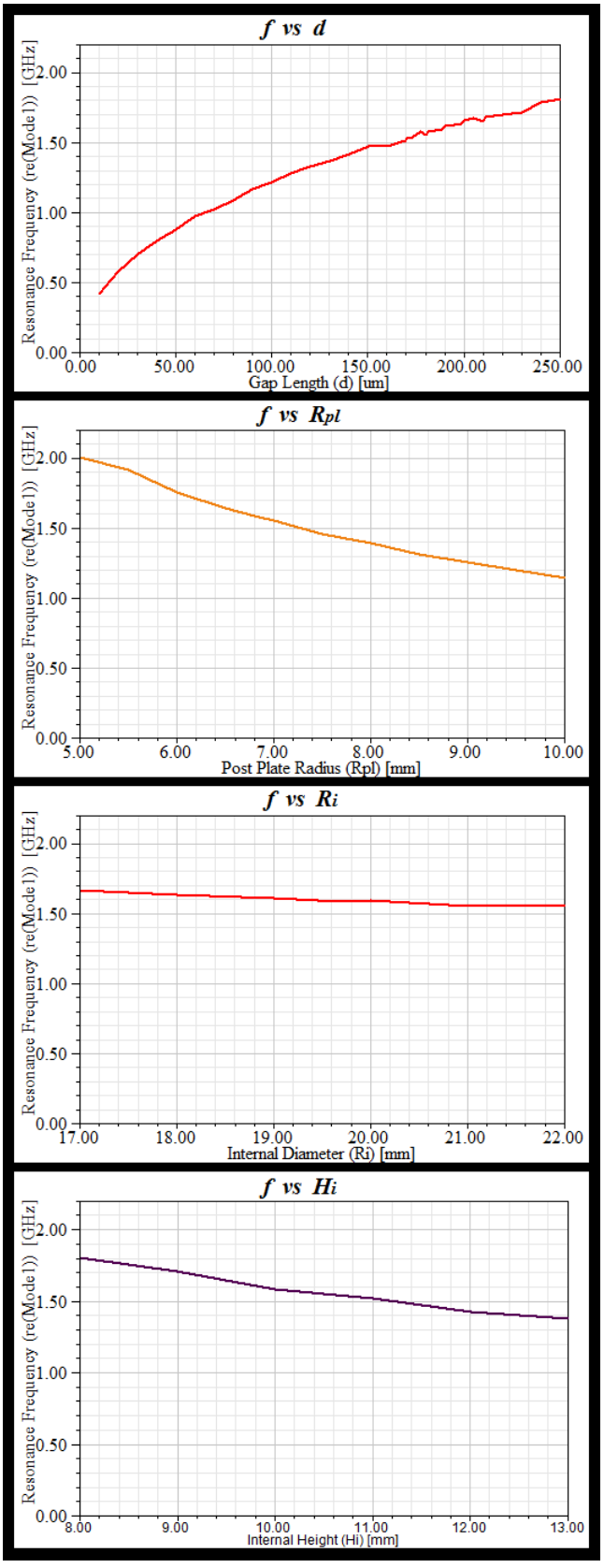

Figure 41. The graphs of the resonance frequency versus other parameters

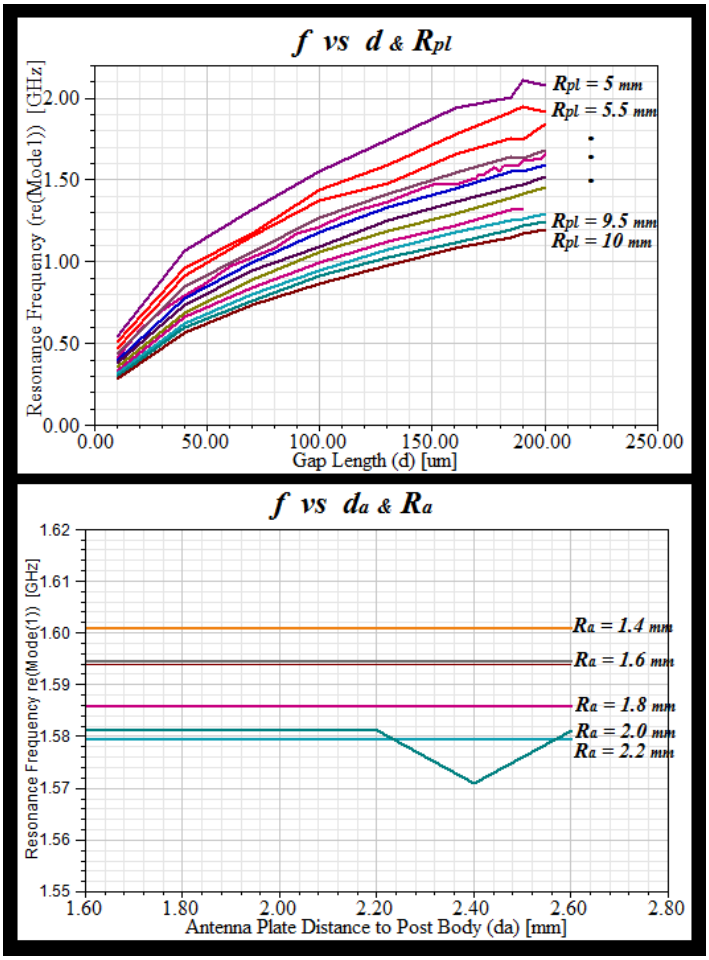

Figure 42. Resonance frequency versus d-R_{pl} and d-d_a parameters

The "*f* vs *d* and R_{pl}" graph in Figure 42 shows the effects of the gap length and plate diameter on the frequency together. The other graph in the figure shows that both the distance of the antenna plate to the central post and the diameter of the antenna plate, have nearly zero effect on the resonance frequency.

The simulation results illustrate that the most critical factor for the resonance frequency of this structure is the width of the gap between the post plate and the cavity wall or diaphragm. Thus the frequency is most sensitive to the gap width. This sensitivity provides the functionality of the device.

3.3.1 Sensitivity Analysis

A sensitivity analysis made for the resonant frequency of Mode 1 as a function of the gap length and it is shown in Figure 43 for several gap length values.

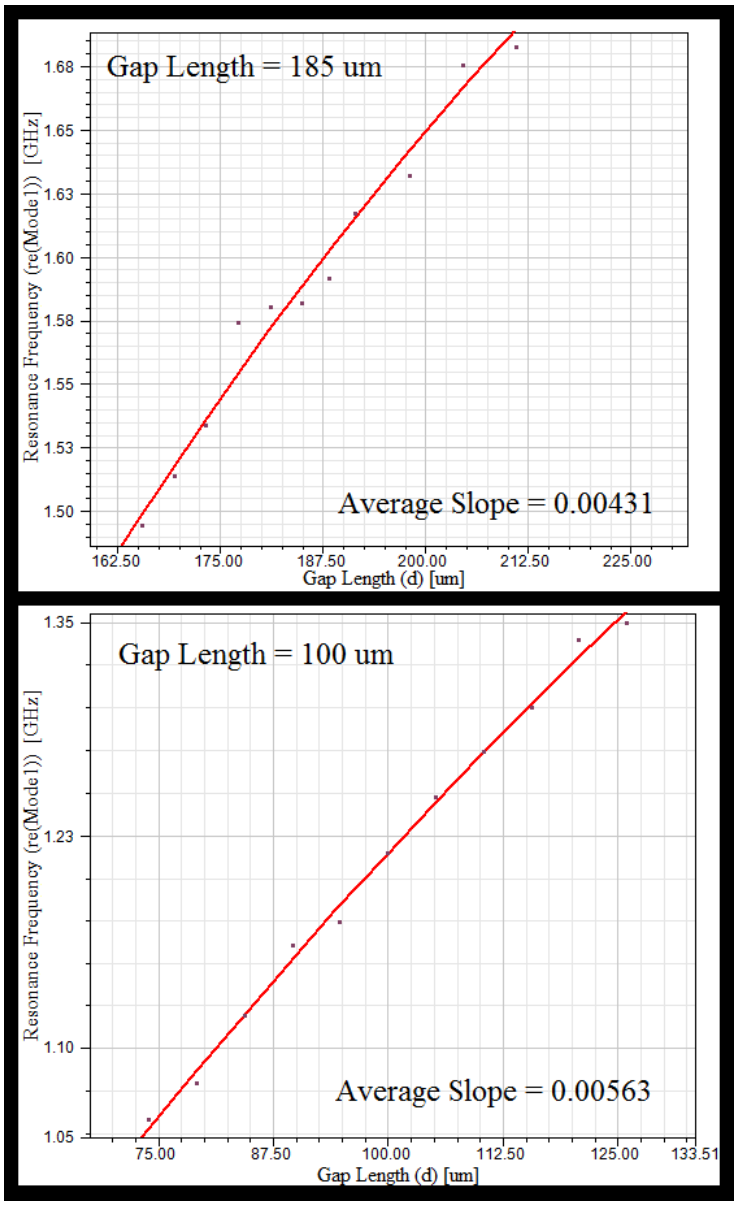

(a)

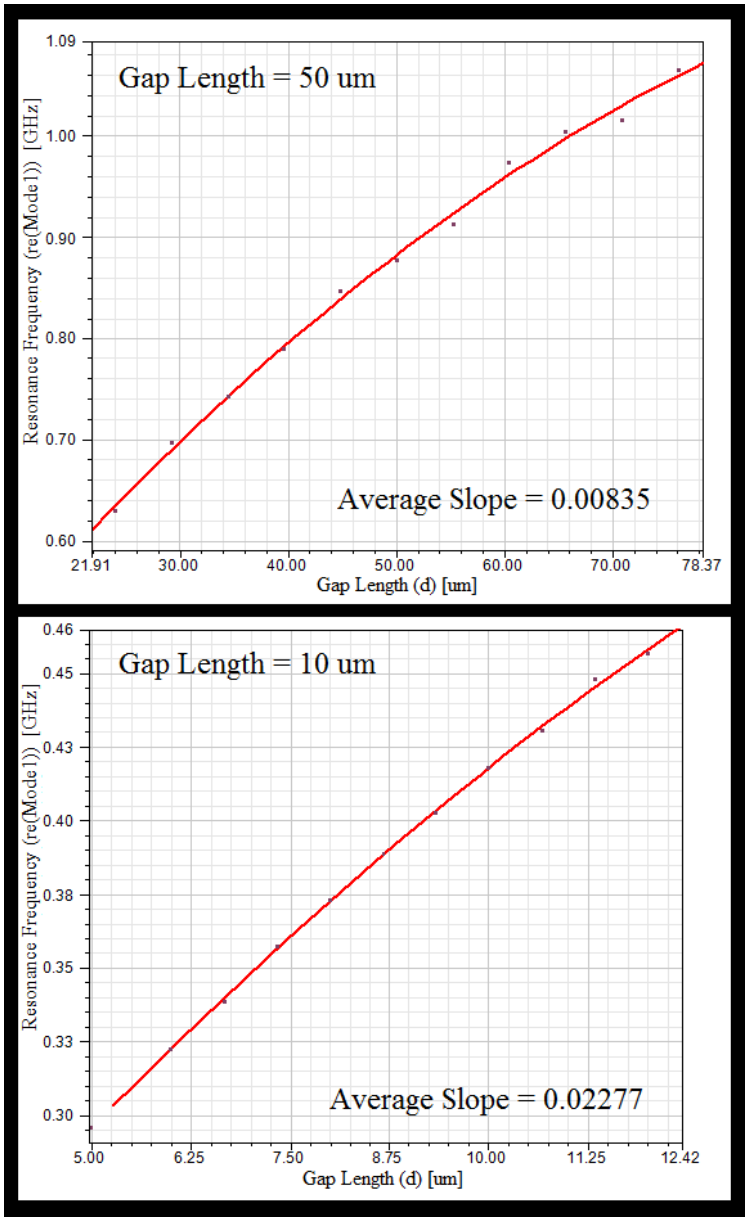

(b)

Figure 43. Sensitivity graphs around several gap length values

The slopes in the graphs are given in terms of frequency by deflection in Table 13 below.

Table 13 Average sensitivities of the device for several gap lengths.

Gap Length	Slope
185 μm	4.31 MHz/μm
100 μm	5.63 MHz/μm
50 μm	8.35 MHz/μm
10 μm	22.77 MHz/μm

As expected, while the gap length decreases the sensitivity of the cavity increases. The reason for this effect is the increasing parallel plate capacitance. For a small gap, the capacitance value will be greater and this greatness causes this capacitance to be more dominant than the other capacitances (i.e., fringing fields and cavity capacitances) in determining the resonant frequency. Thus any change in this capacitance affects the resonance frequency much more. In the same manner when the gap is small, the same amount of deflection in the diaphragm affects the capacitance much more for small gap than the larger one. So the sensitivity is higher for small gaps.

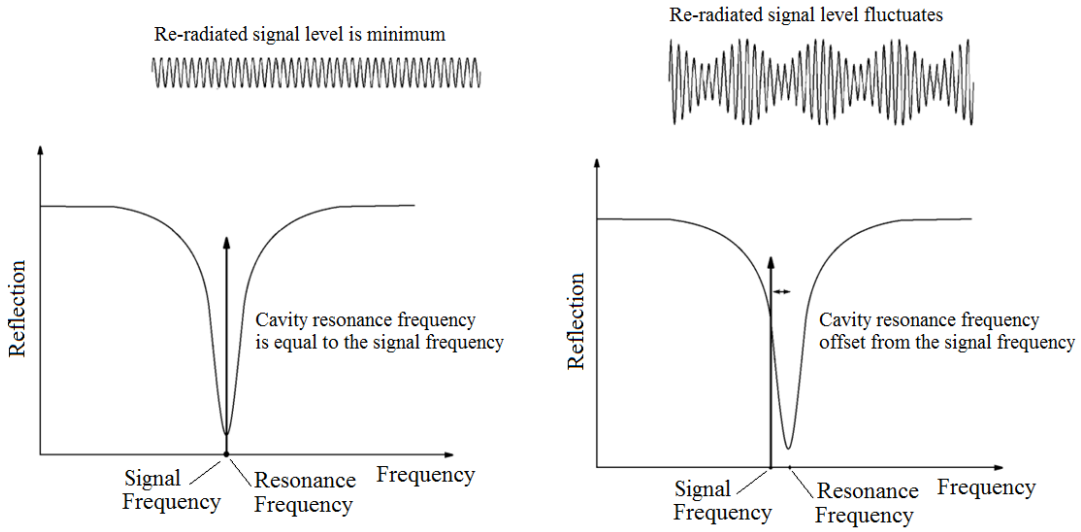

Figure 44. Conversion of diaphragm vibration into an AM modulated signal

Figure 44 illustrates the modulation process of the structure. Acoustically induced displacement of the diaphragm results in changes of the resonant frequency of the device. This means that the loading characteristics of the cavity and thus the reflection characteristics of the antenna change by diaphragm movement. This in turn results in changes in the amplitude of the reradiated signal in a manner similar to an AM modulator. Depending on the Q of the cavity, a reasonably undistorted amplitude modulated signal is produced.

3.3.2 Q Factor

The quality factor of the device is said to be 1000 in a reference as a rough guess and it is approximately calculated as 1948 in section 3.2.2.3. The outputs of the simulation showing the Q factor are given in Figure 45.

Q factor of the cavity highly depends on the gap length as seen on the “Q vs d” graph. Q value is proportional with the frequency so when the gap length decreases the resonant frequency also decreases. Thus the quality factor of the cavity proportionally decreases. Beside, up to some level the change in Q factor by gap length is much more than the higher levels as like the effects on resonance frequency. On the other hand other parameters do not affect the Q factor as much as the gap length. The graphs show that any change in the post plate width, internal diameter and internal height has not significant effect on the quality factor.

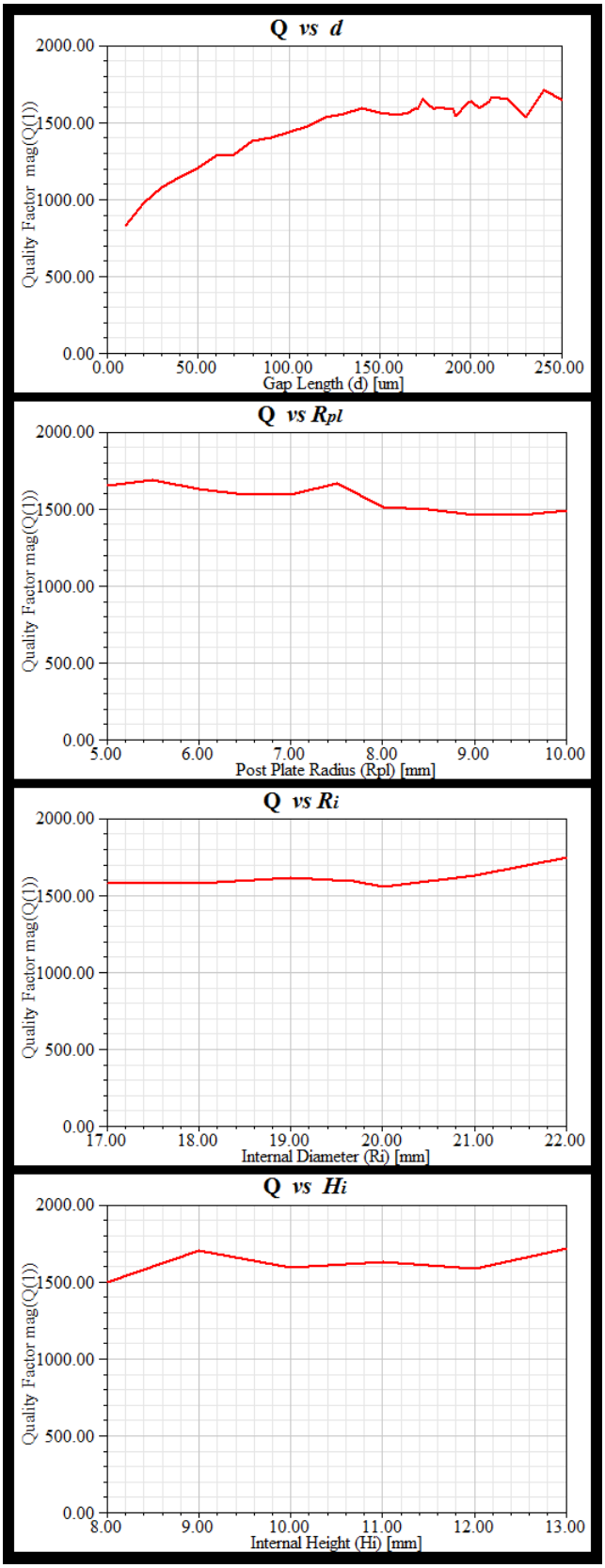

Figure 45. The graphs of the Q Factor versus other parameters

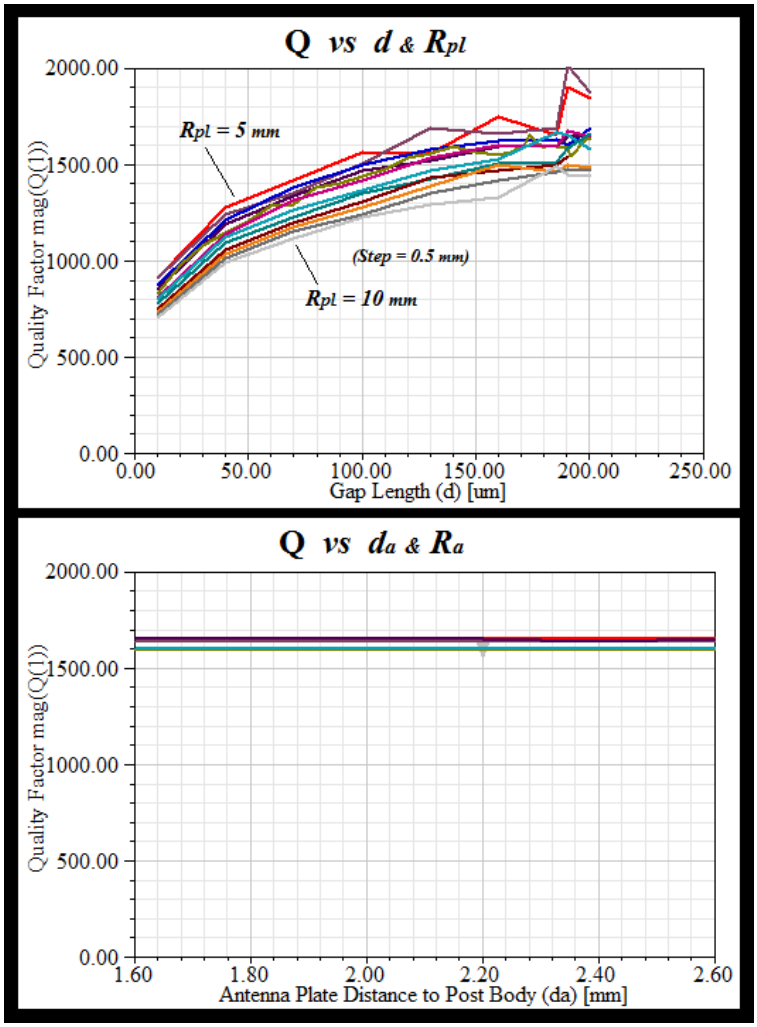

Figure 46. Q Factor versus d-R_{pl} and d-d_a parameters

The parameters of the excitation probe or antenna, i.e., antenna plate diameter and the distance between antenna plate and the post body, nearly have no effect on the Q factor as seen on the graph in the Figure 46 above.

3.4 Design of The Prototypes

3.4.1 Design Considerations

In order to produce a device that can be experimented effectively, some critical parameters must be adjustable. These parameters are the gap length, post plate diameter, internal height, internal radius and diaphragm tension.

Before reaching the final design, in order to test and evaluate the mechanical structure some preliminary plastic prototypes have been designed and produced by using the 3D printing. The plastic prototypes are shown in the Figure 47.

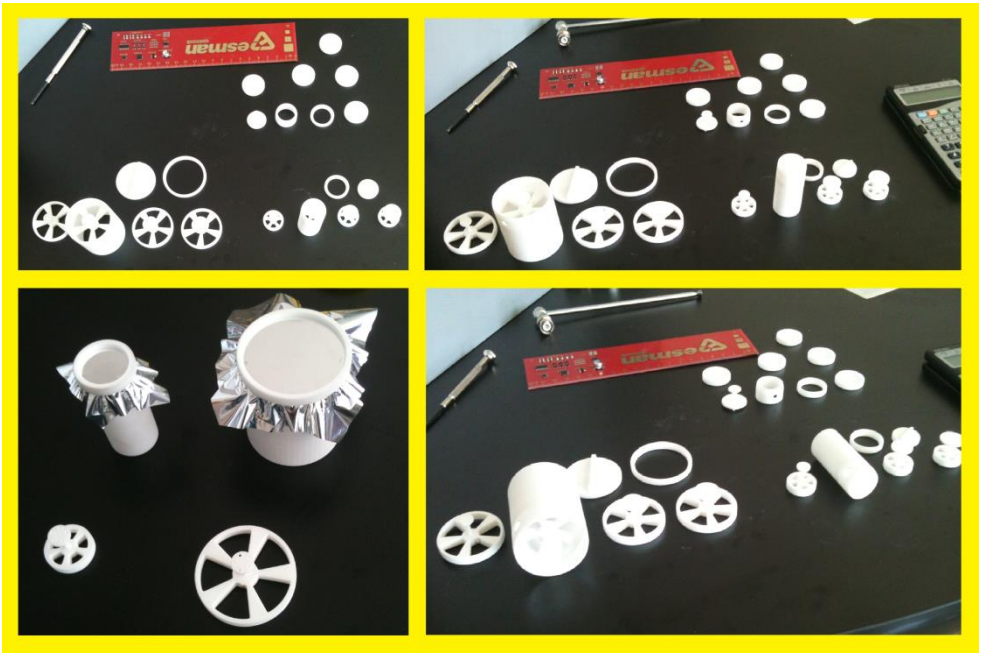

Figure 47. Plastic prototypes

After the evaluation of the plastic prototypes, a practical and producible mechanical design is carried out. The drawing of this mechanical design for the prototypes is given in Figure 48.

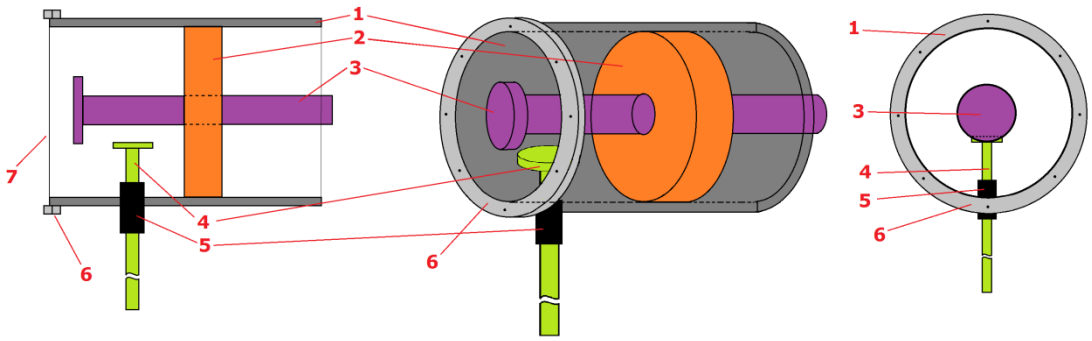

Figure 48. Mechanical drawings of the prototypes

The definition of the prototype parts which are illustrated by the drawing in Figure 48 are as follows.

- Part 1 is the cylindrical body whose inner side wall is threaded. There is also some threaded area on the top most part of the outer wall so that the part 6 is to be mounted. There are two cylinders with the diameter of 39.4 mm and 19.7 mm. The height of the both cylinders is 50 mm.

Figure 49. Part 1, cylindrical body pictures

- Part 2 is the back side wall of the prototype cavity. Its diameters are 19.7 mm and 39.4 mm; and its height is 10 mm. The outer side of this part is threaded so that it moves back and forth to adjust the cavity height. There is a threaded hole of 3 mm diameter in the middle of this part for part 3.

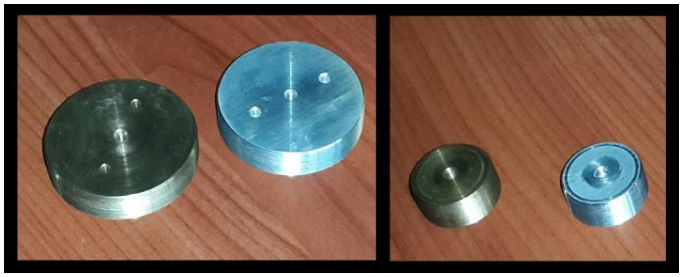

Figure 50. Part 2, backside wall piece

- Part 3 is the central post having a mushroom shape. The body of this part is threaded so that it is movable inside the hole in the middle of the part 2 to adjust the gap width between post plate and diaphragm. This part is produced in different size of plate diameters (5.1 mm, 6.8 mm, 13.6 mm and 27.2 mm). The plate thickness is about 1.5 mm, wedge diameter is 3 mm and total length is 40 mm.

Figure 51. Part 3, central post

- Part 4 is a unified part comprised of antenna and exciting probe of the cavity. Its inner part functions as mushroom shaped exciting probe and its outer portion is monopole antenna. The inner portion and the outer portion are joined with an SMA connector. The plate diameters are 7 mm and 3.5 mm and the plate thickness is 1.5 mm. The probe heights from the internal side of the cavity are 13 mm and 6.5 mm.

Figure 52. Part 4, unified antenna and exciting probe and part 5, SMA connector

- Part 5 is the SMA connector which connects the antenna and probe portion of part 4.
- Part 6 is a two-piece ring structure which holds the diaphragm between its pieces with screws. The inner side of one piece is threaded so that it is screwed to the part 1. This part and the diaphragm constitute the front wall of the prototype cavity. As tightening this part the diaphragm will be stretched more and vice versa.

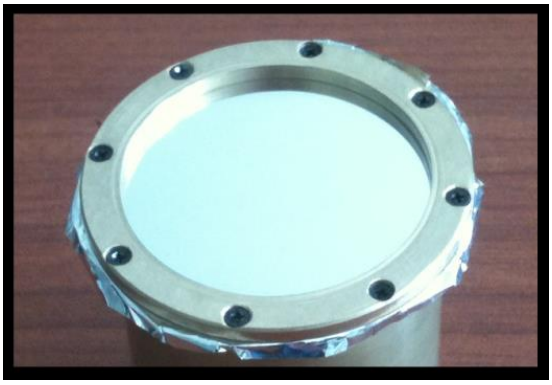

Figure 53. Part 6, diaphragm holding rings and part 7, diaphragm

- Part 7 is the diaphragm. It is aluminum metallized PET (Polyethylene terephthalate) film of 8 μm thickness.

All parts are combined to form the prototypes with adjustable parameters.

Figure 54. Pictures of combined prototypes

Figure 55. Pictures of finished prototypes

3.5 Simulation of The Prototypes

The HFSS models of the prototypes are shown in the Figure 56. It is tried to create the same structure with the real prototypes to minimize the errors.

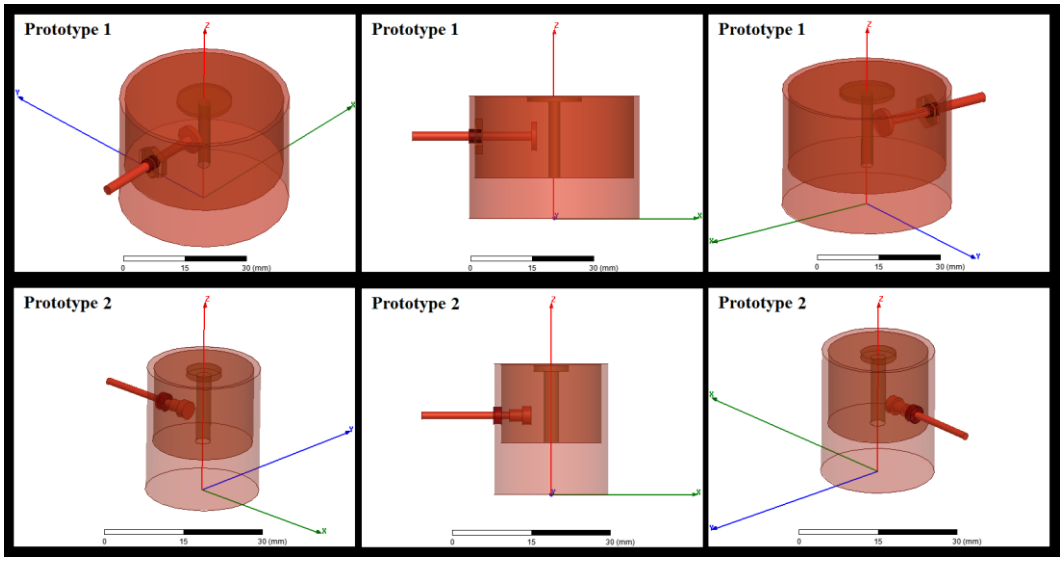

Figure 56. HFSS models of the prototypes

The Resonant frequencies of the Prototype 1 according to the post plate diameter and the internal height are shown in the Table 14.

Table 14 Resonance frequencies (eigenmodes) of the four modes (GHz).

Parameters	Eigenmode 1	Eigenmode 2	Eigenmode 3	Eigenmode 4
Rpl = 6.8 mm Hi = 15 mm	1.20523	3.17656	7.78847	9.41907
Rpl = 13.6 mm Hi = 15 mm	0.665523	3.14251	7.68333	9.39631
Rpl = 27.2 mm Hi = 15 mm	0.358906	3.12828	6.16415	6.19979
Rpl = 6.8 mm Hi = 20 mm	0.999673	3.01526	7.72283	7.99985
Rpl = 13.6 mm Hi = 20 mm	0.577300	3.06320	7.68929	8.01734
Rpl = 27.2 mm Hi = 20 mm	0.307008	3.01098	6.15254	6.17625

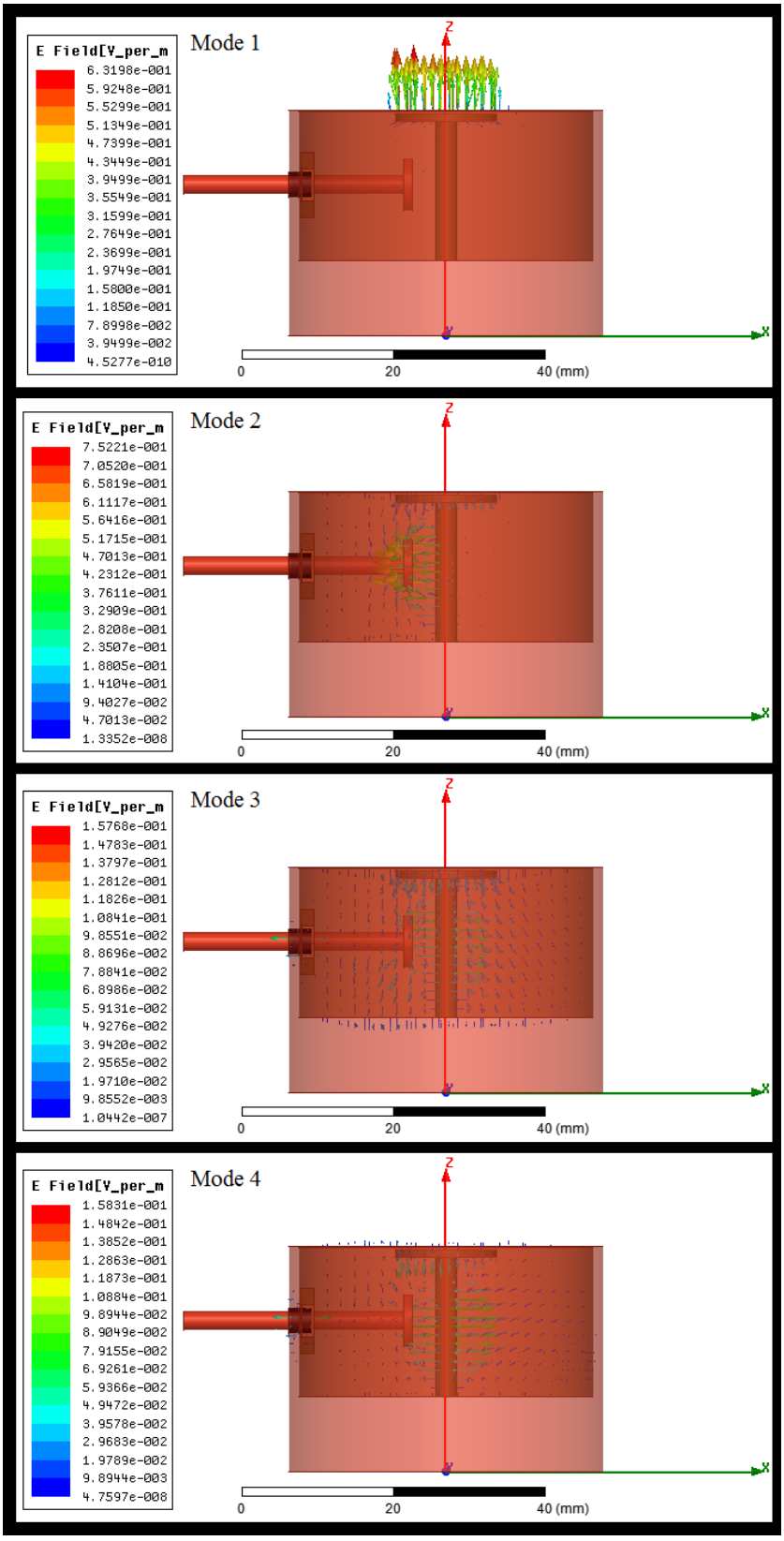

Figure 57. Field distribution of the Prototype 1

The results in Table 14 shows that higher mode resonant frequencies are too high as like the results of the device. However, the resonant frequency values of the first modes are relatively lower.

As in the device model, nearly all electric fields are confined in the gap region as seen on the Figure 57. So the first mode is very sensitive to a change in the gap width.

The Figure 58 below shows that the electric fields inside the Prototype 2. For the first mode the electric fields are accumulated in the gap region. For the third and fourth mode the electric fields are also greatly accumulated in the gap region. But since some amounts of the fields are in other region, the effect of the gap on the resonance frequency is degraded according to first mode for which all fields confined in the gap region.

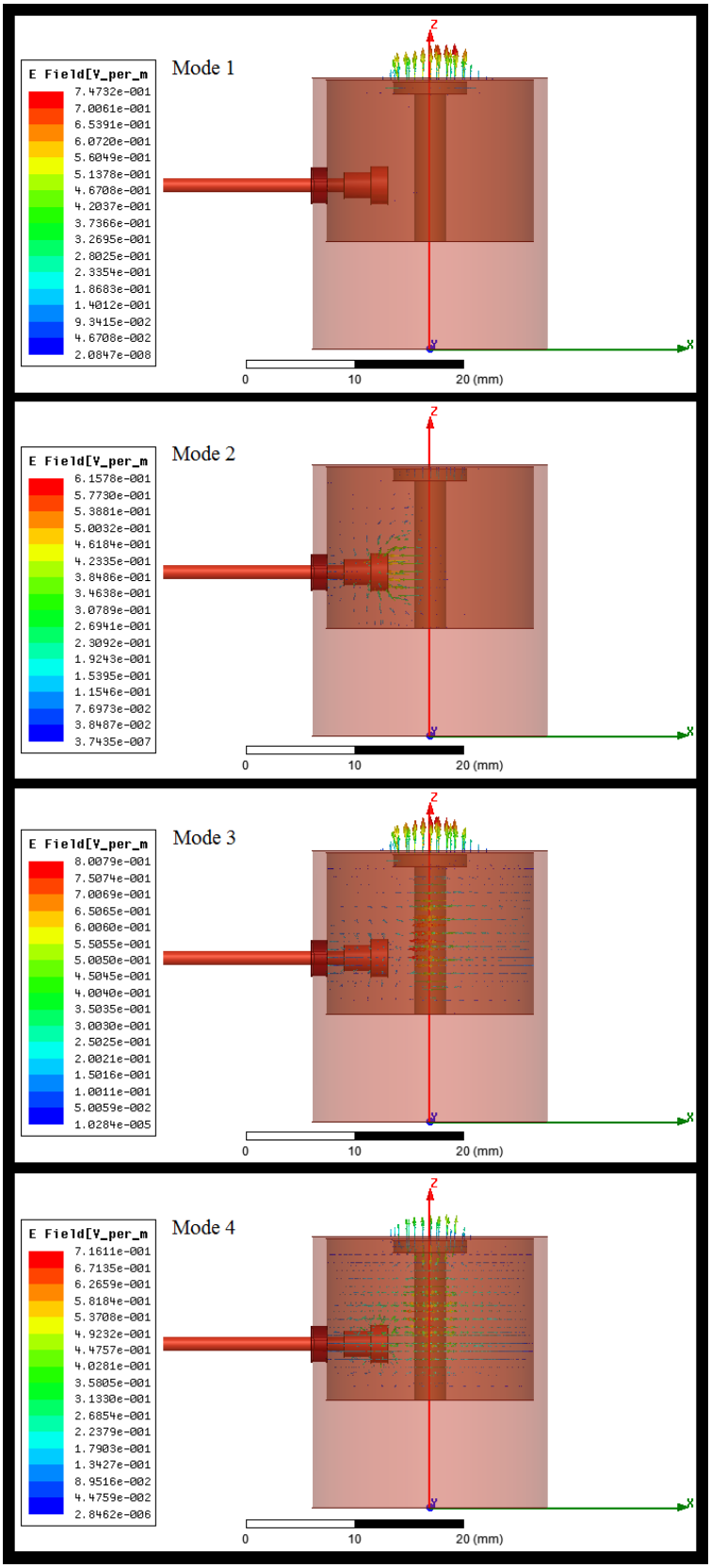

Figure 58. Field distribution of the Prototype 2

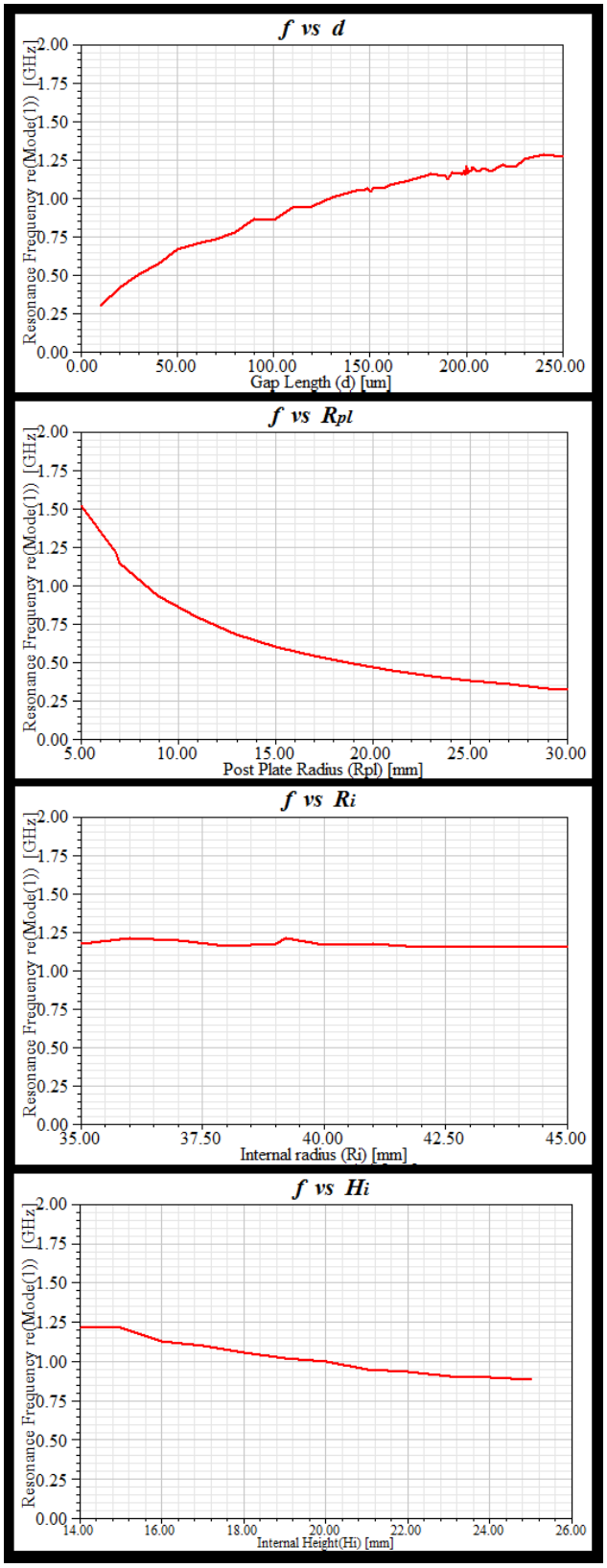

Figure 59. Graphs of resonance frequency versus other parameters

The Figure 59 shows the relationship between the resonance frequency and the dimensional parameters of the Prototype 1. As seen in the figure, the parameter most affecting the resonance frequency of the cavity is the gap width and subsequently the diameter of the post plate. All the graphs are very similar to the device graphs.

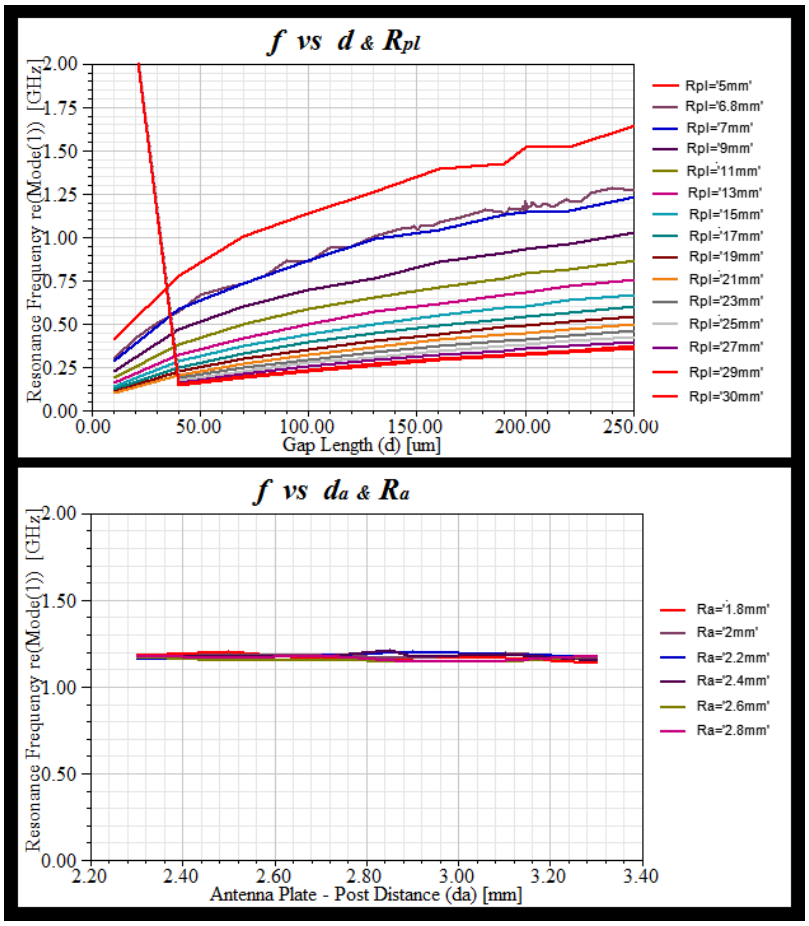

Figure 60. Resonance frequency versus d-Rpl and da-Ra parameters

The first graph in Figure 60 shows the effects of the gap length and plate diameter. The second graph shows the effects of both the distance of the antenna plate to the post and the diameter of the antenna plate on the resonance frequency together. Antenna plate and the space between antenna plate and post have nearly zero effect on the resonance frequency.

3.5.1 Sensitivity Analysis

The sensitivity analysis of the resonant frequency of Mode 1 as a function of the gap length for several gap length values are shown in Figure 61 below.

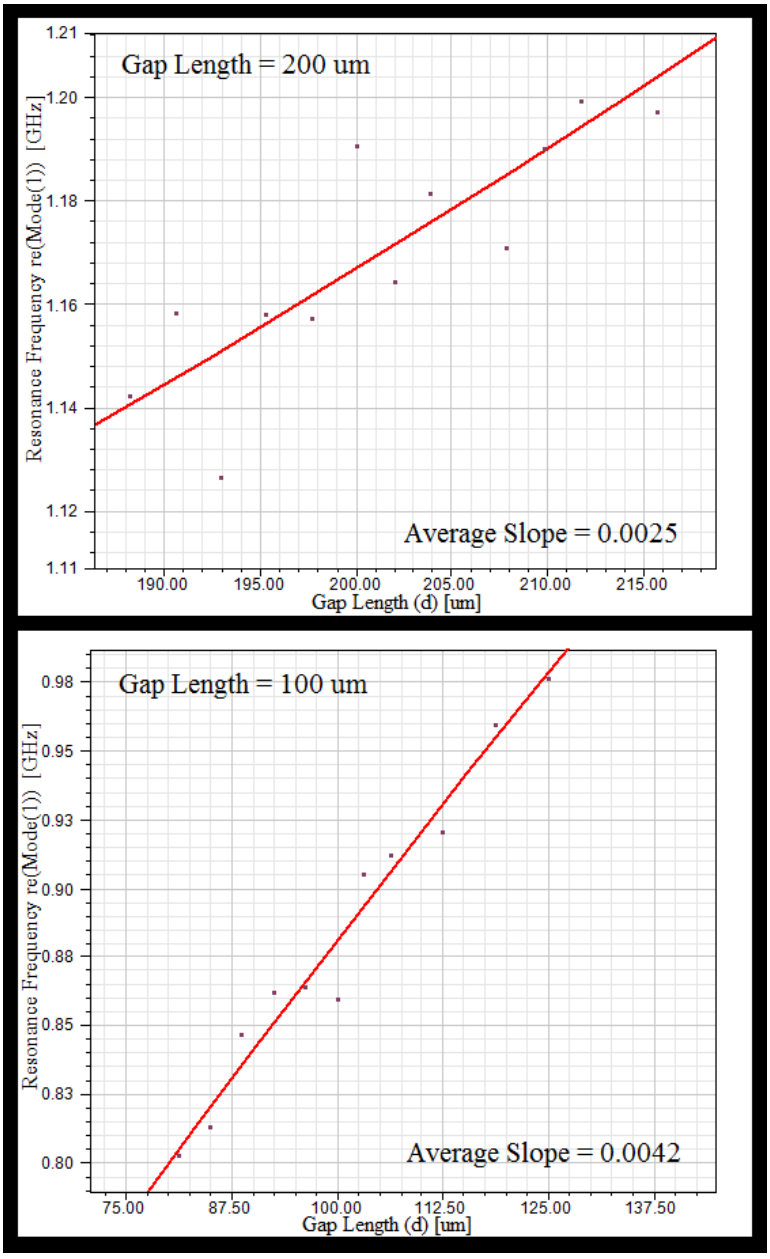

(a)

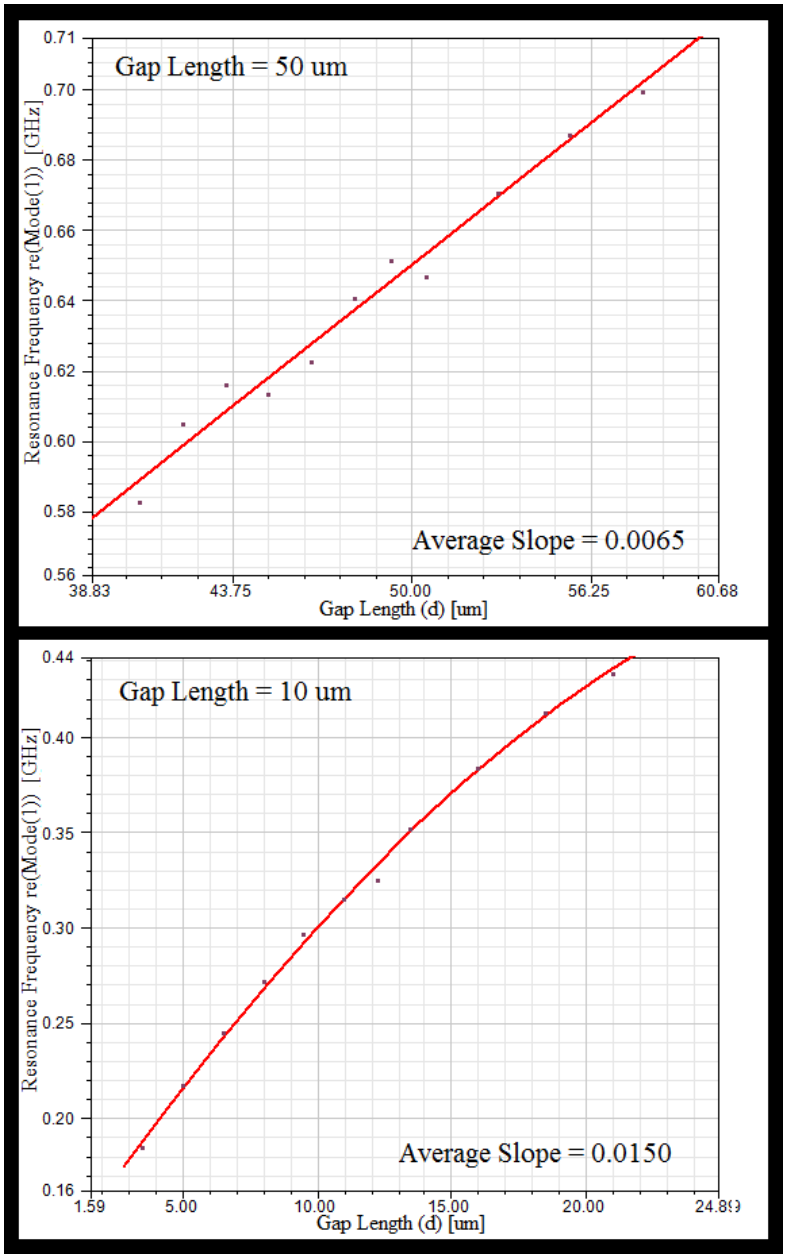

(b)

Figure 61. Sensitivity graphs of Prototype 1 for several gap length

The slopes in the graphs are given in terms of frequency by deflection in Table 15 below.

Table 15 Sensitivity of Prototype 1 for several gap lengths.

Gap Length	Slope
200 μm	2.5 MHz/μm
100 μm	4.2 MHz/μm
50 μm	6.5 MHz/μm
10 μm	15.0 MHz/μm

As in the case of the device analysis and as expected, while the gap length decreasing the sensitivity of the cavity increases.

3.5.2 Q Factor

The quality factor graphs of the Prototype 1 are given in the Figure 62 and Figure 63 below. Graphs show the relationship between the Q factor and the dimensional parameters of the prototype.

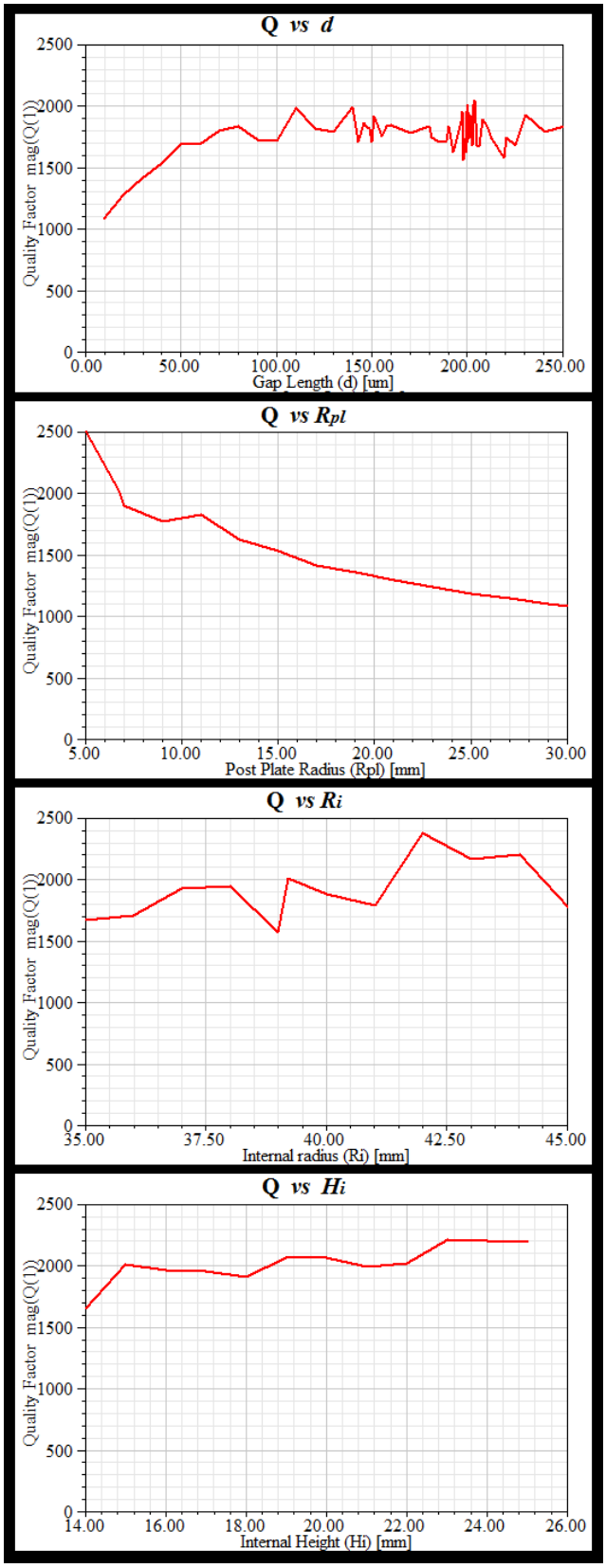

Figure 62. Q Factor graphs

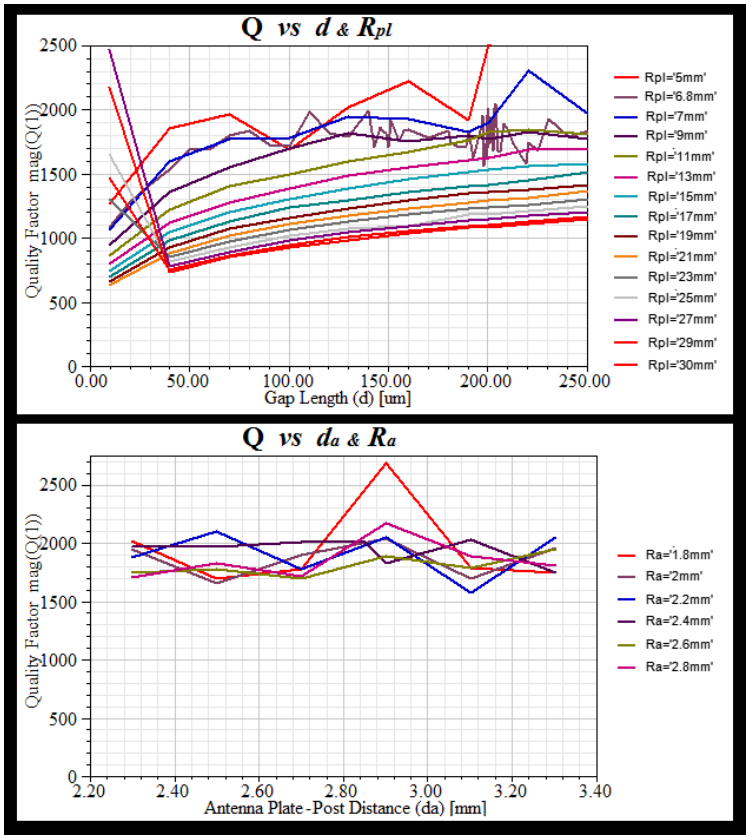

Figure 63. Q Factor versus d – Rpl and da – Ra graphs

The quality factor graphs of the Prototype 1 are given in the Figure 62 and Figure 63 below. Graphs show the relationship between the Q factor and the dimensional parameters of the prototype.

CHAPTER 4

PROTOTYPE MEASUREMENTS AND EXPERIMENTS

In this chapter the experiments performed are described. These are the proof of the concept experiment, resonance frequency measurements and the sound receive experiments.

4.1 Proof of The Concept

Before designing a replica of the Theremin's device, the concept of backscattering from an antenna by load modulation is proved with a capacitor loaded dipole antenna as a concept. In order to do such an experiment a backscattering dipole antenna loaded with a varactor diode and a simple peak detector circuit for detecting the modulated backscatter wave are designed and implemented.

The experiment setup is illustrated in the Figure 64. An RF carrier signal of 13 dBm and 450 MHz is produced by the RF signal generator. A sine signal from 0.5 kHz to 4 kHz and 5 Vpp is applied to the varactor diode by a waveform generator connected to the dipole antenna. Thus the load capacitance of the reflector antenna changes by the applied waveform signal. And this waveform is detected by the simple detector circuit, which is shown in Figure 65.

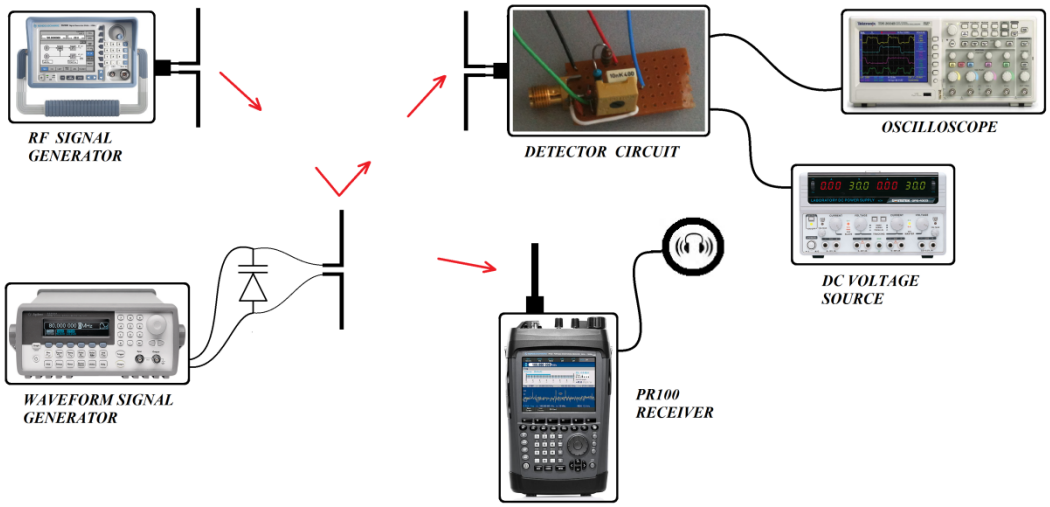

Figure 64. Proof of concept experiment setup illustration

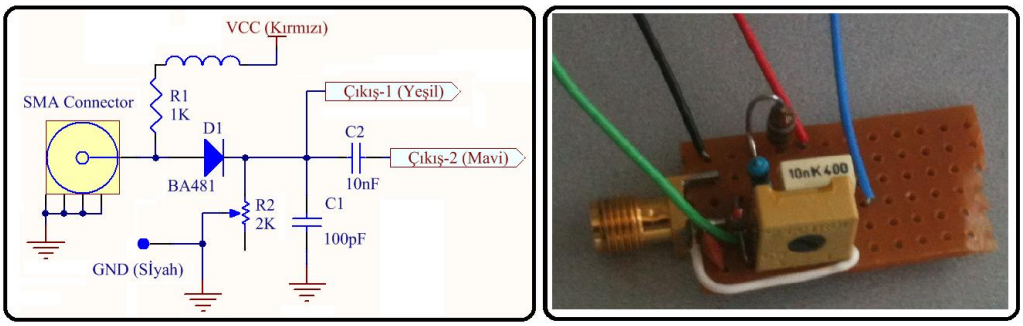

Figure 65. Simple peak detector circuit

Thus it is confirmed that the waveform applied to the varactor diode changes loading of the reflector antenna and thus modulating the reflected or the scattered wave. In the experiment, the demodulated waveform is observed by the oscilloscope and it is listened to as a sound by PR100 receiver as well.

Figure 66. Experiment setup pictures

The experiment setup pictures are shown in Figure 66. By this experiment the concept of antenna load modulation is simply verified.

4.2 Resonance Frequency Measurements

The reflection coefficient (S_{11}) measurement of the prototypes are done with a vector network analyzer. When the cavity is in resonance the reflection coefficient is at minimum. The resonance frequency changes in accordance with the gap length and post plate diameter.

While the frequency changes, the magnitude of the S_{11} changes also and at some point it reaches minimum level. Because of the mechanical tolerances it was very hard to secure the resonance point at which S_{11} is minimum level. Many trials have been done to adjust the gap so that the S_{11} will be minimum level but it was not possible to adjust exactly because even a little movement causes the frequency point change right away. Eventually a point is adjusted but it was not an intended point. It was a minimum level of a series of trials.

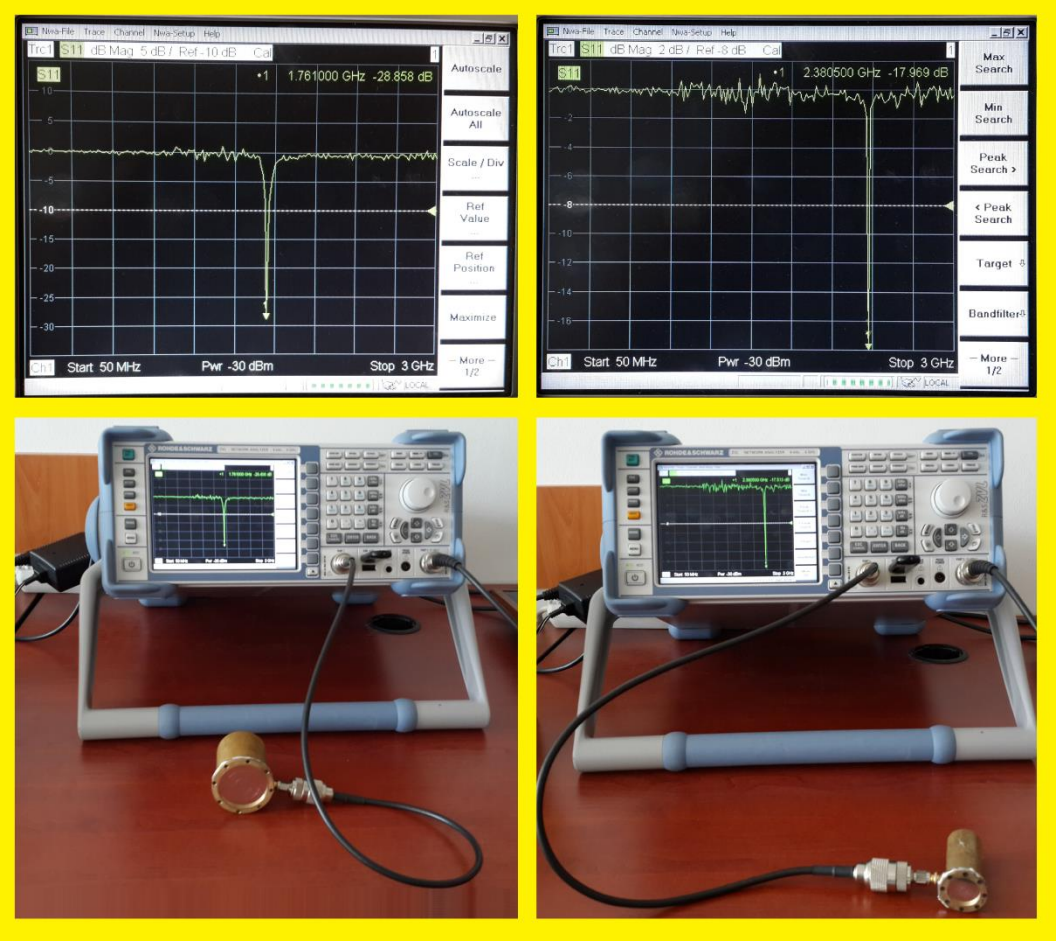

Figure 67. Resonance frequency measurement of prototypes

At some gap length value and post plate diameter it is measured and recorded the resonance frequencies for both prototypes. These results are given in Figure 68 as a graph by comparatively with the simulation results.

As seen in Figure 68 and Figure 69 below the measurement results and the simulation results are consistent at some degree. Small differences are caused by the mechanical tolerances, measurement errors and the modeling errors. The machining errors of the prototypes are at least in the orders of several tens of micrometers which cause significant changes in resonance frequencies. The length measurements are done with a caliper so the caliper tolerances and the reading errors also cause some disparity. And the HFSS models created for the prototypes are tried to be made

exactly the same with the prototypes but because of the design limitation and capability, minor differences would exist which also affects the results.

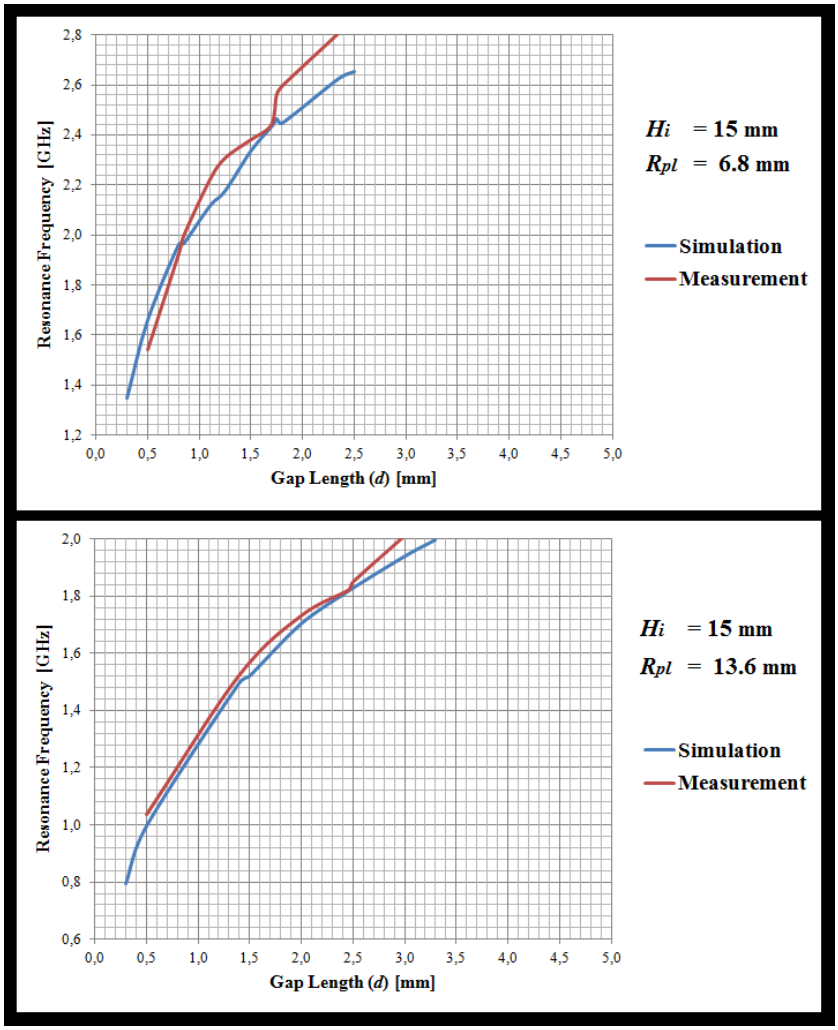

(a)

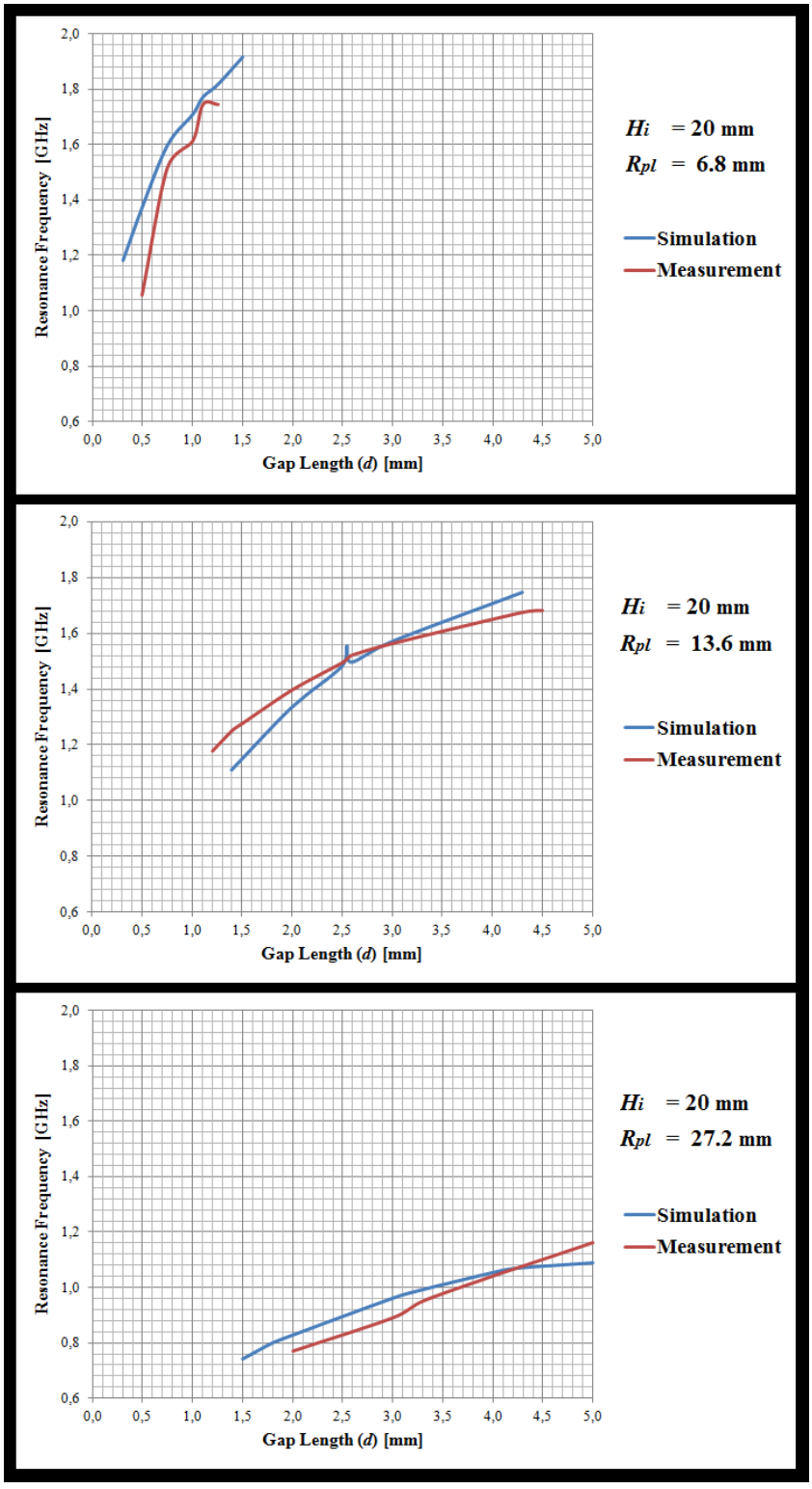

(b)

Figure 68. Comparison of measurement and simulation results for Prototype-1

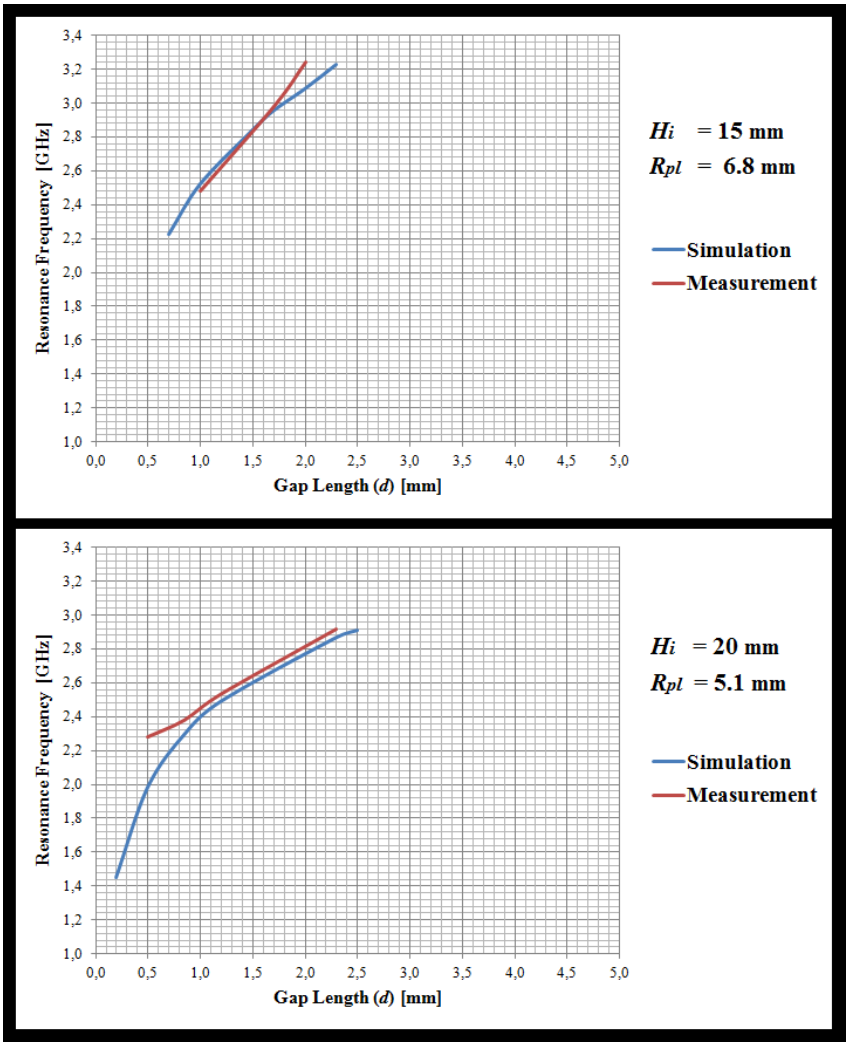
Resonance Frequency [GHz]
3,4
3,2
3,0
2,8
2,6
2,4
2,2
2,0
1,8
1,6
1,4
1,2
1,0
0,0 0,5 1,0 1,5 2,0 2,5 3,0 3,5 4,0 4,5 5,0
Gap Length (d) [mm]
Hi = 15 mm
Rpl = 6.8 mm
Simulation
Measurement
Resonance Frequency [GHz]
3,4
3,2
3,0
2,8
2,6
2,4
2,2
2,0
1,8
1,6
1,4
1,2
1,0
0,0 0,5 1,0 1,5 2,0 2,5 3,0 3,5 4,0 4,5 5,0
Gap Length (d) [mm]
Hi = 20 mm
Rpl = 5.1 mm
Simulation
Measurement

(a)

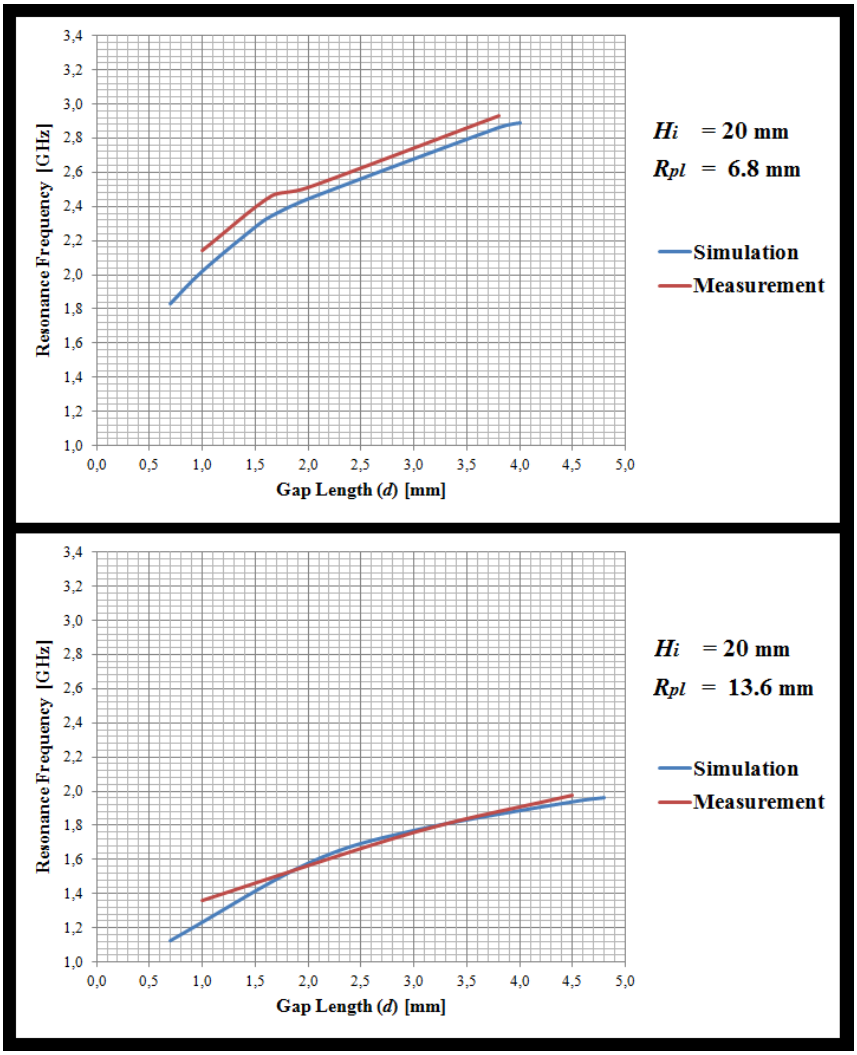

(b)

Figure 69. Comparison of measurement and simulation results for Prototype-2

4.3 Sound Receive Experiments

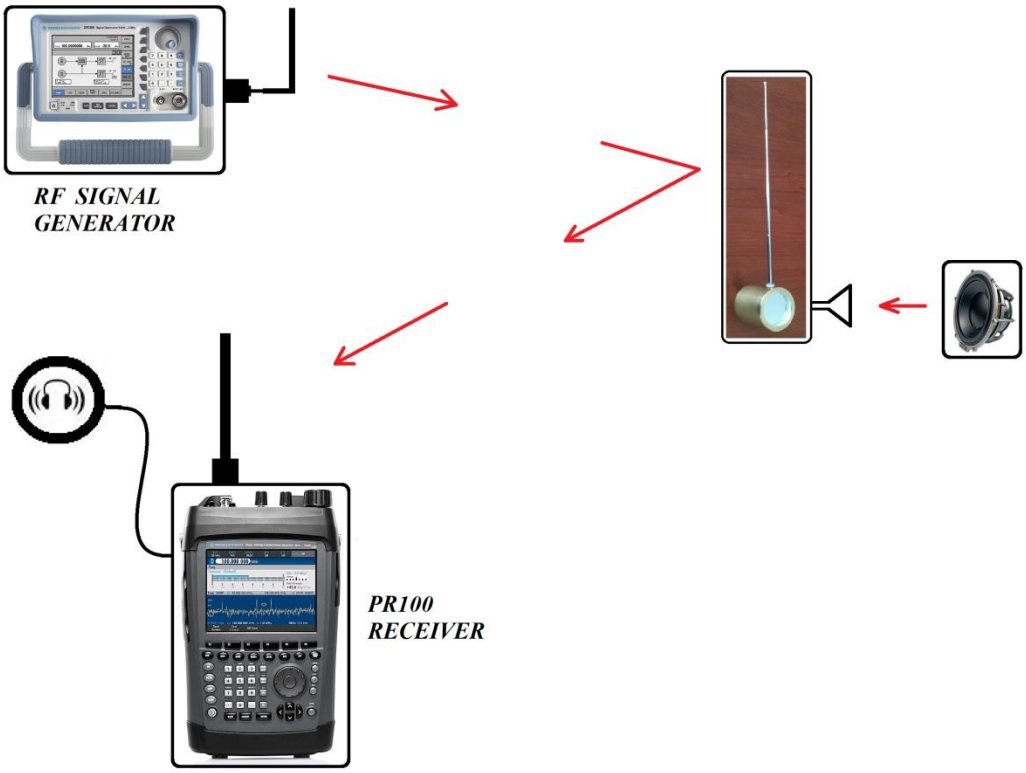

Figure 70. Sound receive experiment setup illustration

The sound receive experiment set up is illustrated in the Figure 70. Before the experiment the determination process of the resonance frequency is performed. In order to adjust the resonance frequency to a value that gives the minimum reflection coefficient a serious efforts were exerted. After many trials the resonance frequency of the prototype was adjusted to the 1.76 GHz eventually and in order to keep this adjustment unchanged the prototype parts were fixed in proper way carefully.

Figure 71. Sound receive experiment setup

A carrier wave is formed as a sine signal with frequency of 1.76 GHz and the amplitude of 13 dBm (maximum amplitude value of the RF generator) was produced by SM300 RF signal generator and transmitted. The prototype cavity resonator was positioned at a distance of about 30 cm from the transmitting antenna of the RF generator. At a distance of approximately 20 cm a speaker was placed towards to the diaphragm side of the cavity resonator prototype. PR100 spectrum analyzer which is capable of AM demodulation and voice recording was used for reception of the scattered signal from the prototype.

The noise floor in the environment of the experiment is about -120 dBm. And the signal level measured with the receiver approximately 1m away from the RF signal generator is about -30 dBm.

Hence the SNR value of the received signal is approximately 90 dB. This is for the total received wave (i.e., the carrier wave and the scattered wave).

When we produce a sine tone with the speaker at the resonance frequency of the diaphragm (i.e., mechanical resonance of the stretched diaphragm) then it can be seen and measured the shifted frequency signals on the receiver. The strong vibration of the diaphragm by a single tone sound causes a clear shift in the frequency of the backscattered signal. The received level of this signal at shifted frequency is approximately -55 dBm. So SNR of the backscattered signal by the prototype is about 65 dB.

The sound produced by the speaker is received by PR100 spectrum analyzer at the same frequency by AM Modulation. The received sound was a bit noisy and low. But it was intelligible and understood well. When one of the speaker, the prototype or the receiver was removed away from the others then the received voice weakened and at some distance it was totally gone. The voice was received from the distance up to 1 m away by the analyzer but beyond that it was so much weakened that there was nearly no voice understood. In the experiment the maximum distance the voice is received is 10 m but it was with very loud sound and not sustainable and repeatable.

The experiments are repeated for several sounds like different kinds of music having different frequency content and sound style, live speaking and recorded speech.

Although AM demodulation is used for the perception of the sound in the experiment, it is observed that the sound is also obtained by using FM demodulation. But the sound obtained by FM demodulation is distorted.

4.3.1 The Obtained Sound

The first graph in Figure 72 belongs to the original sound which is a record of a woman speech played in the test environment, the second graph shows the sound received by using the cavity resonator prototype and the third graph shows the filtered version of the received sound.

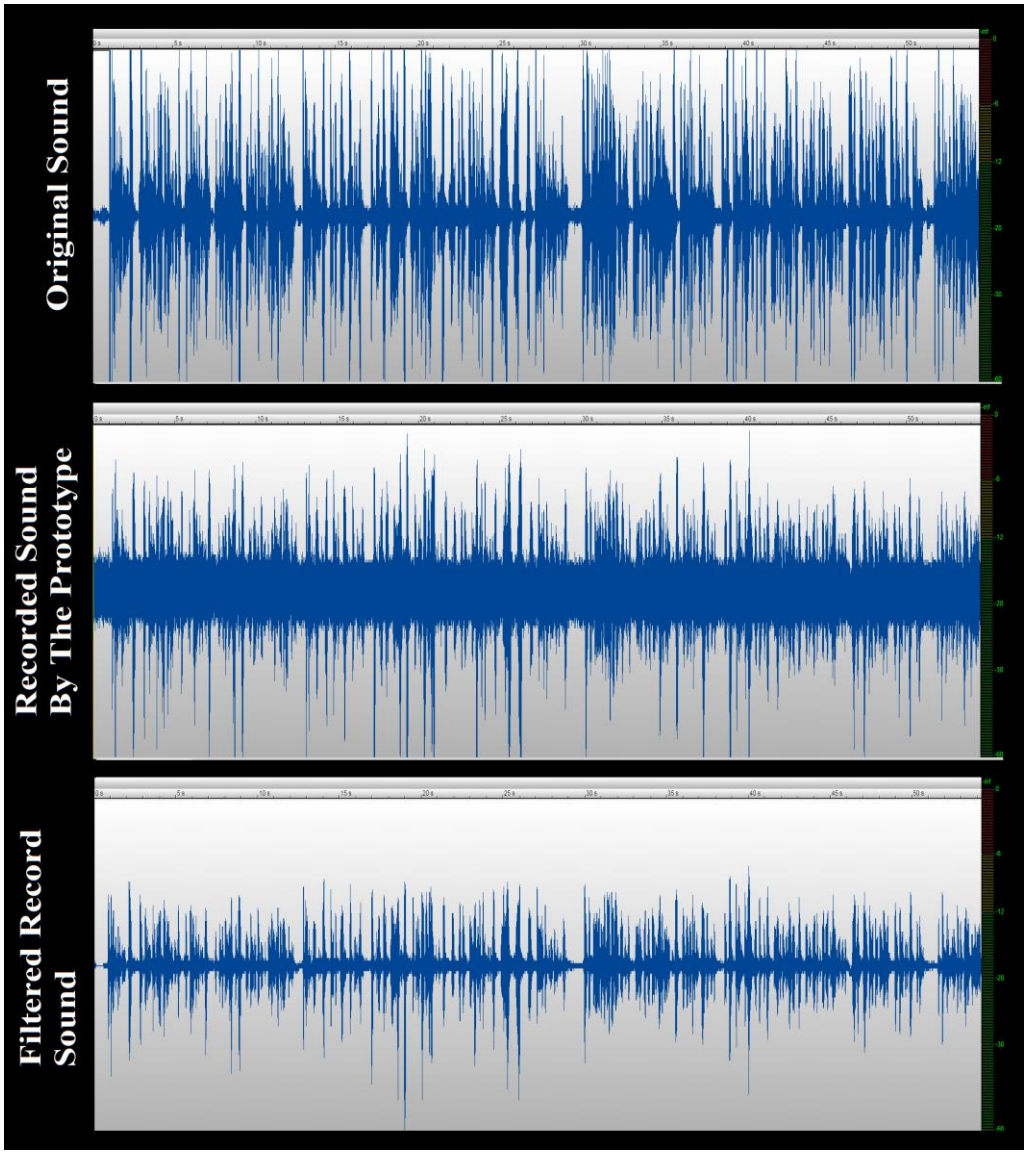

Figure 72. The sound received by the prototype

The sound obtained by the cavity resonator is a bit noisy and this noise reduces the sound quality and voice clarity. But still the speech in the record is understandable. The filtering improves the intelligibility of the sound.

All the audio files which are the original sounds used for the experiment, recorded sounds by the cavity resonator, filtered and amplified version of those are given in Appendix B.

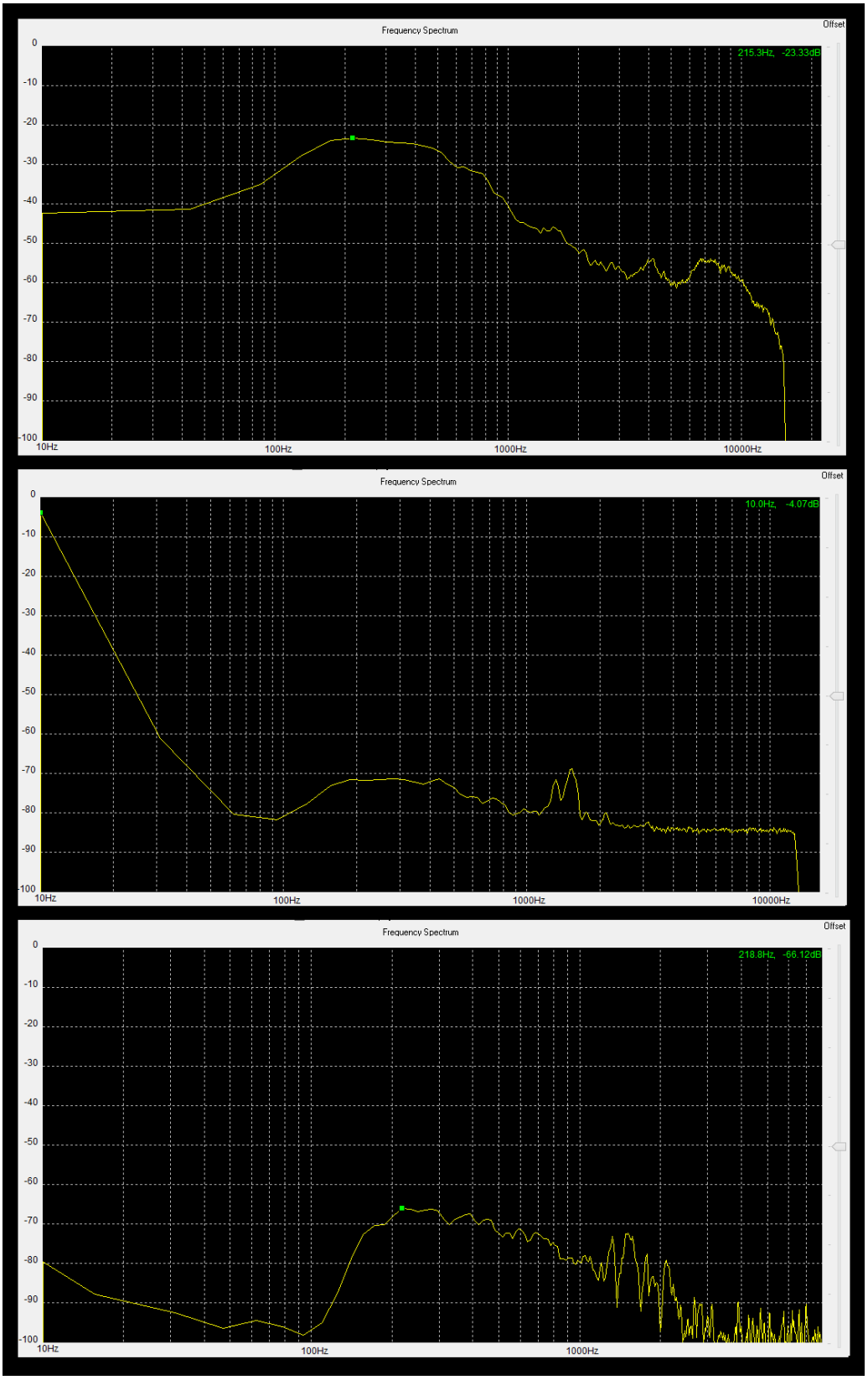

Figure 73. The sound spectrums

Figure 73 shows the frequency content of the sounds. First graph belongs to the original sound, second belongs to the record made by cavity resonator and the third one is the graph of the filtered version of the record. The sound obtained from the cavity contains noise spread across all frequencies but it has additional content especially in low frequency region.
The filtered sound is better than the original received sound in terms of intelligibility although it has some deterioration because of the filtering process.
The filtering process has been performed by Adobe Audition 3.0 and the applied filtering process contains the following transactions.

- Repair DC Offset
- Speech Volume Leveler
- Adaptive Noise Reduction
- Vocal Enhancer

These processes filter the excess noise that distort intelligibility of the sound and enhances the speech clarity thus make the recorded speech more understandable.

4.3.2 Link Budget of the Experiment

The sound receive experiment setup has an architecture of bi-static dislocated backscatter communication link, because the transmitter and the receiver are separate units and located in different places. It is illustrated by a drawing in Figure 74.

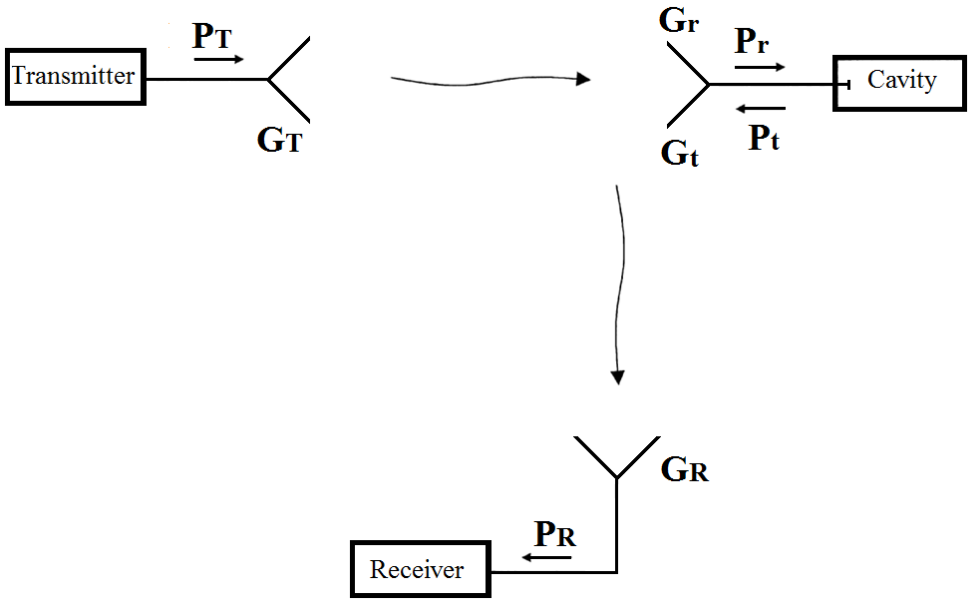

Figure 74. Bi-static dislocated communication link of the experiment

The linear scale link budget for the received modulated backscatter power P_R can be written as

$$P_R = \frac{P_T G_T G_R {G_r}^2 \lambda^4 X_f X_b M}{(4\pi)^4 R_f R_b \Theta^2 B_f B_b F_\alpha} \tag{4.1}$$

where f subscripts denote the forward link parameter and b subscripts denote the backscatter (reverse) link parameters [47].

The parameters in the expression are

P_R : Received power

P_T : Transmitter power

G_T : Transmitter antenna gain

G_R : Receiver antenna gain

G_t : Prototype antenna gain (G_r)

λ : Wavelength of the EM signal

X_f : Forward link polarization mismatch

X_b : Backscatter link polarization mismatch

M : Modulation factor

R_f : Forward link distance

R_b : Backscatter link distance

Θ : On-object gain penalty

B_f : Forward link path blockage loss factor

B_b : Backscatter link path blockage loss factor

F_α : Fading factor

Transition of Eq. (4.1) to the dB format is as follows

$$P_R = P_T + G_T + G_R + 2G_r - L_{FWD} - L_{BACK} \text{ (in dB)}$$

where L_{FWD} represents the forward link losses and L_{BACK} represents the backscatter (reverse) link losses.

The RF signal transmitter output power is 13 dBm and it has a BNC right angle monopole antenna with approximate gain of 3 dBi. The prototype has a monopole antenna with an approximate gain of 2 dBi. The forward link and the backscatter link distances are about 30 cm. The receiver antenna has gain of 5 dBi. Since all three antennas are aligned there is no polarization miss-match loss. Also, since all antennas are in line of sight and there were no object near the antennas which can negatively affects the antennas there are no on-object gain penalty and path blockage loss. A moderate 10 dB fading loss and 6dB modulation loss are assumed.

Table 16 Estimated link budget parameters of the sound receive experiment

Parameter	Value
Transmitter Power (P_T)	13 dBm (-17 dB)
Transmitter Antenna Gain (G_T)	3 dBi
Backscatter Device Antenna Gain (G_r)	2 dBi
Receiver Antenna Gain (G_R)	5 dBi
Free Space Loss (L_{FSL})	-
Polarization Miss-match Loss (L_X)	0 dB
Modulation Loss (L_M)	- 6 dB
On-Object Loss Gain Penalty Loss (L_Θ)	0 dB
Path Blockage Loss (L_B)	0 dB
Fading Loss (L_F)	- 20 dB

The forward and backscatter link losses are

$$\begin{aligned} L_{FWD} &= L_{FSL} + L_X + L_\Theta + L_B + L_F \\ &= L_{FSL} + (0) + (0) + (0) + (-20) \\ &= L_{FSL} + 20\ dB \end{aligned}$$

$$\begin{aligned} L_{BACK} &= L_{FSL} + L_X + L_M + L_\Theta + L_B + L_F \\ &= L_{FSL} + (0) + (-6) + (0) + (0) + (-20) \\ &= L_{FSL} + 26\ dB \end{aligned}$$

The total received power

$$\begin{aligned} P_R &= P_T + G_T + G_R + 2G_r - L_{FWD} - L_{BACK} \\ &= (-17) + (3) + (5) + 2(2) - (L_{FSL} + 20) - (L_{FSL} + 26) \\ &= -2L_{FSL} - 41 \end{aligned}$$

So the SNR level at the receiver

$$\begin{aligned} SNR &= P_R - N_{THR} - NFRec \\ &= (-2L_{FSL} - 41) - 196 - (10) \\ &= 145 - 2L_{FSL} \end{aligned}$$

According to this result, the SNR values for several distances are given in Table 17.

Table 17 Approximately calculated SNR values for several distances

Distance	SNR
10 cm	110.3 dB
20 cm	98.3 dB
30 cm	91.2 dB
50 cm	82.3 dB
1 m	70.3 dB
2 m	58.3 dB
5 m	42.3 dB
10 m	30.3 dB
50 m	2.3 dB

CHAPTER 5

SUMMARY AND CONCLUSION

In this chapter there are three parts. The summary section provides an overview of the thesis. The conclusion section contains the results of the work and inferences obtained from the study. The final section lists suggestions for future work and further studies.

5.1 Summary

This study investigated the passive cavity resonator structure renowned as “Theremin’s Device” or “Great Seal Bug” in detail in order to explore the working principle and technical aspects of the device beyond the rumors and hearsays. The main goal of the work presented in this thesis focused on understanding the structure, theoretically explaining the principles of operation and implementation of a similar structure.

In the first chapter of the thesis, a short story of the device is given and mentioned the motivation aspects and objectives of the study. Besides, some general properties of the topic device are presented and given the organizational structure of the thesis.

In the second chapter of the thesis, the theoretical background information necessary for the study is explained. This includes roughly the topics of resonance and resonators, microwave cavities and features, antennas and the backscatter wave techniques.

The third chapter includes main works performed for this study. First, the theoretical analysis of the device was carried out. Initially the physical structure of the device was examined.

The lumped parameters, quality factor and the resonance frequency of the cavity structure were calculated by using the values obtained from three different references. Also the amount of diaphragm movement by a sound was calculated.
The equivalent circuit of the cavity was found. Modulation issue was formulated and the link budget for the operation of the device was calculated.
After the theoretical analysis, the structure was modeled with the HFSS and simulated with a wide variety of parameters. The eigenmode and field distribution analysis of the structure were realized by simulation. Also sensitivity, quality factor and parameter analysis of the device were performed. After the simulation of the structure, two prototypes were designed and produced. Prototypes were also simulated in the same manner.
The fourth chapter includes the work done for prototype measurements and experiments. Firstly, in order to verify the concept of backscatter modulation a simple experiment setup was prepared. A dipole antenna that is loaded with a varactor diode and a simple AM detector circuit were used for proof of the concept experiment. The resonance frequency measurements of the prototypes were realized by using network analyzer. Later on the actual experiment setup was prepared with the prototype. The ambient sound was gathered via the backscattering from the cavity resonator prototype. The structure was thus successfully replicated and the working theory and the operation concept of the device was verified. The sound obtained was filtered, analyzed and compared with the original sound. Lastly the link budget calculation of the experiment is done.
The fifth chapter, the last one, presents the summary and conclusions of the thesis. It also mentions the future studies and research areas that can be studied further.

5.2 Conclusion

Theremin’s device being the predecessor of modulated backscatter wave communication, RFID and microwave wireless sensor technologies was a covert spy device.

It was invented by Leon Theremin who worked for Soviet secret service and it was used for espionage. The device was found by American intelligence service CIA and resolved by English service. So the device and its story are secret.

Because of this secrecy there is no exact and certain information about the technical details and principle of operation. All the information about the device is consisted of stories, tales and rumors. In the references having information about the device (all information is given in Appendix A) there are many technical inconsistencies about the device, working principle and technical details. So it is used the three references as alternatives and the calculations and analysis are done according to those. And since none of them has all parameters, the missing parameters of one are taken from other two. Thus three alternatives are constituted. The calculated frequencies by using these parameters are approximately 1.62 GHz for the first alternative, 3 GHz for second and 2.63 GHz for the third one. The first result seems reasonable because in some references the working frequency is said to be 1600 MHz. But still the other alternatives may also be close to the original device by use of different measures because the parameters or mechanical measures are approximate values. For example, in some references the inductance of the device is said to be 10 nH but in approximate calculations it is found as approximately 4 nH. And the gap length value used is 185 um for the first alternative but there may be much less for a higher sensitivity. So it is not possible to say an exact value for the working frequency. But 330 MHz, 800 MHz and 1600 MHz are all possible acceptable values. The quality factor cited as an approximate value for the device in some references is 1000. The calculated Q factor is 1948 so that Q factor seems also reasonable.

In the simulation results of the device, the resonant frequency is also approximately 1.6 GHz. This coincides with the calculation result. According to the graph in Figure 41 showing the relationship between the resonance frequency and the gap length, the resonance frequency reduces as low as to 400 MHz. And the graph in Figure 42 shows that the resonance frequency can be as low as 300 MHz with the increasing post plate diameter. In the case of the operating frequency of the device, this suggests the possibility of 330 MHz which is said to be the working frequency of the device in some references.

These graphs also show the significant effect of the gap length to the resonance frequency.

The field analysis of the structure supports this effect. Nearly all the electric fields are concentrated in the gap region. This concentration greatly increases the sensitivity of the resonance frequency to the gap length because any small change in the gap has a great effect on these fields. The sensitivity graphs (Figure 43 and Figure 61) also show the degree of sensitivity for several gap length levels. In these graphs it is seen that the sensitivity increases when the gap length decreases, i.e., the sensitivity is inversely proportional to the gap length. This also coincides with the calculations.

In the graphs (Figure 45, Figure 46, Figure 62, Figure 63) showing the relationship between the quality factor and the gap length and other parameters it is seen that the Q factor ranges from approximately from 800 to 1600. This is compatible with the value of 1000 which is given in some references. Although the roughly calculated Q factor value is 1948, since the post plate and the antenna portion are not taken into account, the correct value must be lower than this. So it can be said that the Q factor graphs are also compatible with theoretical calculations.

The graphs (Figure 41, Figure 42, Figure 59, Figure 60) showing the dependency of the resonance frequency to the dimensional parameters show that the parameter affecting the frequency most after the gap length is plate diameter. When the plate diameter increases then the parallel plate capacitance increases and this increase in capacitance causes a decrease in resonance frequency. The internal height and the internal diameter have very little effect on the resonance frequency because the major factor that determines the resonance frequency is the field distribution inside the cavity and these dimensions have much less effect on the field distribution in this structure. The relationships between the Q factor and the dimensional parameters are nearly in the same manner with the resonance frequency. The gap length has a greater effect on Q factor but the plate diameter has less effect and the internal diameter and the internal height have very little effect.

The production of such a structure are quite challenging because of the need for tight tolerances. Especially the gap length is very important in terms of tolerances because of the greater effect on the resonance characteristic of the cavity.

The measurement and the production tools which used for the production of the prototypes have tolerances up to several tens of micrometers at best. So the precision of the prototype measures are not so good. These tolerances cause difficulties in the adjustment of the gap length such that the slightest move leads to a very large change such as several hundred MHz. So it is not possible to set a desired value for gap length and resonance frequency. Instead it is set and the obtained value is used. Adjusting a proper value is somewhat affordable and it may require so many trials. Moreover, since even a tiny movement could change the gap length the adjusted parts (diaphragm ring, post and back side wall) must be fixed somehow. When doing the sound receive experiment the adjusted parts were fixed with tapes.

The resonance frequency of the prototype cavities were measured with network analyzer. The resonance frequency measurement results of the prototypes coincide with the simulation results. These are illustrated as graphs (Figure 68, Figure 69). The simulation results of the prototypes have also the same characteristic with the device simulation results.

In order to verify the concept of communication with backscattering modulation, a proof of the concept experiment was set up. In this experiment it is seen that by changing the load capacitance of the dipole antenna, the reflected wave from the antenna can be modulated. This experiment proved the concept of backscatter communication.

In the sound receive experiment; the speech from a speaker near the prototype was received. Since the output power of the RF signal generator is low the distance between the prototype and the receiver affects the performance much. It could be received the sound by a maximum distance of several meters. The received sound is very noisy. The noise seems like a white noise and so it cannot be filtered out totally. But the speech is very well understood despite this noise. But still the intelligibility of the received sound is improved by some filtering.

When compared the frequency spectrum of the received sound with the original sound it is seen that the received sound contains noise spread across all frequencies but it has additional content especially in low frequency region.

So the filtering provides better quality in terms of intelligibility despite some distortion.

As shown by Eq. (3.36) in section 3.2.2.5, the reflected wave from the cavity resonator is both AM and PM modulation of the sound. So in the experiments AM demodulation is used for the perception of the sound. But since PM is a special case of FM, it is observed in the experiments that the sound is also obtained by using FM demodulation. But the sound obtained by FM demodulation is distorted as expected.

The link budget calculations for the sound receive experiment as being a bi-static dislocated backscatter communication link show that the approximate SNR value is 70 dB for 1m distance. This theoretical result coincides with the experimental results. The experimental SNR value for the backscattered signal by the prototype is about 65 dB at a 1m distance.

As a general conclusion, this cavity resonator structure has a great capability and opportunity for sensing the continuously changing physical quantities like pressure, vibration, speed, flow, stress, velocity, force etc. passively and remotely. Any physical parameter that can change the gap length of the cavity resonator continuously and thus change the resonance characteristics of the resonator can modulate the scattered wave by the structure and can be sensed or monitored remotely by demodulation. Since the structure is passive and does need no power for functioning, it can be used in applications for which power is a critical issue such as submarine applications, high altitude air applications, rural area applications and applications carried out in terrestrial depths. For instance; by implanting such a structure inside the body of an animal, the existence of the respiration or the heart beat can be monitored remotely and detected that whether it is alive or not. Another application may be that a design of this structure can be placed in a very high altitude in the air and the air flow or wind speed can be monitored remotely and wirelessly, moreover it will not need power so long lasting.

5.3 Future Work

There are several issues that can be studied as future work on this topic. Firstly, some references claim that the operation of the device take place in two different frequencies such that the incoming and the outgoing or backscattered wave have different frequencies. It is asserted that the device produces a harmonic of the incoming frequency and re-radiates it after modulation. This case can be further investigated and studied.

An issue that can be studied further is the subject of utilizing the signal existing already in the environment, instead of transmitting a carrier signal. Since there is no transmitting signal, this method will be totally passive. Today there are many signals in the environment such as GSM, Wi-Fi, TV broadcast etc. The concept of using these signals as a carrier for a backscatter communication may be researched.

Another issue that can be studied may be the cable version of the Theremin's device. Such a structure would also consist of only the mechanical parts and not contain any electrical or electronic parts. So it would be a device that cannot be detected by the device detectors. And it would also be a device that cannot be damaged by electrical or electromagnetic methods.

The cavity resonators have also many application areas especially in RF MEMS sensor technologies. Any physical parameter that can change the gap of the coaxial cavity resonator may be the subject of a sensor application. The sensing of the position, force, stress, pressure, flow and many more parameters may be a research area for RF MEMS cavity resonators.

REFERENCES

[1] U.S. Department of State. (2011). *History of the Bureau of Diplomatic Security of the United States Department of State* (No: 176589). Hillsborough: Global Publishing Solutions

[2] S. David Pursglove. (1962, January). How Russian Radio Works. *Electronics Illustrated*, 5, 89-91.

[3] *Great Seal Bug*. (2012). Retrieved January 07, 2015. From: http://spymuseum.com/dt_portfolio/great-seal-bug/

[4] *Cold War: Great Seal Exhibit*. (2015). Retrieved February 12, 2015. From: National Security Agency Web Page, National Cryptologic Museum - Exhibit Information: https://www.nsa.gov/about/cryptologic_heritage/museum/virtual_tour/museum_tour_text.shtml#great_seal

[5] *Spaso House*. (2015). Retrieved April 02, 2015. US Department of State, Moscow Embassy of The United States of America Web Site http://moscow.usembassy.gov/spaso.html

[6] A. Glinsky. (2000). *Theremin: Ether Music and Espionage*. Chicago: University of Illinois Press.

[7] Wright Peter, Greengrocer Paul. (1987). *Spycatcher*. Australia: Heinemann Publishers.

[8] Kevin D. Murray. (2012). *The Great Seal Bug Story*. Retrieved September 25, 2014. Murray Associates Web Site: http://www.spybusters.com/Great_Seal_Bug.html

[9] Michael E. Mauel.(2012). *Understanding the Great Seal Bug*. Retrieved October 9, 2014. Columbia University, Department of Applied Physics and Applied Mathematics With Materials Science and Engineering Web Site: http://sites.apam.columbia.edu/courses/apph4903x/Great_Seal_Bug.pdf

[10] S. David Pursglove. (1968, March). Little Radio Transmitters for Short-Range Telemetry. *Scientific American*, 218(3), 128-134.

[11] H. Meith Kelton. (1996) *The Ultimate Spy Book*. Canada: Dorling Kindersley

[12] Pavel Nikitin. (2012). Leon Theremin (Lev Termen). *IEEE Antennas and Propagation Magazine, 54(5), 252-257*.

[13] The Thing (listening device). (2014). Retrieved February 11, 2015. Wikipedia: http://en.wikipedia.org/wiki/The_Thing_(listening_device)

[14] Graham Brooker, Jairo Gomez. (2013, November). Lev Termen's Great Seal bug analyzed. *Aerospace and Electronic Systems Magazine, IEEE*, 28(11), 4-11.

[15] David M. Pozar. (2012). *Microwave Engineering*. Danvers MA: JohnWiley & Sons Inc.

[16] Frederick Emmons Terman. (1943). *Radio Engineer's Handbook*. New York: McGraw-Hill Book Company.

[17] Robert E. Collin. (1992). *Foundations for Microwave Engineering*. New York: McGraw Hill

[18] Roger F. Harrington. (2001). *Time-Harmonic Electromagnetic Fields*. New York: John Wiley & Sond Inc.

[19] Herbert P. Neff, Jr. (1991). *Introductory Electromagnetics*. New York: John Wiley & Sond Inc.

[20] Kazuo Fujisawa. (October 1958). General Treatment of Klystron Resonant Cavities. *IEEE Transactions on Microwave Theory and Techniques, 6(4), 344-358.*

[21] Richard P. Feynman. (2005). *The Feynman Lectures on Physics*. United States: Caltech. Available online: http://www.feynmanlectures.caltech.edu/

[22] Li X., Jiang Y. (2010). Design of a Cylindrical Cavity Resonator for Measurements of Electrical Properties of Dielectric Materials (Master's thesis, University of Gävle, Gävle, Sweden). Retrieved from: http://www.diva-portal.org/smash/get/diva2:354559/fulltext01

[23] Constantine A. Balanis. (2012). *Advanced Engineering Electromagnetics*. USA: John Wiley & Sond Inc.

[24] Ali Akdagli. (2011). Electromagnetic Waves in Cavity Design, Hyoung Suk Kim, *Behavior of Electromagnetic Waves in Different Media and Structures,* (77-100). China: In Tech.

[25] Peroulis D., Naglich E., Sinani M., Hickle M. (2014). Tuned to Resonance: Transfer-Function-Adaptive Filters in Evanescent-Mode Cavity-Resonator Technology. IEEE Microwave Magazine, *15(5),* 55-69.

[26] Muhammad-Ahmad, Makki El-Tayyid. (1987). *Resonant cavity method for broadband dielectric measurements* (Doctoral thesis, University of Durham, Durham, UK). Available at Durham E-Theses Online: http://etheses.dur.ac.uk/6671/

[27] Arif, M.S., Peroulis, D. (2014). All-Silicon Technology for High-Q Evanescent Mode Cavity Tunable Resonators and Filters. *Journal of Microelectromechanical Systems, 23(3),* 727-739.

[28] Barroso, J.J., Castro, P.J., Carneiro, L.A., Aguiar, O.D. (September 2003) Reentrant Klystron Cavity as an Electromechanical Transducer. *Proceedings of the 2003 SBMO/IEEE MTT-S International, 2(20-23),* 1081-1084.

[29] Joshi H., Sigmarsson H.H., and Chappell W.J. (August 2008). Analytical Modeling of Highly Loaded Evanescent-mode Cavity Resonators for Widely Tunable High-Q Filter Applications. *Proceedings of Union Radio Scientifique Internationale (URSI), No: D09.6.*

[30] Barrow W. L., Mmieher W. W. (April 1940). Natural Oscillations of Electrical Cavity Resonators. *Proceedings of the IRE, 28(4),* 184-191.

[31] Sophocles J. Orfanidis. (2003). *Electromagnetic Waves and Antennas*. Available Online: http://eceweb1.rutgers.edu/~orfanidi/ewa/orfanidis-ewa-book.pdf.

[32] Andersen, J. B., Frandsen, A. (2005). Absorption Efficiency of Receiving Antennas. *IEEE Transactions on Antennas and Propagation, 53(9),* 2843-2849.

[33] Best, S.R., Kaanta, B.C., (October 2009) A Tutorial on the Receiving and Scattering Properties of Antennas. *IEEE Antennas and Propagation Magazine, 51(5),* 26-37.

[34] Roger F. Harrington. (September 1958) Electromagnetic Scattering by Antennas. *IEEE Transactions on Antennas and Propagation, 11(5)*, 595-596.

[35] Harry Stockman. (1948). Communication by Means of reflected Power. *Proceedings of the Institute of Radio Engineering, 36(10)*, 1196-1204.

[36] Daniel Gregory Kuester. (2013). *Passive Binary-Modulated Backscatter in Microwave Networks with Applications to RFID* (Doctoral thesis, University of Colorado, Colorado, USA). Available Online: http://ecee.colorado.edu/microwave/docs/theses/kuester_thesis.pdf

[37] Jack H. Richmond. (1955). A modulated scattering technique for measurement of field distributions. *IRE Transactions on Microwave Theory and Techniques, 3(4)*, 13-15.

[38] Pavel V. Nikitin, K.V.S. Rao. (April 2008). Antennas and Propagation in UHF RFID Systems. *In Proceeding of The International Conference on RFID*, 277-278

[39] Louis E. Frenzel. (2008). *Principles of Electronic Communication System*. New York: The McGraw Hill

[40] Bates, A. (Narrator), Robbins, A. (Producer/Director). (1999). *The Spying Game - "Walls Have Ears"*. [TV Series] (Available from British public-service television broadcaster Channel 4 archive)

[41] Bob Atkins. (1989). A Simple Cavity Filter for 2304 MHz. In *The ARRL UHF/Microwave Project Manual* (Page 6-4). Newington, CT: American Radio Relay League

[42] Colin H. Hansen. (2001). Fundamentals of Acoustics. In World Health Organisation Special Report, *Occupational Exposure to Noise: Evaluation, Prevention and Control* Germany: Federal Institute of Occupational Safety and Health.

[43] Werner Karl Schomburg. (2011). *Introduction to Microsystem Design*. New York: Springer.

[44] Bernard Rembold. (2009). Optimum Modulation Efficiency and Sideband Backscatter Power Response of RFID-Tags. *Frequenz, 63(1-2).*

[45] Kai Chang. (2000). *RF and Microwave Wireless Systems*. New York: John Wiley & Sons.

[46] Daniel M. Dobkin. (2008). The *RF in RFID Passive UHF RFID in Practice*. Massachusetts: Elsevier Inc.

[47] Joshua D. Griffin, Gregory D. Durgin. (2009, April). Complete Link Budgets for Backscatter-Radio and RFID Systems. *IEEE Antennas and Propagation Magazine, 51(2),* 11-25.

[48] Kai Chang. (2000). RF and Microwave Wireless Systems. New York: John Wiley & Sons

[49] Ferreira, L., Kuipers, M., Rodrigues, C., Correia, L.M. (September 2006). Characterisation of Signal Penetration into Buildings for GSM and UMTS. *3rd International Symposium on Wireless Communication Systems (ISWCS '06),* 63-67.

[50] H. Keith Melton. (1994). *CIA Special Weapons & Equipment: Spy Devices of the Cold War*. New York: Sterling Pub Co Inc.

[51] Design How To Eavesdropping using microwaves – Addendum. (December 11, 2005). *EETimes*. Retrieved December 17, 2014. http://www.eetimes.com/document.asp?doc_id=1274748

[52] Martin L. Kaiser III. (2006). *Odyssey of an Eavesdropper: My Life in Electronic Countermeasures and My Battle against the FBI*. New York: Carroll & Graf Publishers.

[53] John G. Truxal. (1990). *The Age of Electronic Messages*. Cambridge MA: The MIT Press.

[54] Wallace, R., Melton H. K., Schlesinger, H. R. (2009). *Spycraft: The Secret History of the CIA's Spytechs, from Communism to Al-Qaeda*. New York: Penguin Group (USA) Inc.

[55] David Wise. (1992). *Molehunt: The Secret Search for Traitors That Shattered the CIA*. New York: Random House.

[56] M.L. Shannon. (1992). *Don't Bug Me: The Latest High-Tech Spy Methods*. Colorado: Paladin Press.

[57] Winfield R. Koch. (1941). U.S. Patent No: US2238117A. Washington DC: U.S. Patent and Trademark Office.

[58] Robert M. Brown. (1967) *The Electronic Invasion*. United States: Hayden Book Co. Inc.

[59] National Security Agency. (2015). *Cold War: Great Seal Exhibit.* National Cryptologic Museum - Exhibit Information. Available online: https://www.nsa.gov/about/cryptologic_heritage/museum/virtual_tour/museum_tour_text.shtml#great_seal

APPENDIX A

ALL AVAILABLE INFORMATION OF THEREMIN'S DEVICE

There are dozens of formal and informal sources that provide information about the Theremin's Bug. In this appendix, all gathered information is presented in filtered and classified manner. The information contained herein has been compiled from [1-14,40,50-58].

Device Definitions

Here are some definitions which define the type of device.

- Predecessor of RFID technology
- Passive Cavity Transmitter
- Passive Radiator
- High-Q (Sharply Tuned) Cavity
- Passive tuned-cavity listening device

Pictures and Drawings of the Device

There are several picture and drawings of the Theremin's Device in some references but there is no clear evident that whether these pictures and the drawings belong to the original device or not. So the information used here is not so definite. Nevertheless, we will use all these existing information in this work.
The pictures and drawings of the device are as follows.

Figure 75. Director of Security John Reilly (right) holds the cavity resonator [1]

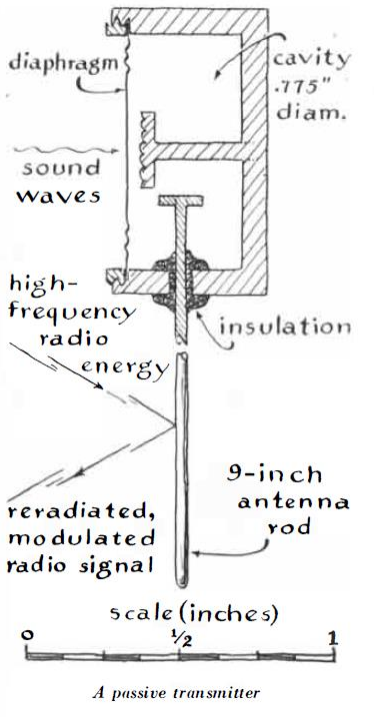

Figure 76. Scaled drawing from "Scientific American" science magazine [10]

Figure 77. A scene from Channel 4 TV Series “The Spying Game - Walls Have Ears" [40]

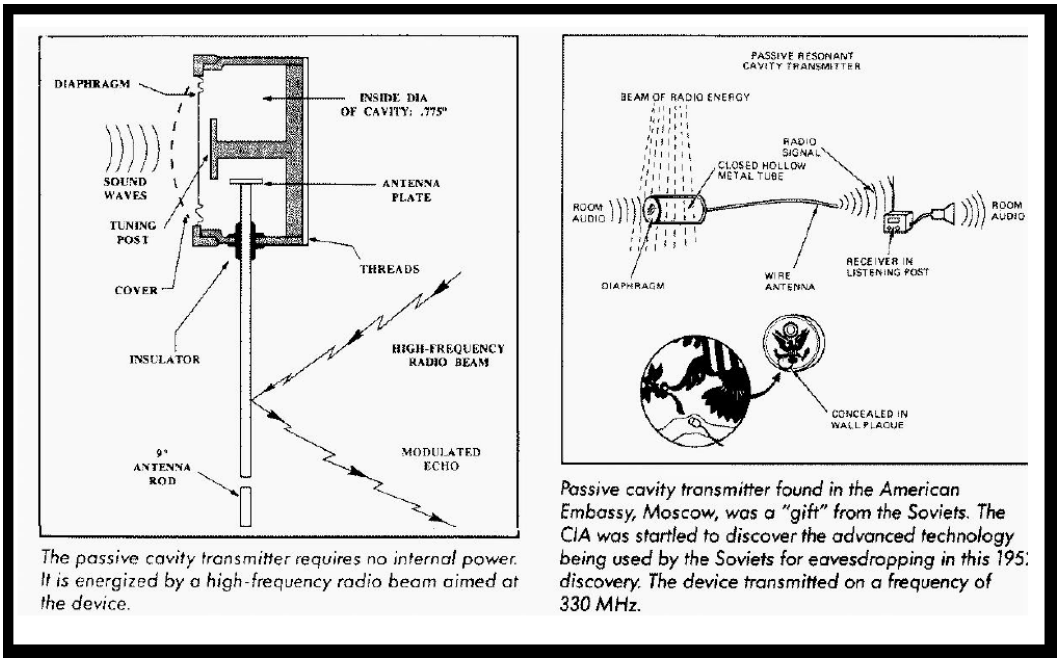

Figure 78. The Drawings of the device and its operation from the “CIA Special Weapons & Equipment: Spy Devices of the Cold War” [50]

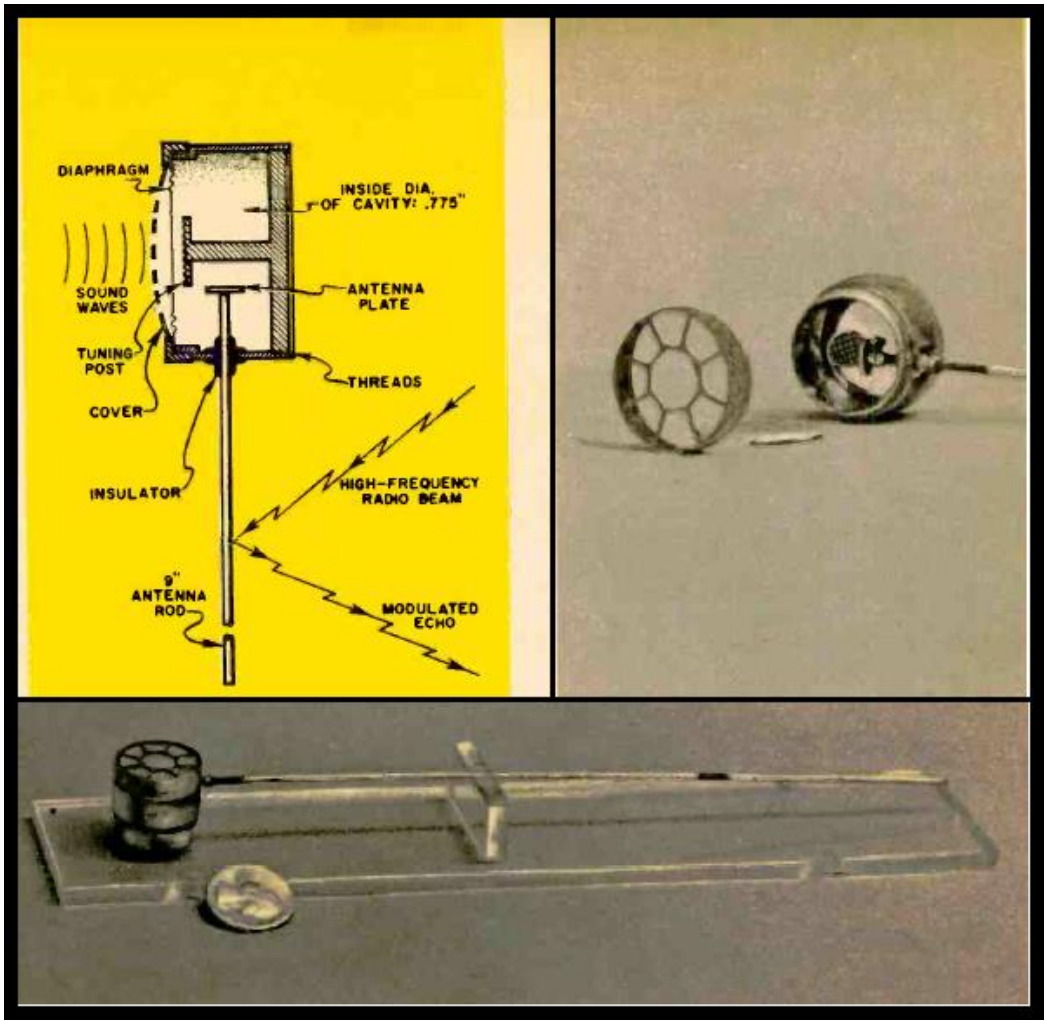

Figure 79. Pictures and drawings from "Electronics Illustrated" Magazine [2]

Figure 80. An old picture of the replica exhibited in National Cryptologic Museum of NSA [59]

Figure 81. A recent picture of the replica exhibited in National Cryptologic Museum of NSA [13]

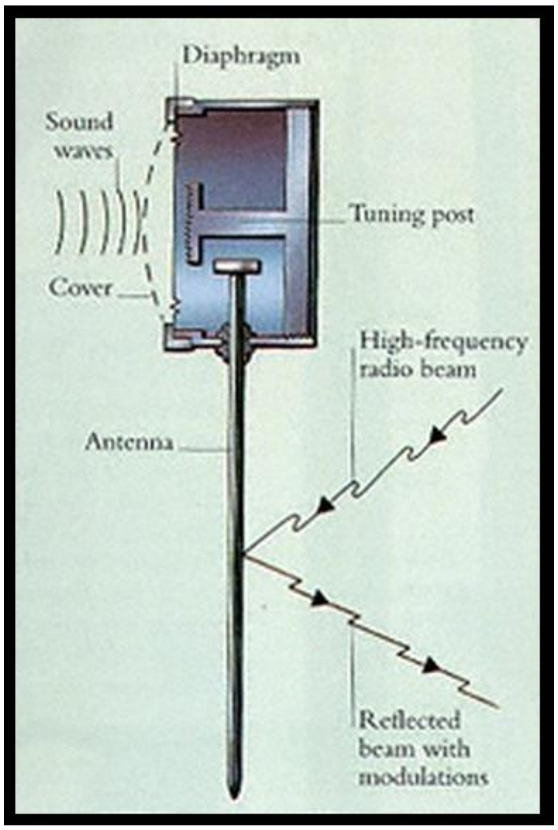

Figure 82. A picture from The Ultimate Spy Book [11]

Device Dimensions

In some sources, the body dimension of the device are given as numerically and in some others it is defined as comparing some other things like quarter coin. Besides, there are several published drawings and some pictures of the device.

It can be obtained some attributes from those drawings and pictures by using them as an additional source and as a crosscheck. In some pictures and drawings, it can be determined the relative ratio between the dimensions in order to find unknown sizes from the known ones. But in other pictures and drawings in which no number exist, it can be used the proportions between the sizes.

This data can be used when analyzing the device and in calculations to reach some additional support.

Table 18 Theremin's Device Parameter from several sources

Parameters	Reference-1 [14]	Reference-2 [10]	Reference-3 [2]	Reference-4 [13]
Internal Diameter	1.97 cm	1.9685 cm	-	1.9685 cm
Outer Diameter	2.1569 cm	2.374 cm	2.426 cm	-
Internal Height	1 cm	0.9463 cm	1.7463 cm	1.7463 cm
Post Plate Diameter	0.68 cm	0.7969 cm	0.635 cm	-
Post Plate Thickness	0.0585 cm	0.1162 cm	-	-
Post Height	0.86 cm	0.8301 cm	-	-
Post Body Diameter	0.1961 cm	0.1494 cm	-	-
Gap Length	0.0185 cm	0.9961mm	-	-
Diaphragm Thickness	-	-	76.2 µm	76.2 µm
Antenna Plate Diameter	0.35 cm	0.3652 cm	-	-
Antenna Plate Thickness	0.0464 cm	0.08799 cm	-	-
Antenna Body Diameter	0.1078 cm	0.08799 cm	-	-
Antenna Length	22.8 cm	22.86 cm	22.86 cm	22.86 cm
Antenna Height	0.65 cm	0.7886 cm	-	-
Cylinder Thickness	0.0784 cm	0.2158 cm	-	-
Quality Factor	-	-	1000	-
Inductance	-	-	10 nH	10 nH
Weight	-	-	1.1 oz	1.1 ounce
Frequency	330 MHz	-	1600 MHz	800 MHz

In the Table 18 all the parameter information about the device is given. These parameters are exactly given as definite. But there are inconsistencies between them.

Table 19 The approximate proportional measures of the device from pictures and drawings

Parameter	Picture-1 [11]	Picture-2 [50]	Picture-3 [2]
Internal Diameter *	1	1	1
Internal Height	0.6	0.507	-
Post Plate Diameter	0.379	0.358	0.353
Post Plate Thickness	8.276	0.0405	-
Post Body Diameter	0.152	0.1074	-
Antenna Plate Diameter	0.221	0.189	0.353
Antenna Plate Thickness	0.069	0.0338	0.04082
Antenna Body Diameter	0.0897	0.061	0.07143
Cylinder Thickness	0.069	0.0541	-

* All the parameters are expressed in terms of Internal diameters as a ratio.

The Table 19 contains the proportionality of the parameters. In some drawings there is no value but if they are scaled then the proportionality of the dimensions can be used as additional information or a crosscheck.

Antenna

There are many different rumors about the antenna length and definition. According to the sources the antenna is

- A quarter wave antenna
- A monopole
- A half wave antenna (one says no ground)
- A full wave antenna
- A quarter wave antenna for 330MHz
- 9 inch monopole (a silver-plated copper rod)
- 8.5 inch full wave antenna
- 8 inch
- 1800 MHz resonating antenna

It is observed in the pictures from CIA museum, the antenna is almost 7 times the diameter.

Structure

The information about what the device is made of exists in some sources. Here are those:

- It did not contain any ferrous materials (and therefore had eluded metal detectors).
- The device was constructed of precision-tooled steel and comprised a long pencil-thin antenna with a short cylindrical top.
- The cylinder is made of copper and silver plated.
- Diaphragm was made from the thinnest copper sheet and silver-plated.
- It is made of brass and silver plated.

Working Frequency

In the sources there are many different frequency values and definitions for the Theremin's device. The list is as follows.

- 330 MHz
- 1800 MHz
- 800 MHz
- 1600 MHz
- Somewhere between 1.1 – 1.5 GHz
- VHF
- UHF
- Usually in MW region, 1 GHz and up
- A wideband signal including many different frequency components
- Radar like signal, not pulsed

Discovery Methods

There are many different stories about how the device is discovered and which kind of device is used.

The statements defining the device which is used to discover Theremin's Device are given below.

- Un-tuned Video Receiver.
- A wideband receiver with a simple diode detector/demodulator.
- Audio amplifier from a thing called a Schmidt Kit. The amplifier had a crystal diode in series with a short wire rod that acted as an antenna at the audio input connector.
- Un-tuned crystal video receiver.
- Radio.
- VHF receiver which is used to monitor Russian military aircraft traffic.
- Discovered during a routine physical, not electrical, security check.

Working Principle

Although there are many story and explanation about the working principle of the device, mainly there are only two types of working style.

- It is a device, which reflects the incoming wave and the reflecting wave is modulated by the diaphragm movement.
- It is a device, which absorbs the incoming wave and sends back a harmonic of that wave, and the outgoing wave is modulated by the diaphragm movement.

According to the first definition it is a reflecting device. And the diaphragm affects the reflected wave. This provides the modulation by the sound. Here are some explanations about this approach.

- Vibration of membrane changes the capacitance seen by the antenna which in turn modulated the radio waves that struck and were re-transmitted by the Thing
- The membrane and the post formed a variable capacitor acting as a condenser microphone and providing amplitude modulation (AM), with parasitic frequency modulation (FM) for the re-radiated signal
- A radio beam was aimed at the antenna from a source outside the building. A sound that struck the diaphragm caused variations in the amount of space (and the capacitance) between it and the tuning post plate. These variations altered the charge on the antenna, creating modulations in the reflected radio beam.
- The pedestal and diaphragm together made up a sort of air-variable capacitor, which altered the resonant behavior of the cavity.
- To excite passive tuned-cavity listening devices. Microwave energy is directed toward the cavity using a directional antenna from the monitoring location. The microwave oscillator is connected to the antenna using a directional coupler having forward and reverse power detectors. The instantaneous VSWR is an indication of diaphragm displacement as the cavity power absorption changes through detuning.

- The RF beam struck the bug's tiny antenna and a minuscule signal echoed back. As long as the antenna kept the same electrical length the echo remained at a set frequency. The sound waves which struck diaphragm, causing it to vibrate. This altered the cavity's size ever so slightly and varied the capacitive values (“post plate – diaphragm” and “post – antenna plate”). The changes in capacitances altered the charge on the antenna rod (radiated to it from the transmitter) and caused its echoed signal to vary accordingly. In effect, the bug modulated a little piece of the beamed signal before sending it back as an echo.

According to the second idea, it is a regenerating device. And the diaphragm affects the regenerated wave which is a harmonic of the incoming wave. This provides the modulation by the sound. Here are some statements about this harmonic regeneration approach.

- A harmonic of the inbound radio frequency energy is rebroadcast. It is important to note that the microwave signal that “powers up” the device is not the same frequency as the outbound signal.
- The length of the antenna and the dimensions of the cavity were engineered in order to make the re-broadcast signal a higher harmonic of the illuminating frequency. (Note that the transmitting frequency is higher than the illuminating one.)
- The size of the cavity and the length of its antenna are carefully calculated so that a harmonic (multiple) of the inbound radio frequency energy that bathes the cavity is rebroadcast.
- The high-Q, silver plated cavity is "tuned" via the adjustable "mushroom" (a 1/4-wavelength shorted stub) to parallel-resonant at an odd-harmonic frequency (3 times higher) than the transmitted RF carrier. The use of higher frequencies will allow for a physically smaller cavity. Also, a RF carrier which is 3 times higher can share an antenna which is for a frequency 3 times lowers, due to the way the current is distributed in the antenna.

Modulation

All stories say that the vibration of the diaphragm by sound modulates the wave. So what is that modulation? Here are some statements about the modulation.

- Amplitude modulation (AM), with parasitic frequency modulation (FM)
- The modulation was partially both amplitude modulated and frequency modulated
- Also discussed was how much of the bug's emission was either AM or FM or did it do both
- Inherently created both AM and FM modulation
- Straightforward zero-IF receiver that delivered the amplitude modulation of the re-emitted signal as audio output.

APPENDIX B

ENCLOSED CD-ROM

The CD-ROM containing the sound files is attached on the back cover.

CD-ROM Content

1- Original Audio Files [FOLDER]

1- *Woman Speech [54 sec]*

2- *Music [72 sec]*

2- Audio Recordings By Cavity Resonator [FOLDER]

1- *Recording of Woman Speech [54 sec]*

2- *Recording of Woman Speech [54 sec] (Amplified)*

3- *Recording of Music [72 sec]*

4- *Recording of Music [72 sec] (Amplified)*

5- *Recording of My Speech [46 sec]*

6- *Recording of My Speech [46 sec] (Amplified)*

3- Filtered Audio Recordings [FOLDER]

1- *Recording of Woman Speech [54 sec] (Filtered 1)*

2- *Recording of Woman Speech [54 sec] (Filtered 1,Amplified)*

3- *Recording of Woman Speech [54 sec] (Filtered 2)*

4- *Recording of Woman Speech [54 sec] (Filtered 2,Amplified)*

5- *Recording of Music [72 sec] (Filtered)*

6- *Recording of Music [72 sec] (Filtered, Amplified)*

7- *Recording of My Speech [46 sec] (Filtered)*

8- *Recording of My Speech [46 sec] (Filtered, Amplified)*

Info

Content